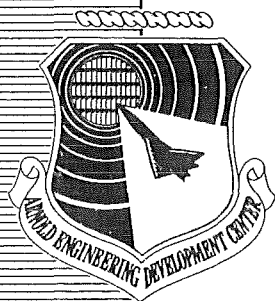DOT/FAA/CT-86/35
AEDC-TR-86-26

An Analytical Study
of Icing Similitude
for Aircraft Engine Testing

C. Scott Bartlett
Sverdrup Technology, Inc.

October 1986

Final Report for Period September 1985 — June 1986

Approved for public release; distribution is unlimited.

U. S. Department of Transportation   U. S. Air Force

Federal Aviation Administration   Air Force Systems Command

FAA Technical Center   Arnold Engineering Development Center

Atlantic City Airport, NJ 08405   Arnold Air Force Station, TN 37389

NOTICES

When U. S. Government drawings, specifications, or other data are used for any purpose other than a definitely related Government procurement operation, the Government thereby incurs no responsibility nor any obligation whatsoever, and the fact that the Government may have formulated, furnished, or in any way supplied the said drawings, specifications, or other data, is not to be regarded by implication or otherwise, or in any manner licensing the holder or any other person or corporation, or conveying any rights or permission to manufacture, use, or sell any patented invention that may in any way be related thereto.

Qualified users may obtain copies of this report from the Defense Technical Information Center.

References to named commercial products in this report are not to be considered in any sense as an endorsement of the product by the United States Air Force or the Government.

This report has been reviewed by the Office of Public Affairs (PA) and is releasable to the National Technical Information Service (NTIS). At NTIS, it will be available to the general public, including foreign nations.

APPROVAL STATEMENT

This report has been reviewed and approved.

CARLOS TIRRES
Facility Technology Division
Directorate of Technology
Deputy for Operations

Approved for publication:

FOR THE COMMANDER

LOWELL C. KEEL, Lt Colonel, USAF
Director of Technology
Deputy for Operations

REPORT DOCUMENTATION PAGE

1a. REPORT SECURITY CLASSIFICATION UNCLASSIFIED		1b. RESTRICTIVE MARKINGS
2a. SECURITY CLASSIFICATION AUTHORITY		3 DISTRIBUTION/AVAILABILITY OF REPORT Approved for public release; distribution is unlimited.
2b. DECLASSIFICATION/DOWNGRADING SCHEDULE		

4. PERFORMING ORGANIZATION REPORT NUMBER(S) AEDC-TR-86-26	5. MONITORING ORGANIZATION REPORT NUMBER(S)

6a. NAME OF PERFORMING ORGANIZATION Arnold Engineering Development Center	6b. OFFICE SYMBOL (If applicable) DOT	7a. NAME OF MONITORING ORGANIZATION
6c. ADDRESS (City, State and ZIP Code) Air Force Systems Command Arnold Air Force Station, TN 37389-5000		7b. ADDRESS (City, State and ZIP Code)

8a. NAME OF FUNDING/SPONSORING ORGANIZATION Federal Aviation Administration	8b. OFFICE SYMBOL (If applicable)	9. PROCUREMENT INSTRUMENT IDENTIFICATION NUMBER

8c. ADDRESS (City, State and ZIP Code) FAA Technical Center Atlantic City Airport, NJ 08405	10 SOURCE OF FUNDING NOS			
	PROGRAM ELEMENT NO 921H06	PROJECT NO DB81EW	TASK NO	WORK UNIT NO

11. TITLE (Include Security Classification) An Analytical Study of Icing Similitude for Aircraft Engine Testing

12. PERSONAL AUTHOR(S)
Bartlett, C. Scott, Sverdrup Technology, Inc., AEDC Group

13a. TYPE OF REPORT Final	13b. TIME COVERED FROM 9/85 TO 6/86	14. DATE OF REPORT (Yr., Mo., Day) October 1986	15 PAGE COUNT 111

16. SUPPLEMENTARY NOTATION

Available in Defense Technical Information Center (DTIC).

17.	COSATI CODES		18 SUBJECT TERMS (Continue on reverse if necessary and identify by block number)
FIELD	GROUP	SUB GR	aircraft icing ice scaling icing tests
01	02		engine icing ice accretion icing environment
21	01		icing similitude ice scaling laws

19. ABSTRACT (Continue on reverse if necessary and identify by block number) An analytical study was conducted of the requirements for achieving similitude for icing as test conditions were varied. The application is aimed at engine icing tests conducted in ground spray rig facilities. The analysis considers the changes in the icing test conditions, including static temperature, static pressure, liquid water content, droplet size, and flow velocity, that are required to achieve similitude if any of the conditions are changed. The analysis uses a math model of icing scaling which has been validated by experimental data collected at the AEDC icing research tunnel. The requirements for similitude were analyzed for changes in both temperature and pressure. Expressions to describe the influence of test condition changes on the value of the scaling parameter were developed. The effect of icing caused by free-stream static temperature changes and temperature rise through a generic high-bypass turbofan engine was studied. The icing test points listed for compliance testing for aircraft icing certification under guidelines given in the Federal Aviation Administration Advisory Circular (AC) 20-73 were used as test points for the analyses.

20. DISTRIBUTION/AVAILABILITY OF ABSTRACT UNCLASSIFIED/UNLIMITED ☐ SAME AS RPT ☒ DTIC USERS ☐	21 ABSTRACT SECURITY CLASSIFICATION Unclassified	
22a. NAME OF RESPONSIBLE INDIVIDUAL William O. Cole	22b. TELEPHONE NUMBER (Include Area Code) (615) 454-7813	22c. OFFICE SYMBOL DOS

DD FORM 1473, 83 APR   EDITION OF 1 JAN 73 IS OBSOLETE

PREFACE

The work reported herein was conducted by the Arnold Engineering Development Center (AEDC), Air Force Systems Command (AFSC), at the request of the United States Department of Transportation, Federal Aviation Administration (FAA). The analytical study was conducted by Sverdrup Technology, Inc., AEDC Group, operating contractor for the propulsion test facilities at AEDC, AFSC, Arnold Air Force Station, Tennessee, under Project Number DB81EW. The Air Force Project Monitor was Mr. Carlos Tirres, AEDC/DOTR, and the FAA Contracting Officer Technical Representative was Mr. Gary Frings. The analysis was completed in April 1986 and the manuscript was submitted for publication in June 1986.

CONTENTS

ILLUSTRATIONS

TABLES

Table   Page

LIST OF ABBREVIATIONS

A   Area

AC   Advisory Circular

A_c Accumulation parameter

AEDC   Arnold Engineering Development Center

Btu   British thermal unit

b, B   Relative heat factor

c   Characteristic length

c_p Specific heat at constant pressure, Btu/lbm

C_t Concentration factor

Em   Total collection efficiency

FAA   Federal Aviation Administration

FAR   Federal Aviation Regulations

ft   Feet

g_c Universal gravitational constant, 32.174 lbm×ft/(lbf×sec)

gm   Gram

h_c Convective heat transfer coefficient, Btu/ft²/hr/°F

I   Inlet conditions

i   Enthalpy, Btu/lbm

J   Mechanical equivalent of heat, 788 ft×lbf/Btu

K	Inertia parameter
K_o	Modified inertia parameter
lbf	Pounds force
lbm	Pounds mass
LC	Leading edge characteristic length
L_f	Latent heat of fusion, Btu/lbm
LWC	Liquid water content, gm/m^3
L_v	Latent heat of vaporization, Btu/lbm
m	Mass flow rate or meters
MF	Mass fraction
min	Minutes
MMD	Mass median droplet diameter
MVD	Mean volume droplet diameter
N,n	Freezing fraction
P	Static pressure, psia
psia	Pounds per square inch, absolute
$Q_{cv,}$	Control volume heat transfer, Btu
q_k	Conductive heat transfer, Btu/lbm
q	Dynamic pressure, psia
r	Droplet radius

s   Surface length increment

sec   Seconds

T   Static temperature

t   Icing time, min

U   Flow velocity

V   Flow velocity

W   Mass flux, lbm/ft/sec

$W_{c.v.}$ Control volume work

w   Mass flow rate

Z   Elevation

SYMBOLS

β Local collection efficiency

μ Micro (10^{-6}) or absolute viscosity, $lbf \times sec/ft^2$

θ Air energy driving potential, °R

ϱ Density, lbm/ft^3

ϕ Droplet energy driving potential, °R

°F   Temperature, degrees Fahrenheit scale

°K   Temperature, degrees Kelvin scale

°R   Temperature, degrees Rankine scale

Σ	Numerical summation
$<$	Less than
$>$	Greater than
λ/λ_o	Droplet range parameter (Ref. 9)

SUBSCRIPTS

a,air	Air
cf	Compressor face conditions
d	Droplet
d_i	Particular droplet diameter, microns
e	Evaporative
i	Ice, Input
I	Inlet
k	Kelvin temperature scale
o	Baseline value, specified value
proj	Projection
r	Runback
rem	Removed
s	Static
stored	Amount stored
ST	Stream tube

sur   Surface

T   Stagnation (Total) conditions

total   Total, sum

v   Vapor

w   Liquid water

∞   Infinity (Free-stream)

EXECUTIVE SUMMARY

The formation of ice on aircraft surfaces including engines, occurs during flight through clouds of supercooled water drops. The resulting ice accretions on these surfaces can be a hazard to operational safety. For safety reasons the effectiveness of ice protection systems must be evaluated. These tests are often conducted in either ground spray facilities or ground-based altitude facilities. Ideally, the ground-based altitude facilities duplicate the flight icing conditions of temperature, pressure, air velocity, liquid water content, and water droplet size. However, the outdoor spray rigs must rely on ambient values of temperature and pressure. To test at the specified value of temperature, ground spray rigs must wait and test in the "time window" during which the desired temperature occurs. The impact on the validity of data collected on ground spray rigs which are unable to meet specified values of temperature and pressure for icing tests is not well understood.

An analytical study was conducted to determine the significance of variations in test temperature and pressure on icing testing. The study utilized an ice scaling model that has been experimentally substantiated at the Arnold Engineering Development Center (AEDC) icing research wind tunnel in a previous effort. This model predicts what changes are required in the other icing test conditions to overcome variations from the required values in temperature and pressure to achieve the same effective icing test. It was shown that for this model, if one condition was varied, all of the remaining conditions must vary. These variations are not obtainable for engine testing in ground spray facilities where the pressure and temperature are not controllable, and where the engine operating condition dictates the airflow velocity over the engine components.

The influences of changes in test conditions on similitude are addressed. A method to evaluate the influence that each individual test condition exerts on each scaling parameter is discussed. If the influence of test condition changes on the scaling parameters and a tolerance limit within which the scaling parameters must be held are known, then the range over which each test condition can be allowed to vary and still achieve icing similitude can be determined. The tolerance limit within which the scaling parameters must be held, however, is unknown and impossible to determine analytically. A follow-on effort is planned to address this issue.

This investigation also addressed various flight and engine operating points for different components within the engine as the free-stream test temperature was varied.

INTRODUCTION

BACKGROUND.

The formation of ice on aircraft surfaces including engines and induction systems occurs during flight through clouds of supercooled water drops. Ice accretion on these surfaces usually results in a degradation of both performance and operational safety. Protective techniques are normally utilized to remove accumulated ice (deicing) or continually maintain ice free surfaces (anti-icing). For safety reasons the effectiveness of these protection techniques must be evaluated before their use; therefore, each technique must be tested under conditions which closely simulate or, if possible, duplicate naturally occurring icing conditions.

There are three main techniques currently used to conduct icing tests: (1) flight testing under naturally occurring icing conditions, (2) flight testing under man-made icing conditions created by tanker aircraft, or (3) testing based on creating an icing environment in a ground test facility. Research and development testing and much component certification are accomplished by one or more of the various icing environment simulation techniques.

The Federal Aviation Administration (FAA) Advisory Circular (AC) 20-73 (Ref. 1) states that the design and design analysis of an ice protection system should be such that no combination of meterological conditions in the Federal Aviation Regulation (FAR) 25 Appendix C envelopes (Ref. 2), coupled with any engine-airplane operational envelope, will result in an accumulation of ice on any surface which will cause an unsafe operation condition. If ice protection systems have been designed as described in AC 20-73, and if the design points can be justified as most severe, testing at the design points is all that is required to show compliance with the regulations. Furthermore, all certification tests should be adequate to verify the manufacturer's icing criticality analysis and subsequent selection of critical design points.

The meterological conditions to be considered and simulated during icing tests are characterized and documented in the FAR 25 Appendix C (Ref. 2). The ranges of temperature, liquid water content, and droplet size at various altitudes for stratiform and cumuliform clouds are shown in Fig. 1. These envelopes define the maximum probable ranges of the parameters that would occur in nature (that is, 99.9 percent of the icing observations in nature are within the envelopes). As mentioned previously, every combination of the parameters represented by the envelopes, along with the mission scenario of the aircraft, should be utilized to determine the specific conditions which result in the most severe icing conditions for each aircraft or engine component. These discrete conditions become the design and test conditions for certification testing of aircraft, engine, and induction icing protection systems.

For testing purposes, the icing conditions are simulated by duplicating the principal factors that characterize a natural icing cloud: (1) air temperature, (2) water droplet size distribution (including the mean effective droplet diameter for the distribution), and (3) cloud liquid water content. Also to be considered in aircraft flight through icing clouds is the cloud extent which, along with the aircraft flight speed, result in an icing duration. Ideally, an engine icing test should duplicate the flow condition at the engine compressor face that is experienced by the engine in flight through an icing cloud. The flow condition is defined by (1) the proper static air temperature (T), (2) the proper static air pressure (P), (3) the air velocity (V), (4) the liquid water content (LWC), (5) the diameter of the water droplet, and (6) time of exposure (t).

For this report, the water droplet size is characterized by the mean volume droplet diameter (MVD). One half of the water volume (mass) lies below the MVD and one half lies above the MVD.

Flow conditions at an engine compressor face are seldom the same as flight conditions, the air having been either accelerated or decelerated from free stream before entering the engine (Fig. 2). It is necessary to relate the test flow conditions to those at the engine compressor face and not necessarily to the free-stream values. Selection of the correct test conditions to provide adequate simulations at the compressor face will depend on the icing simulation test technique used. This report will address icing condition simulation tests conducted in ground test facilities, specifically altitude test cells and ground spray rigs. Natural flight icing and tanker testing will not be discussed, although the work presented herein may apply to tanker testing. The constraints imposed by testing in either the altitude test cell or the ground spray rig will be discussed, along with problems which may be encountered during certification tests conducted in ground test facilities.

Verification testing of engine ice protection systems in icing conditions is generally accomplished in one of two ways:

1. Tests are conducted in a facility capable of simulating altitude conditions and using an artificially produced icing cloud.

2. Tests are conducted in a sea level or ground level facility with an artificially produced icing cloud.

Engine manufacturers presently utilize both methods to demonstrate compliance with the FAA regulations.

For the altitude facility, two separate techniques may be employed for icing tests direct connect or free jet. The entire test cell flow is seen by the engine compressor face in the direct connect test (Fig. 3a). The selection of the proper flow conditions to achieve adequate icing simulation for direct connect testing is addressed in Refs. 3 and 4. For testing in a free-jet mode, the velocity of the flow will reach the compressor face as it would during flight through a natural icing cloud (Fig. 3b). The test cell conditions should be set to the actual free-stream (flight) conditions of the natural cloud when testing in the free-jet mode.

Ground spray rigs (Figs. 3c and 3d) can be categorized as either indoor or outdoor rigs, and the spray cloud can be either fan blown or wind blown. Since the altitude pressure of ground spray rigs cannot be varied, studies of altitude pressure effects on ice accretion should be accomplished through ice scaling. Usually the values of the other conditions defining an icing environment are varied to compensate for altitude pressure mismatch. A comprehensive analysis of the scaling technique is given in Ref. 5. The outdoor ground spray facilities rely on ambient temperature for testing. Tests must be accomplished in the "time window" during which the desired temperature occurs. Since all systems including test article, instrumentation, facility, and support personnel must be on standby, any delay in achieving the desired temperature may increase test costs significantly. One question that is frequently asked during these tests is how much the actual temperature can differ from the desired temperature and still achieve adequate simulation of the desired icing environment.

PURPOSE.

The purpose of this report is to utilize the icing scaling equations to investigate engine icing certification testing and to provide, if possible, ways to aid the certification process. Specifically, this report will address three topics:

1. Expansion of the "test window" for ground spray rigs through applications of icing similitude.

2. Identification of areas of concern in the determination of critical engine icing conditions, including which engine locations should be considered most critical.

3. Provide guidance for the use of altitude facilities to simulate altitude pressures which may have been found to contribute to a severe icing condition during the engine icing test design point analysis, to study the effects of altitude pressure on icing severity, and to look at test techniques that can be utilized to overcome the altitude pressure mismatch that may be experienced on ground spray rigs.

Investigation of these topics will provide a technical background of the sensitivity of icing test results to mismatches between available test conditions and those found to be most severe during the engine and flight scenario analysis.

This knowledge will be useful in judging the impact of conducting an icing test at available test temperatures. Also, such knowledge will be useful in judging the applicability of other test techniques utilized to overcome the mismatches that occur during ground spray rig tests.

SCOPE.

The investigations reported herein are analytical in nature and utilize computerized math models of the ice scaling process. The models have been validated experimentally at AEDC. A comprehensive analysis of the scaling technique is given in Ref. 5, along with results from the experimental verification. In general, the scaling code was developed for unheated surfaces only. (Highlights and example cases of the technique are included in Appendix A.) The code will be used to investigate means of overcoming mismatches in temperature and pressure on ground spray rigs.

The icing test conditions serve as inputs to the similitude code. The code calculates the values of the five different scaling parameters, and then calculates the test conditions required to hold the value of each of the scaling parameters constant for a change in any one of the test conditions. The code was used to determine what condition tradeoffs, called parameter substitutions, were required to achieve the same icing test point (icing criticality) for variations in temperature and/or pressure. Additionally, the code was used to calculate the value of the ice scaling parameters and to determine the sensitivity of those scaling parameters to changes in any of the icing condition variables in an icing test.

REPORT OUTLINE.

This report is organized as follows: first, the problems frequently encountered during icing certification testing are discussed, then approaches to overcome these problems are discussed. The icing points of AC 20-73 which are used as acceptable points for compliance testing will be used as example test conditions for analytical evaluation. Test conditions where the airplane flight Mach number equals the engine inlet Mach number are considered. The requirements to ensure exact similitude (exact equality of the scaling parameters) as the test conditions are changed were studied. The effect that different collection surfaces have on the similitude requirements is discussed. The investigation also addressed the effect which temperature

mismatches have on exact equality of the scaling parameters and the interrelationships which changes in liquid water content and mean volume droplet diameter exhibit as a result of temperature mismatches.

The effect a change in temperature has on various components within the engine at various flight conditions such as ground idle and sea-level cruise was studied. The effect of temperature rise through the engine and the effect of free-stream temperature changes on the icing characteristics and icing criticality of various components through the engine is explained.

The effect altitude pressure changes have on ice scaling was investigated by evaluating the sensitivity of the similitude parameters to changes in static pressure. Finally, a direct comparison of tests at sea level and at altitude was made to determine what conditions must be changed to achieve exact equality of the scaling parameters between sea level and altitude icing tests.

DISCUSSION

EFFECT OF TEMPERATURE ON SIMILITUDE REQUIREMENTS.

A review of present FAA aircraft engine icing certification tests showed that a major area of concern and the most troublesome was that of meeting the test temperature specified as most severe by the icing design point analysis. This situation occurs frequently in ground spray rigs where no control of the temperature is available, and, in many cases, much time and money are spent waiting for the "test window" during which the desired temperature is available. Numerous proposals have been offered such as changing liquid water content, mean volume droplet diameter, or increasing the icing test duration to cancel effects of temperature mismatch and thereby achieve the same or more severe icing test. However, none of the proposals have been validated experimentally.

In this investigation the scaling code was used to determine the changes in the test conditions that are required to achieve exact equality of the scaling parameters between test points if the static test temperature could not be met. AC 20-73 has three test points normally used as acceptable means of compliance in the FAA icing certification process. These values are shown in Table 1. The revised AC 20-73 now specifies a range of conditions for test point 3. The conditions used in this report were selected to match the test points most frequently used in certification work. These points were used as baseline test conditions for analysis of test temperature mismatches.

To ensure "exact similitude" under different icing conditions, the values of the ice scaling parameters must be maintained. The scaling parameters to be maintained are:

1. K_o, the modified inertia parameter

   K_o is a term describing the affinity of an obstruction in a flow path to collect droplets entrained in that flow path. The larger the value of K_o, the more affinity a body has to collect drops.

2. A_c, the accumulation parameter

   A_c is a water catch term relating the LWC, V, icing time, and collection efficiency terms to a rate of water catch for a particular collection surface. It is not an ice collection term if no accounting has been made for changes in the collection surface attributable to ice formation.

3. N, the freezing fraction

   N is defined as the amount of impinging liquid water that freezes on impact with the collection surface. When N is zero, none of the impinging liquid will freeze on impact. When N is one, all of the impinging liquid will freeze on impact (rime ice).

4. ϕ, the water droplet energy driving potential

   ϕ is a measure of the energy transfer potential of the liquid droplets impinging on an icing surface. It is the total enthalpy of the droplets ratioed to the specific heat of the droplets.

5. θ, the air energy driving potential

   θ is a term describing the heat transfer potential of the air passing over an icing surface. It is formulated by the convective heat transfer term plus the product of the rate of evaporative mass flux and the latent heat of vaporization, all divided by the convective heat transfer coefficient. If θ is negative, there is probably not sufficient heat transfer to freeze the impinging liquid.

It should be understood that maintaining all five of these scaling parameters at some given value has been shown sufficient to ensure exact icing similitude for certain geometries in the AEDC icing tunnel (Ref. 5), but it is not known if maintaining all of these is necessary for similitude. It also is not known how much any one of these parameters may vary from its designated value before affecting similitude. In data in Ref. 5 a 10-percent variation in the ice shape can be considered sufficient for similitude as determined by repeatability of the tunnel.

The icing similitude code, used here as an analytical tool, was written to solve a set of scaling equations while maintaining the values of the scaling parameters. The icing test variables that must be determined from these equations are as follows (Ref. 5):

1. Air velocity

2. Static pressure

3. Static temperature

4. Liquid water content

5. Mean volume droplet diameter

6. Icing time

It should be noted that there are six icing test variables but only five scaling parameters (equations) available. This indicates that the problem is underspecified and that any one of the test variables can be arbitrarily selected to be varied. The selection of this variable should be made to overcome a mismatch in existing and required test conditions. For this study, test temperature will be the variable selected. This allows examination of the requirements necessary to achieve exact equality of the scaling parameters when the available test temperature is not the design test point temperature.

For clarity, it should be understood that the velocity term refers specifically to the velocity of the airflow over a particular object in the icing cloud. It is not the velocity of the airplane. The velocity of air flow over any engine component may vary depending on the location within the engine or engine inlet and the particular engine operating point.

During icing certification tests in ground spray rigs, the most difficult of the AC 20-73 test points to meet from a temperature standpoint is the −4°F condition. This point was the first analyzed. For simplicity the icing test point was chosen so that the airplane flight Mach number and the engine compressor face Mach number are equal, and a value of Mach = 0.2 was chosen as typical. At a static temperature of −4°F this corresponds to an air velocity of ~200 ft/sec. Choosing equal airplane and inlet Mach numbers indicates that no spilling or gulping of the air by the engine occurs, thus creating a more easily analyzed case where free-stream icing conditions are equal to the compressor face icing conditions.

A specific icing surface must be selected to determine the "exact similitude" requirements. The collection surfaces chosen were: (1) an NACA 0012 airfoil with 6.0-in. chord and 0.19-in. leading edge diameter at 0-deg angle of attack, approximating a fan stator, (2) a 10.0-in.-diam sphere, approximating a bullet nose spinner, and (3) a 1.0-in.-diam cylinder, normal to the flow, approximating an instrumentation probe. These different collection surfaces showed the influence of collection surface geometry on the similitude requirements. An icing condition not yet specified must be arbitrarily chosen. A static pressure of 14.2 psia is chosen to represent a ground spray rig at approximately 1,000 ft altitude. The icing time will be chosen as 1 min. A summary of the six icing test conditions follows:

Velocity: 200 ft/sec
Static pressure: 14.2 psia
Static temperature: $-4°F$
Liquid water content: 1.0 gram/m^3
Mean volume droplet diameter: 15 μm
Icing time: 1.0 min

These conditions are for AC 20-73 test point 1. Depending on which of the three AC 20-73 points is under study, the static test temperature (T), the liquid water content (LWC), and the droplet size (MVD) will change accordingly.

The code utilized in this investigation in its present form allows only velocity to be the test condition parameter which can be varied. Simple cross plotting allows the code to be used to vary the other test condition parameters. The changes in the test condition parameters required to achieve exact equality of the scaling parameters at various temperatures for the NACA 0012 airfoil are shown in Table 2. Figure 4 is a graphical representation of the values that each of the test condition parameters must assume to achieve exact equality of the scaling parameters as the static temperature is changed. It shows these requirements for all three of the collection surfaces (airfoil, sphere, and cylinder). When reviewing the figure, remember that all of the test condition parameters must change according to the curves. Changing less than all of the conditions will not achieve exact equality of the scaling parameters. For example, if AC 20-73 point 1 is used (where T = -4°F is specified) to achieve similitude for the NACA 0012 airfoil as T is raised to $-3.5°F$, the pressure must rise to 18.4 psia, the velocity must decrease to 112 ft/sec, the liquid water content must rise to 1.52 gm/m^3, the MVD must increase to 19.9 μm, and the icing time must increase to 1.18 min. All of these values must be satisfied to achieve exact equality of the scaling parameters.

Similar analyses were conducted for the remaining two test points by using test temperature, liquid water content, and droplet diameter as specified in the AC 20-73 points 2 and 3 (Table 1). Results of the analyses for the 23°F and 29°F test points using the NACA 0012 airfoil are shown in Tables 3 and 4, respectively. Figures 5 and 6 show graphical representations of the similitude requirements for test points 2 and 3, respectively, for the three collection surfaces. The calculated values of the scaling parameters are also listed in the tables.

As the value of temperature rises above the specified value, the value of static pressure rises above the ambient value, sometimes quite drastically, as does the required LWC, MVD, and icing time (t). The velocity of the airstream approaching the icing surface must decrease. It should be noted that all points listed in Tables 2, 3, and 4 are below the dynamic pressure (q) value of 1.6 which Ruff utilized as an upper limit on scaling velocity (Ref. 5). However, some points do fall outside the range of parameter variations that have been validated experimentally. A table of the ranges of test parameters investigated in Ref. 5 is reproduced in Table 5.

Specifying one test condition parameter results in changes of the remaining parameters to obtain exact solution to the scaling equations. This observation follows from the nature of the problem which, as mentioned previously, allows only one variable to be specified. The functional dependencies of each scaling parameter to the test condition variables are given in Table 6. The observation that all of the test conditions must change if the temperature changes should present no problem in the event that all of the variables are controllable. This is rarely the case in engine testing. When tests are performed on ground spray rigs, the pressure is an uncontrollable variable which assumes the value of the ambient pressure. The velocity of airflow across the engine components is largely dictated by the air density (strongly proportional to pressure) and the engine operating point. Therefore, the pressure and velocity represent two uncontrollable variables. To achieve exact equality of the scaling parameters requires all of the test conditions to vary and since velocity and pressure cannot be varied in a controlled way, it is not possible to achieve exact similitude on ground spray rigs if a temperature mismatch exists.

The conclusion reached here is that exact equality of the scaling parameters is not possible unless all of the six test condition parameters are forced to vary in a controlled way. This is not to imply that effective icing tests cannot be conducted on ground spray rigs. Past experience shows that effective tests are conducted on ground spray rigs. It does mean that all six of the test variables must be controlled to obtain exact solutions to the energy and mass balance equations which are based on a stagnation line analysis of the collection surface. It is not known how closely the test variables must be held to the values required by the

stagnation line analysis to obtain sufficient similitude. Quantative data are required to make that judgement. An effort is underway to address this issue.

The effect of the geometry of the icing surface on similitude requirements is shown in Figs. 4, 5, and 6; these figures indicate that differences in the similitude requirements exist for different collection surfaces. This points out that a change in a test condition which ensures exact equality of the scaling parameters for a particular icing surface does not necessarily ensure exact equality of the scaling parameters for another surface exposed to the same test conditions. No effect of hub rotation has been included in this anlaysis.

SENSITIVITY OF THE SCALING PARAMETERS TO TEST CONDITION CHANGES.

The preceding analyses showed that exact quality of the scaling parameters is not possible unless all of the six test condition parameters are forced to vary in a controlled way. It may, therefore, be asked how much effect on the scaling parameters a variation in test temperature has. A sensitivity analysis indicates what effect a change in any one of the test conditions has on the value of each of the five scaling parameters. To conduct such an analysis it is necessary to understand the functional relationship of each scaling parameter to the test conditions.

For tests conducted on a ground spray rig, the pressure is an uncontrollable variable and equal in value to the existing ambient pressure. The velocity over each collection surface in the engine is largely dictated by the prevailing pressure and the engine operating point. For a particular collection surface the geometry is invariant. This leaves LWC, MVD, and t as the variable test conditions. By investigation of the icing scaling parameters (Table 6), one sees that only the accumulation parameter, A_c, is a function of time.

$$A_c = \frac{LWC \; \beta \; Vt}{\varrho_i \; c}$$

Assume the ice density (ϱ_i) is constant between test conditions. Knowing that collection efficiency (β) is a function of only droplet size for a constant pressure and that flow velocity (V) and body geometry (c) are not variable, the equation is seen to be a function of only liquid water content, droplet size, and time:

$$A_c = f(LWC, MVD, t)$$

By specifying that the body geometry does not change, the A_c term is descriptive only of water catch and cannot be used as an ice collection term. This is because any accumulation of ice will change the geometry of the collection surface and thus its collection characteristics.

25

Since t appears explicitly in the formulation of A_c, any changes in A_c attributable to changes in LWC or MVD can be offset by variations in time. This must be done to maintain water catch similitude. Throughout this report A_c was evaluated at a reference time arbritrarily chosen as $t = 1.0$ min. This allows the water catch to be calculated easily for any cloud exposure time desired. Since t is an easily controllable variable for ground test facilities, and since the only scaling parameter in which t appears is the A_c, the A_c term may be temporarily disregarded from the analysis and the problem encountered on ground spray rigs is simplified to one of determining the effect that changes in LWC, MVD, and test temperature (T) have on the scaling parameters. Once the values of LWC and MVD are known, determined by the remaining four scaling parameters, the time can be chosen to yield the required water catch. The relationship of A_c to changes in LWC and MVD are presented in the following analysis.

Again the test points specified in AC 20-73 will be utilized for analysis.

The functional relationships of each of the scaling parameters to each of the test conditions of LWC, MVD, and T were studied. The AC 20-73 test points (Table 1) were used as baseline test conditions from which changes were made in LWC, MVD, and T. The ice scaling code was used to calculate the value of each scaling parameter as LWC, T, or MVD were varied. By knowing the functional relationship of each of the scaling parameters to changes in T, LWC, or MVD, expressions for the sensitivity of each scaling parameter to a change in T, LWC, or MVD can be developed. The same flight condition (flight Mach number equal to compressor inlet Mach number) and icing test conditions as used in the analysis of similitude requirements were used here. The 6-in. chord NACA 0012 airfoil was used as the ice collection surface. The ranges over which each of these variables was allowed to vary are as follows:

$$-10°F \leq T \leq 29°F$$
$$0.2 \text{ gm/m}^3 \leq LWC \leq 3.0 \text{ gm/m}^3$$
$$10 \text{ } \mu m \leq MVD \leq 60 \text{ } \mu m$$

These ranges were arbitrarily selected to demonstrate the effect that the test variables, T, LWC, and MVD have on the calculated values of the scaling parameters. Recall that the scaling parameters are mathematical expressions describing the mass and energy balances at the stagnation line of a collection surface. Although application of the scaling parameters has been validated over a limited range of conditions (Ref. 5 and Table 5), mathematical solutions to the equations themselves are valid over any range desired. The values of the scaling parameters were calculated for discrete points within the ranges and the results were put into graphical form in Figs. 7 - 11.

The analysis was carried out for each of the three test points from AC 20-73. When reviewing the graphs, the reader should remember that during the analysis all icing test conditions were held constant and only one of the three test variables (T, LWC, or MVD) was varied, as shown by the abscissa for each plot. The scaling parameters themselves may or may not be functions of all these variables (see Table 6). The scaling parameters are shown plotted against only those variables, (T, LWC, or MVD) of which they are functionally dependent.

Figure 7 shows that the value of modified inertia parameter (K_o) is a strong function of drop size.

Figure 8 shows that the value of freezing fraction (N) is a function of LWC, T, and MVD at some point within the range of parameter variations. The effect of LWC is seen to be almost asymptotic at the lower values of LWC as the value of N approaches unity. As T is raised, the value of N drops towards zero. At N = 0, none of the impinging water will freeze on impact. Freezing fraction is only slightly affected by droplet size (MVD). It is also worthy of note that lower LWC, lower T, and smaller MVD all tend to cause the freezing fraction to rise, and that once N = 1.0 (rime ice) further reductions in the values do not change the value of N.

In Fig. 9 the air energy driving potential (θ) is also seen to be a function of LWC, T, and MVD. Here it is interesting to note that there seems to be an upper limit on the value of θ and that limit is a function of T. As the values of LWC and MVD are raised toward the limit where freezing fraction falls below a value of unity, this upper limit is met. This occurs at approximately LWC = 1.6 gm/m^3 for AC 20-73 point 1 in Fig. 9. This indicates that once the LWC, MVD, or T is raised to a point where N < 1.0, θ becomes a function of T only.

The droplet energy driving potential (ϕ) is seen in Fig. 10 to be a function of T only and is linear in nature. No effect of body geometry or any other test condition except velocity is experienced.

The value of the accumulation parameter (A_c) ratioed to time (t) is shown in Fig. 11. A_c is seen to be a strong function of LWC and weakly affected by MVD which shows up in the collection efficiency term of A_c. The influence which drop size has on the A_c is reduced when the drop size increases and the collection efficiency approaches a value of unity.

Figures 7 - 11 show that for a given change in T, LWC, or MVD the relative influence on any of the scaling parameters may be different, depending on which of the AC 20-73 points is under study. To better explain this influence, the percentage change in each scaling parameter as a function of changes in either T, LWC, or MVD will be analyzed.

The percentage change in each scaling parameter as a function of changes in either T, LWC, or MVD is shown in Figs. 12 - 17. The percentage change is defined as the value of the parameter less the value of that parameter at the specified test point divided by the specified value and multiplied by one hundred to yield percentage. The difference of T, LWC, or MVD from the specified values (T_o, LWC_o, or MVD_o) is termed ΔT, ΔLWC, or ΔMVD. For example, the value of freezing fraction at the specified condition for AC 20-73 test point 2 (23°F) is N_o = 0.18 and T_o = 23°F. If the test were conducted at a temperature of 20°F, the value of N is calculated to be N = 0.25, and the change in N is:

$$\Delta N = 0.25 - 0.18 = + 0.07$$

The percentage change in N is:

$$\frac{\Delta N}{N_o} \times 100 = \frac{0.07}{0.18} \times 100 = 38.9\%$$

The change in test temperature (T) is given by

$$\Delta T = 20°F - 23°F = -3°F$$

Thus, a ΔT of 3 degrees results in a 39-percent change in freezing fraction.

Since the modified inertia parameter is unaffected by ΔLWC or by ΔT the percentage change is given for changes in MVD only. The curves of Fig. 12 are for three sizes of MVD: 15, 25, and 40 μm. If one were to plot $\Delta MVD/MVD_o$ on the abscissa, the curve would collapse and can be well represented by a single curve (Fig. 13). This shows that for a given ΔMVD, the percentage change is dependent only on whether the value of MVD_o is 15, 25, or 40 μm.

The percentage changes in freezing fraction (N) attributable to ΔT, ΔLWC, and ΔMVD are shown in Fig. 14. Figure 14a shows that there is no change in N over the range of ΔT for AC 20-73 point 1, but there are significant changes for AC 20-73 points 2 and 3. This is illustrated with a simple example. Suppose a value of ΔT = 1°F. For point 1 at ΔT = 1.0°F, the value of N = 1.0. Therefore, there is no change in the value of N. In fact, there is no change until N drops below 1.0, and this does not happen until T $\cong$ 7°F (ΔT = 11°F). For point 2 at ΔT = 1.0°F, there is a 12-percent reduction in N while for point 3 at ΔT = 1.0°F, there is a 79-percent reduction in N. It is obvious from this figure that as the value of N drops below unity and approaches zero, the effect of temperature changes grows increasingly significant. As LWC is decreased the value of N rises toward unity (Fig. 8). As LWC is dropped

to the point that N approaches unity, further reductions in LWC have no effect on N (Fig. 14b). At a value of $\Delta LWC = +0.5$ gm/m^3, there is no change in the value of N for point 1. $\Delta LWC = +0.5$ gm/m^3 causes a 10-percent reduction in N for point 2, and a 52-percent reduction in N for point 3. As seen in Fig. 14c the change in N attributable to ΔMVD is quite pronounced as MVD is reduced, but the effect lessens as MVD is increased. There is no change for a reduction in MVD once $N = 1$ is reached (as seen for point 1 in Fig. 14c.).

The percentage of change in the droplet energy driving potential (ϕ), is seen in Fig. 15. It is plotted for ΔT only since it is not a function of ΔLWC or ΔMVD. Since ϕ is a linear function of T, the value of ϕ is directly proportional to ΔT. For a given ΔT, the value of $\Delta\phi$ is fixed. The divergence of the curves in Fig. 15 is explained by the fact that for a given ΔT, thus $\Delta\phi$, the value of ϕ_0 in the $\Delta\phi/\phi_0$ term is different, depending on which value of T_0 was used to calculate ϕ.

The effect of both LWC and T on the value of the air energy driving potential (θ) is quite dependent on whether the value of N is less than or equal to unity (see Fig. 9).

When the value of N is unity, the effect of ΔT on $\Delta\theta/\theta_0$ is slight and positive in slope as compared to the effect when N is less than unity where the slope of $\Delta\theta/\theta_0$ ratioed to ΔT is steep and in the negative direction as seen in Fig. 16a. As discussed previously, when N is less than unity, the value of θ is a function of T only and the lines of Fig. 16a for AC 20-73 points 2 and 3 have different slopes only because of the different values of T_0 and hence different values of θ_0.

The breaking point of the curves of $\Delta\theta/\theta_0$ versus ΔLWC of Fig. 16b are determined by the value of N. As the value of LWC is increased to the point where N drops below unity, the value of θ is no longer affected by changes in LWC (Figs. 8 and 9) but by T only. This is reflected in the $\Delta\theta/\theta_0$ versus ΔLWC plot of Fig. 16b. Thus θ is quite sensitive to ΔLWC and large changes are observed for small changes in ΔLWC. The sensitivity of θ to ΔLWC exists until LWC is raised to a point where N is less than unity at which point $\Delta\theta/\theta_0$ is no longer affected by increases in LWC.

Similarly, $\Delta\theta/\theta_0$ versus ΔMVD is affected by the value of N. Figure 16c shows that the value of θ is shown to increase as MVD is increased up to the point where N less than unity is reached; thereafter, further increases in ΔMVD do not affect $\Delta\theta/\theta_0$.

Figure 17a shows that the accumulation parameter, A_c, is a strong function of ΔLWC. Figure 11 showed the value of A_c as being nearly a linear function of LWC for all three of the AC 20-73 test points, and that approximately the same ΔA_c is calculated for a given ΔLWC

29

for each of the three curves. Hence, for a given ΔLWC, the value of $\Delta A_c/A_{c_0}$ will be larger for small values of A_{c_0}. This is shown in Fig. 17a where A_{c_0} for test point 1 is calculated at $LWC_0 = 1.0$ gm/m^3, 2.0 gm/m^3 for test point 2, and 0.3 gm/m^3 for test point 3. Figure 17b shows the effect of ΔMVD on A_c and it is seen that the influence of ΔMVD is reduced at higher values of ΔMVD. This is due primarily to the leveling of the collection efficiency term which approaches unity for larger drops. Once the collection efficiency reaches unity, all of the water in the icing cloud that can be intercepted by the ice collection surface is collected. Further increases in the droplet size cannot increase collection efficiency past unity, hence A_c is no longer affected by droplet size increase.

It is obvious from these discussions that the relationship of the scaling parameters to the test condition parameters of T, LWC, and MVD (Figs. 7 - 11) is important in understanding the percent change in the scaling parameter due to ΔT, ΔLWC, and ΔMVD (Figs. 12 - 17).

To determine the combined effects which changes in the test conditions have on each of the scaling parameters, an error analysis (Ref. 6) was performed. In this analysis the similitude parameters were expanded as functions of their independent variables, the test conditions. From these expansions the changes in each scaling parameter were determined for small changes in the independent variables.

Generally, the change in value of a parameter can be expressed as a function of its independent variables. A function, f, of several independent variables can be represented by a Taylor series expansion

$$\Delta f = \frac{\delta f}{\delta X_1} \Delta X_1 + \frac{\delta f}{\delta X_2} \Delta X_2 + \frac{\delta f}{\delta X_3} \Delta X_3 + \ldots + \frac{\delta f}{\delta X_n} \Delta X_n$$

where the partial derivatives are evaluated at known values of X. If ΔX is small, second-order effects can be ignored as was done in the above expansion (Ref. 6).

In a like manner the similitude parameters are expanded as follows:

Modified inertia parameter, K_0

$$\Delta K_0 = \frac{\delta K_0}{\delta T} \Delta T + \frac{\delta K_0}{\delta LWC} \Delta LWC + \frac{\delta K_0}{\delta MVD} \Delta MVD$$

Freezing fraction, N

$$\Delta N = \frac{\delta N}{\delta T} \Delta T + \frac{\delta N}{\delta LWC} \Delta LWC + \frac{\delta N}{\delta MVD} \Delta MVD$$

Droplet driving potential, ϕ

$$\Delta \phi = \frac{\delta \phi}{\delta T} \Delta T + \frac{\delta \phi}{\delta LWC} \Delta LWC + \frac{\delta \phi}{\delta MVD} \Delta MVD$$

Air driving potential, θ

$$\Delta \theta = \frac{\delta \theta}{\delta T} \Delta T + \frac{\delta \theta}{\delta LWC} \Delta LWC + \frac{\delta \theta}{\delta MVD} \Delta MVD$$

Accumulation parameter, A_c

$$\Delta A_c = \frac{\delta A_c}{\delta T} \Delta T + \frac{\delta A_c}{\delta LWC} \Delta LWC + \frac{\delta A_c}{\delta MVD} \Delta MVD$$

To evaluate the effect of changes in the independent parameters of ΔT, ΔLWC, and ΔMVD on the scaling parameters for the three AC 20-73 test points, the values of the partial differentials were evaluated from Figs. 7 - 11. The curves in these figures represent the change in one scaling parameter as one of the independent variables was changed. Thus, the slope of the curves at any point represents the partial derivative of the function which describes the scaling parameter. The test conditions are the same as for all previous examples utilizing the NACA 0012 airfoil at a static pressure of 14.2 psia and an air velocity of 200 ft/sec. Some terms in the expansion equations will drop out if the slope of the curve is zero. The following expansions for each scaling parameter were obtained.

For AC 20-73 point 1:

ΔK_o	=	$+0.02\Delta MVD$
ΔN	=	no effect due to ΔT, ΔLWC, or ΔMVD
$\Delta \phi$	=	$-1.0\Delta T$
$\Delta \theta$	=	$+0.225\Delta T + 27.0\Delta LWC + 0.57\Delta MVD$
ΔA_c	=	$+0.021\Delta LWC + 0.0003\Delta MVD$

AEDC-TR-86-26

For AC 20-73 point 2:

$$\Delta K_o = +0.02\Delta MVD$$
$$\Delta N = -0.025\Delta T - 0.073\Delta LWC - 0.0015\Delta MVD$$
$$\Delta\phi = -1.0\Delta T$$
$$\Delta\theta = -1.44\Delta T$$
$$\Delta A_c = +0.023\Delta LWC + 0.0003\Delta MVD$$

For AC 20-73 point 3:

$$\Delta K_o = +0.02\Delta MVD$$
$$\Delta N = -0.18\Delta T - 0.172\Delta LWC - 0.0005\Delta MVD$$
$$\Delta\phi = -1.0\Delta T$$
$$\Delta\theta = -1.55\Delta T$$
$$\Delta A_c = +0.024\Delta LWC + 0.00005\Delta MVD$$

The reader should recall that these equations are valid only over ranges where the second-order terms of the Taylor series expansion are negligible.

Neglecting terms within these expansions which are an order of magnitude smaller than the others, the test condition changes that most strongly influence the value of the scaling parameters can be seen. Neglecting these terms, the expansions reduce to the following

For AC 20-73 point 1:

$$\Delta K_o = +0.02\Delta MVD$$
$$\Delta N = \text{no effect due to } \Delta T, \Delta LWC, \text{ or } \Delta MVD$$
$$\Delta\phi = -1.0\Delta T$$
$$\Delta\theta = +27\Delta LWC$$
$$\Delta A_c = +0.021\Delta LWC$$

For AC 20-73 point 2:

$$\Delta K_o = +0.02\Delta MVD$$
$$\Delta N = -0.025\Delta T - 0.073\Delta LWC$$
$$\Delta\phi = -1.0\Delta T$$
$$\Delta\theta = -1.44\Delta T$$
$$\Delta A_c = +0.023\Delta LWC$$

For AC 20-73 point 3:

$$\Delta K_o = +0.02\Delta MVD$$
$$\Delta N = -0.18\Delta T - 0.172\Delta LWC$$
$$\Delta\phi = -1.0\Delta T$$
$$\Delta\theta = -1.55\Delta T$$
$$\Delta A_c = +0.024\Delta LWC$$

It is seen in these expressions that if T, LWC, or MVD is allowed to vary from the specified point, at least one of the scaling parameters will change in value. Further, if a change in T occurs, no change in LWC or MVD will compensate for it. For example, for test point 2, if $\Delta T = +1.0°F$, N will be changed by $\Delta N = -0.025$. To compensate for this change, LWC can be changed by $\Delta LWC = -0.342$ gm/m^3. Now $\Delta N = 0.025 + 0.025 = 0$, but $\Delta\phi = -1.0°R$ $\Delta\theta = -1.44°R$, and $\Delta A_c = -0.008$.

If the scaling parameters are allowed to vary within some tolerance band, some deviations from test condition temperature can be offset by changes in LWC and MVD. For example, for AC 20-73 point 1, the deviation allowable for each scaling parameter will be arbritarily set at ±10 percent. For this particular test condition this relates to the following actual tolerances in the scaling parameters and the resulting deviations in test conditions:

$$\Delta K_o = \pm 0.01 \rightarrow \Delta MVD = \pm 0.5 \ \mu m$$
$$\Delta N = -0.10 \rightarrow N/A$$
$$\Delta\phi = \pm 3.5 \rightarrow \Delta T = \pm 3.5°F$$
$$\Delta\theta = \pm 3.1 \rightarrow \Delta LWC = \pm 0.11 \ \text{gm/m}^3$$
$$\Delta A_c = \pm 0.002 \rightarrow \Delta LWC = \pm 0.10 \ \text{gm/m}^3$$

Using the most restrictive of these yields, the following allowable tolerance to keep the scaling parameters within ± 10 percent of those values required for "exact similitude" for AC 20-73 point 1 is as follows:

$$\Delta T = \pm 3.5°F$$
$$\Delta LWC = \pm 0.10 \ \text{gm/m}^3$$
$$\Delta MVD = \pm 0.5 \ \mu m$$

ALLOWABLE TOLERANCES IN TEST CONDITIONS.

It was arbitrarily decided in the previous example to let the scaling parameters vary by ± 10 percent. What effect would a 10-percent change in K_o, N, θ, ϕ, or A_c have on similarity? Would a 10-percent change in K_o be insignificant while a 10-percent change in θ would be significant? If this question could be answered, then the expansions relating the test conditions to the scaling parameters could be used to determine an acceptable tolerance range within which each test condition could be held to achieve acceptable similitude. It is reasonable to assume that the significance of each scaling parameter will not be the same. The ability to eliminate one or more of the scaling parameters, if it were insignificant in maintaining similitude, would, of course, relax constraints on the necessity to hold test conditions within tight tolerances.

With the knowledge now at hand, it is impossible to answer these questions of significance for the scaling parameters, and thus it is impossible to define tolerance limits for the test conditions. A summary of past ice scaling investigations and the combinations of scaling parameters proposed by each is shown in Table 7. It is obvious that all possible combinations have not been tried. The questions concerning the significance of each scaling parameter in similitude studies would be best answered with experimental data gathered under test conditions well controlled to illustrate that information. Some guidelines then may be given to specify what test condition tolerances are allowed and the implications of deviations from those tolerances.

TEMPERATURE EFFECTS ON ICING AT VARIOUS ENGINE COMPONENTS.

The preceding analyses were performed at specific points from the AC 20-73 and at flight conditions where free-stream values of T, LWC, MVD, and P were the same as those experienced by an ice collection surface. An analysis of the effects of temperature changes on each scaling parameter for various engine components was performed to identify the influence which temperature mismatches have on engine components susceptible to icing. This type of analysis will aid in the determination of which engine components should be considered critical during an icing encounter. Both the effects of free-stream temperature change and of temperature rise through the engine should be included in the analysis. To properly study the influence which flight and engine operations have on the LWC and MVD on various components within the engine, the behavior of icing clouds as they are ingested by the engine (including water ingestion, LWC and MVD changes due to component blockage and droplet impingement, and ice accumulation characteristics) was included in the analysis.

A math model was used to predict the icing conditions which exist at various component such as fan stators, compressor blades, splitters, and probes within an engine. This model was used to predict the icing conditions at each engine component by considering the flight speed, the free-stream conditions, and the engine operating point. The model was based on a generic high-bypass turbofan engine in the 30,000-pound-thrust class. A sketch of the engine geometry with pertinent component callouts is shown in Fig. 18. The engine has an inlet with constant duct area leading to the fan. The static temperatures and static pressures through the inlet, fan, and fan stators were modeled with a computer program from data available at the AEDC. Water ingestion analysis was added to this unpublished computer model and was based on work similar to that discussed in Ref. 5 and Appendix B. The static conditions from the engine inlet cowl to the fan face were arbritrarily assumed constant, as were the static conditions aft of the fan leading to an instrumentation probe and the fan exit guide vanes. The LWC and MVD are assumed uniform across the component under consideration. This assumption has limited validity depending on the application. The fan was modeled at two locations, the fan root and the fan tip. The fan blade velocity of approach was calculated as the resultant of angular velocity of the blades and the axial component attributable to airflow.

The icing conditions calculated by the engine model for each component were used as inputs to the ice scaling model. In this way the scaling parameters for each component at each icing condition were calculated and the changes in the scaling parameters due to changes in the free-stream test temperature were analyzed.

The ice scaling model uses only simple geometries for which extensive data such as collection characteristics and heat transfer coefficients are available. This limitation forces the actual collection surfaces in the engine to be modeled by simple geometries. Table 8 gives a listing of the engine components and the simple geometries used to model them. The characteristic length (c) is the diameter for the spherical and cylindrical components and the leading edge diameter for the airfoil components.

The extent of possible icing through the engine can be judged by the values of N and θ at each component. If N is very close to zero, none of the impinging water will freeze, and if θ is negative there is not sufficient energy transfer to cause the drops to freeze on the collection surface.

Ground idle (GI) and 50-percent maximum continuous thrust (0.5 MCT) were the two engine operational points used to analyze the effect of temperature changes on the scaling parameters. The flight conditions chosen to match these engine operation points were sea-level-static for GI and 0.4 flight Mach number for the 0.5 MCT point. Baseline free-stream

icing conditions of T = -4°F, LWC = 1.0 gm/m³, and MVD=15 μm are used as specified in the AC 20-73 point 1.

The results of the model analyses are shown in Table 9 for the GI flight points, and in Table 10 for the 0.5 MCT points.

Tables 9 and 10 list the values of the icing test conditions for each component as the value of free-stream static temperature is varied. Also shown are the values of the scaling parameters for each icing condition at each component. As shown previously, only θ, ϕ, and N are significantly affected by changes in T.

The important influence of free-stream temperature change can be seen by investigation of Table 10 which shows that at $T_\infty = -4°F$, icing conditions exist (positive values of θ) at the cowl, spinner, and fan root only. As T_∞ is raised to +6°F, the value of θ at the fan root goes negative, indicating little or no ice formation.

It can be seen from Table 9 that as the value of T_∞ is raised, the value of N remains equal to unity at the spinner for temperatures up to $T_\infty = 11°F$. Casual observation could lead to the conclusion that $T_\infty = -4°F$ and $T_\infty = 11°F$ are basically the same icing point since the spinner ice would probably look similar at the different points. The truth is that the nature of the ice buildup further downstream in the engine may be changing from a glaze ice with a high potential for growth and blockage to no ice at all. This could lead to acceptance of a point run at a value of T_∞ higher than the specified value, that would be rejected if run at the specified value of T_∞.

Tables 11 and 12 are breakdowns of Tables 9 and 10, respectively. These tables show the variations in the icing condition parameters and the scaling parameters as flow passes through the engine at a constant value of free-stream temperature. These tables show the free-stream static temperature ($T_\infty = -4°F$) and the icing conditions existing at each component. The temperature rises through the engine, as does pressure. Notice that drastic changes in LWC can occur since the volume contractions through the engine decrease the volume of air while the mass of water remains the same. This increases the amount of water per volume of air, thus increasing LWC. The high values of LWC can easily bring about a critical icing condition since the accumulation of ice is highly dependent on the level of LWC (Fig. 11). The A_c goes up substantially at the high values of LWC, especially for the probe because of its high collection efficiency. This could easily be a critical component if the other conditions, especially T, were conducive to icing.

The temperature rise through the engine does affect the extent of icing in the engine. From Table 12 it is seen that for the 0.5 MCT case the value of N approaches zero and Θ becomes negative at the fan blade tip and further downstream indicating no more icing in these regions. Also the component with the highest A_c, the cylindrical probe, is no longer in danger of icing and thus is no longer a critical component.

These observations indicate that flight and engine operating conditions have a significant effect on the criticality of icing within the engine. Every combination of the icing cloud envelopes, flight condition, and engine operating point should be considered. This will ensure that a combination leading to high liquid water content and other conditions promoting formation of ice at a component with high collection efficiencies will not be overlooked.

INFLUENCE OF STATIC PRESSURE ON SIMILITUDE.

To compare the use of altitude test facilities to ground icing spray rigs, three areas were considered: (1) the difference in test techniques of altitude and ground spray rigs; (2) determination of the effect of static pressure (P) changes on the value of the scaling parameters; and (3) comparison of the test conditions run on ground spray rigs to those required at altitude to ensure exact similitude based on equality of the scaling parameters.

The basic differences in test techniques were discussed in the introduction of this report. The obvious advantage of the altitude facility is that generally any value of P can be supplied at the request of the test conductor. This naturally allows more flexibility in testing. One disadvantage of testing in a ground spray rig is the inability to control P. The ground spray rig is constrained to operate at the naturally existing value of P.

To determine the effect of static pressure on the scaling parameters, an analysis similar to that conducted previously for variations in T was performed. The influence of changes in P on the scaling parameters was analyzed through use of the ice scaling code (Ref. 5). The test points as specified in AC 20-73 were used to study the effect of pressure change on icing similitude. The ice collection surface was a 6.0-in. chord NACA 0012 airfoil. The pressure was varied from 14.2 to 4.4 psia which represents an altitude range of 1,000 to 30,000 ft. The results of the variation in P on the scaling parameters are shown in Figs. 19 and 20. As seen in Table 6, there is no functional dependency of ϕ on the value of P. Therefore, there was no analysis performed to study the effort of ΔP on ϕ.

Figure 19a shows that the value of K_o increases as the static pressure is dropped. The freezing fraction is relatively unaffected by changes in P, as seen in Fig. 19b. Figure 19c shows

37

that θ increases as P is decreased. Figure 19d shows that A_c/t_0 increases slightly as P is decreased because of the slight increase in collection efficiency.

The percentage changes in the scaling parameters versus ΔP are shown in Fig. 20. Percentage change is given, using N as an example, by $\Delta N/N_0 \times 100$, and ΔP is given by $\Delta P = P - P_0$. The influence of ΔP on the scaling parameters may best be illustrated by developing expressions similar to those previously developed for ΔLWC, ΔT, and ΔMVD. Since, in Fig. 19, all of the test conditions except P were held constant, the slope of those curves at a particular point represents the value of the partial derivative for P at the selected point. The point was chosen as $P = 14.2$ psia for each AC 20-73 test point. This allows expressions describing the influence of P on the scaling parameters to be combined with the expressions previously developed to describe the influence of LWC, T, and MVD (developed at $P = 14.2$). Details of the technique to develop the expressions for LWC, T, and MVD apply here and are found in the section on the Allowable Tolerance of Test Conditions. The following expressions were obtained for the influence of ΔP:

For AC 20-73 point 1

$$\Delta K_0 \quad = \quad -0.003\Delta P$$
$$\Delta N \quad = \quad \text{no effect due to } \Delta P$$
$$\Delta \theta \quad = \quad -1.08\Delta P$$
$$\Delta A_c \quad = \quad \text{no noticeable effect due to } \Delta P$$

For AC 20-73 point 2

$$\Delta K_0 \quad = \quad -0.006\Delta P$$
$$\Delta N \quad = \quad -0.002\Delta P$$
$$\Delta \theta \quad = \quad -0.315\Delta P$$
$$\Delta A_c \quad = \quad \text{no noticeable effect due to } \Delta P$$

For AC 20-73 point 3

$$\Delta K_0 \quad = \quad -0.013\Delta P$$
$$\Delta N \quad = \quad -0.004\Delta P$$
$$\Delta \theta \quad = \quad -0.083\Delta P$$
$$\Delta A_c \quad = \quad \text{no noticeable effect due to } \Delta P$$

Combining these expressions with those previously developed for ΔLWC, ΔT, and ΔMVD,

and neglecting terms which are an order of magnitude smaller, the following expressions are obtained for the AC 20-73 test points:

For point 1

$$\Delta K_o = +0.02\Delta MVD - 0.003\Delta P$$
$$\Delta N = \text{no effect due to } \Delta P$$
$$\Delta\phi = -1.0\Delta T$$
$$\Delta\theta = +27 \,\Delta LWC$$
$$\Delta A_c = +0.021\Delta LWC$$

For point 2

$$\Delta K_o = +0.02\Delta MVD - 0.006\Delta P$$
$$\Delta N = -0.025\Delta T - 0.073\Delta LWC$$
$$\Delta\phi = 1.0\Delta T$$
$$\Delta\theta = -1.44\Delta T - 0.315\Delta P$$
$$\Delta A_c = +0.023\Delta LWC$$

For point 3

$$\Delta K_o = +0.02\Delta MVD - 0.013\Delta P$$
$$\Delta N = -0.18\Delta T - 0.172\Delta LWC$$
$$\Delta\phi = -1.0\Delta T$$
$$\Delta\theta = +1.55\Delta T - 0.08\Delta P$$
$$\Delta A_c = +0.024\Delta LWC$$

From this analysis it is seen that the influence of ΔP on the scaling parameter is slight compared to the effect of ΔT, ΔLWC, and ΔMVD. An exception is the modified inertia parameter (K_o) where a significant effect is experienced attributable the effect of P on the air density, which affects the droplet trajectory and hence the collection efficiency of a collection surface. The effect of P is also noted in the air energy driving potential (θ) and comes into play in the evaporation term in that expression (see Appendix A). This influence is on the order of 1/4 to 1/3 as strong as that encountered for ΔT. The affect of slight fluctations in P, on the order of ≈ 0.5 psia, would seem to have little impact on the value of θ.

EFFECT OF STATIC PRESSURE ON SIMILITUDE REQUIREMENTS.

Another question that may be asked is what changes are required to achieve "exact similitude" between a test run in a ground level spray rig and a test run at altitude in an altitude test facility. The analytical approach used to answer this question is similar to that conducted

earlier, and the reader is referred to the section on temperature effects on similitude requirements. This question is addressed in Tables 13, 14, and 15 which show the required values the test conditions must assume to maintain the values of all of the scaling parameters. These tables represent data obtained using the icing scaling code. Again, the test conditions specified in AC 20-73 at a velocity of V = 200 ft/sec were used. These tables show that as altitude increases (decreasing pressure), the test temperature must be reduced slightly, the velocity of air over the airfoil must increase, the LWC must be reduced, the MVD must be decreased, and the icing time must be slightly increased.

The reverse situation is addressed in Table 16. which lists the requirements to return to lower altitude from a test conducted at an altitude of ~20,000 ft at the test conditions specified in AC 20-73 point 2 at a velocity of 200 ft/sec. To lower altitude (that is, to raise P) the velocity soon approaches zero and this quickly limits this test technique.

CONCLUSIONS

An analytical study is presented investigating applications of the icing similitude laws to aircraft engine certification work. The results of the analytical study lead to several conclusions:

1. The analysis of the effect of static temperature (T) changes on icing show that all of the test conditions must change when any one of them changed in order to obtain "exact similitude." Since the value of static pressure, P, is uncontrollable on ground spray rigs and the flow velocity, V, is set by P and engine operation, it can quickly be seen that "exact similitude" cannot be obtained on a ground spray rig if a temperature mismatch exists.

2. The requirements for exact similitude change for different collection surfaces, indicating that any application of icing similitude should consider the icing conditions as they exist at a particular component and not for a combination of different components unless those components are effectively similar with respect to similitude requirements.

3. A sensitivity analysis of each of the scaling parameters to changes in test conditions can be used to determine tolerances which may be allowed when setting icing test conditions. These tolerances must be based on some arbitrarily selected range of values within which each scaling parameter may be allowed to vary. The influence of each test condition upon a particular scaling parameter may vary, depending or whether the ice accretion in question is rime or glaze ice. Without experimental data to quantify the effect that changes in each of the scaling parameters have on the ice accretion process, conclusive results cannot be deduced on allowable tolerances within which

the temperature, pressure, liquid water content, or mass median droplet diameter can vary without significantly altering the ice accretion.

4. Changes in pressure on the scaling parameters were found to be generally less influential than changes in temperature, liquid water content, or mean volume droplet diameter. If all of the test conditions are allowed to vary, "exact similitude" requirements can be met to reproduce sea level conditions at altitude or to reproduce altitude conditions at sea level. The transition from altitude to sea level, however, requires the flow velocity to decrease quickly and approach zero. This will generally not allow a transition to sea level unless the initial value of velocity is quite high.

5. A study of the effect of temperature rise through the engine and of changes in free-stream temperature on typical engine icing components indicates that changes in icing condition may not be evident on the visible engine hardware such as the spinner, but significant changes in the criticality of icing conditions further downstream may exist. Free-stream temperature changes affect the extent of icing through the engine and can alter the criticality of any particular component.

6. The requirements for similitude change for different components (different geometries) and for different baseline conditions. Since different geometries and different conditions exist throughout an engine, there is not any one set of conditions that will ensure exact similitude for all of the engine components. Application of similitude should concentrate on critical components. The conditions required to achieve similarity at that component may not necessarily ensure similarity at other components. Likewise, allowable tolerances in the test conditions are not necessarily the same for different components.

7. The technique of ice scaling has been verified as a valid tool in icing testing (Ref. 5), but its use in icing certification is limited without knowledge of the changes that can be allowed for each scaling parameter and still achieve either effective similitude or, possibly a more severe icing condition, if desired. So far, this question has been addressed only analytically. Experimental data are required to more completely understand the influence of each scaling parameter on the similitude and severity of an icing test point.

REFERENCES

1. FAA Advisory Circular AC No. 20-73: *Aircraft Ice Protection*. April 21, 1971.

2. "Airworthiness Standards: Transport Category Airplanes; Appendix C." *Federal Aviation Regulations*, Part 25, Federal Aviation Administration.

3. Willbanks, C. E. and Schulz, R. J. "Analytical Study of Icing Simulation for Turbine Engines in Altitude Test Cells." AEDC-TR-73-144 (AD-770069), November 1973.

4. Pfeifer, G. D. and Maier, G. P. "Engineering Summary of Power Plant Icing Technical Data." FAA-RD-77-76, July 1977.

5. Ruff, G. A. "Analysis and Verification of the Icing Scaling Equations, Vol. I." AEDC-TR-85-30, (AD-A162226), November 1985.

6. Abernethy, R. B. and Thompson, J. W., "Handbook, Uncertainty in Gas Turbine Measurements." AEDC-TR-73-5 (AD-755356), February 1973.

7. Hauger, H. H. and Englar, K. G. "Analysis of Model Testing in an Icing Wind Tunnel." Douglas Aircraft Company, Inc. Report No. SM14933, 1954.

8. Sibley, P. J. and Smith, R. E., Jr. "Model Testing in an Icing Wind Tunnel." Lockheed Aircraft Corporation, Report No. LR10981, 1955.

9. Dodson, E. O. "Scale Model Analogy for Icing Tunnel Testing." Boeing Airplane Company, Transport Division, Document No. D66-7976, March 1962.

10. Jackson, E. T. "Development Study: The Use of Scale Models in an Icing Tunnel to Determine the Ice Catch on a Prototype Aircraft with Particular Reference to Concord." British Aircraft Corporation (Operating) Ltd., Filton Division, SST/B75T/RMMcK/242, July 1967.

11. Armand, C., et al. "Techniques and Facilities Used at the Onera Modane Centre for Icing Tests." North Atlantic Treaty Organization Advisory Group for Aerospace Research and Development, AGARD-AF-127, November 1978.

12. Langmuir, I. and Blodgett, K. B. "A Mathematical Investigation of Water Droplet Trajectories." Army Air Force Technical Report No. 5418, 1946.

13. Bowden, D. T., Gensemer, A. E., and Skeen, C. A. "Engineering Summary of Airframe Icing Technical Data." FAA Reports ADS-4, 1964.

14. Messinger, B. L. "Equilibrium Temperature of an Unheated Icing Surface as a Function of Airspeed." *Journal of the Aeronautical Sciences,* January 1953, pp. 23-42.

15. Gelder, T. F. "Droplet Impingement and Ingestion by Supersonic Nose Inlet in Subsonic Tunnel Conditions." NACA 4268, 1958.

16. Wilder, R. W. "Techniques Used to Determine Artifical Ice Shapes and Ice Shedding Characteristics of Unprotected Airfoil Surfaces." Presented at the Federal Aviation Administration Symposium on Aircraft Icing Protection, Washington, D. C., April 1969.
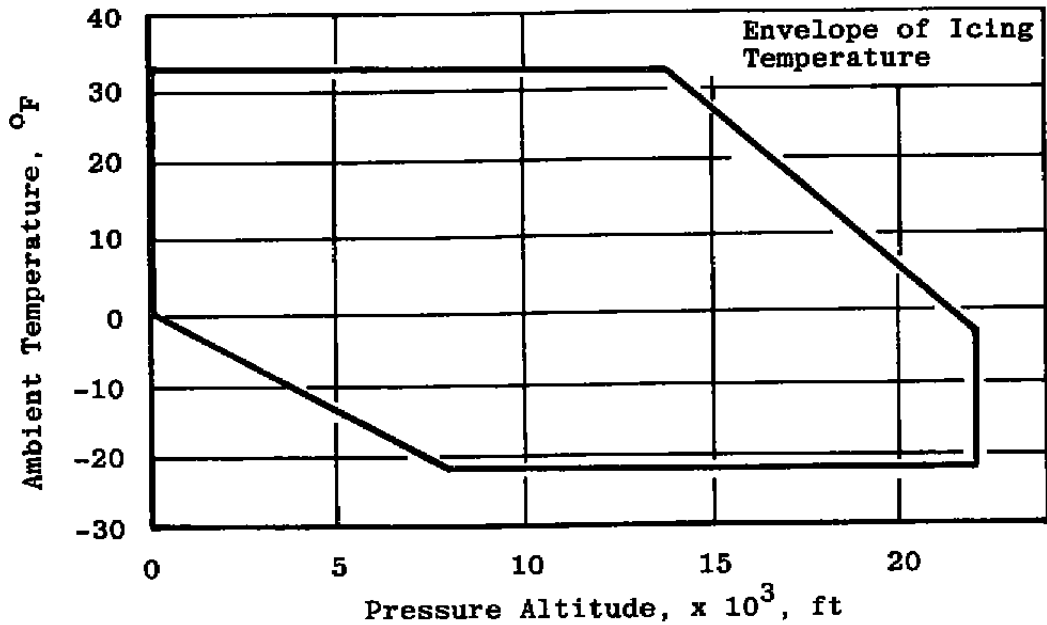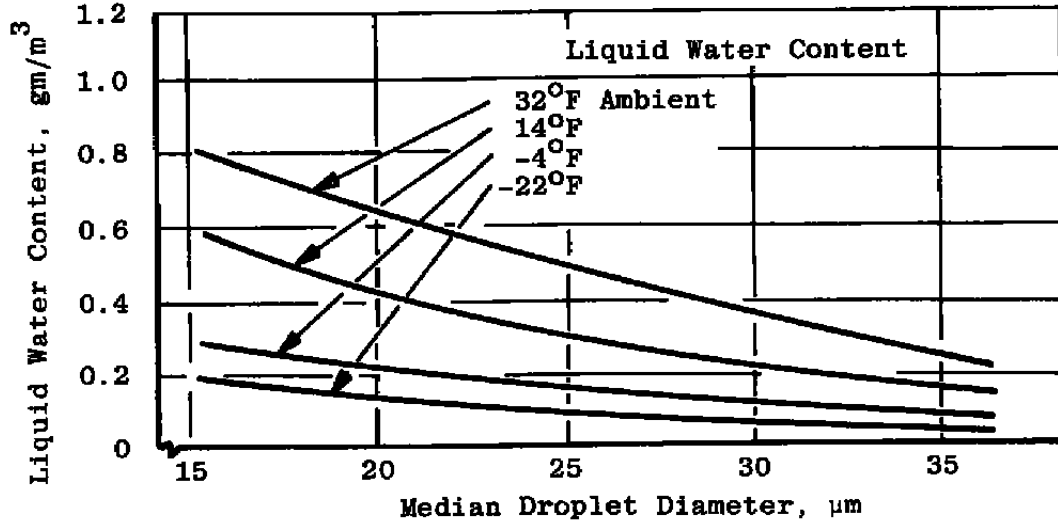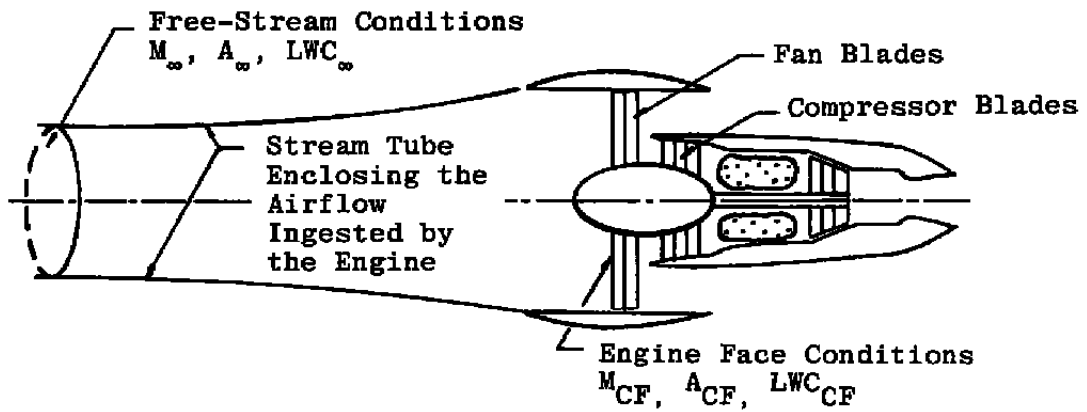
a. Continuous maximum (stratiform clouds)

FIGURE 1. CLOUD ICING CONDITIONS.

45

Altitude: 4,000 to 22,000 ft
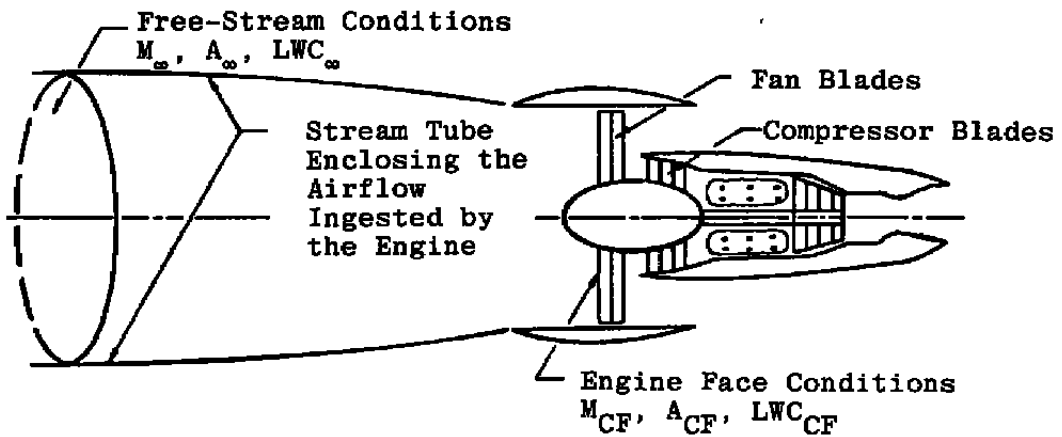Horizontal Extent: 3 miles
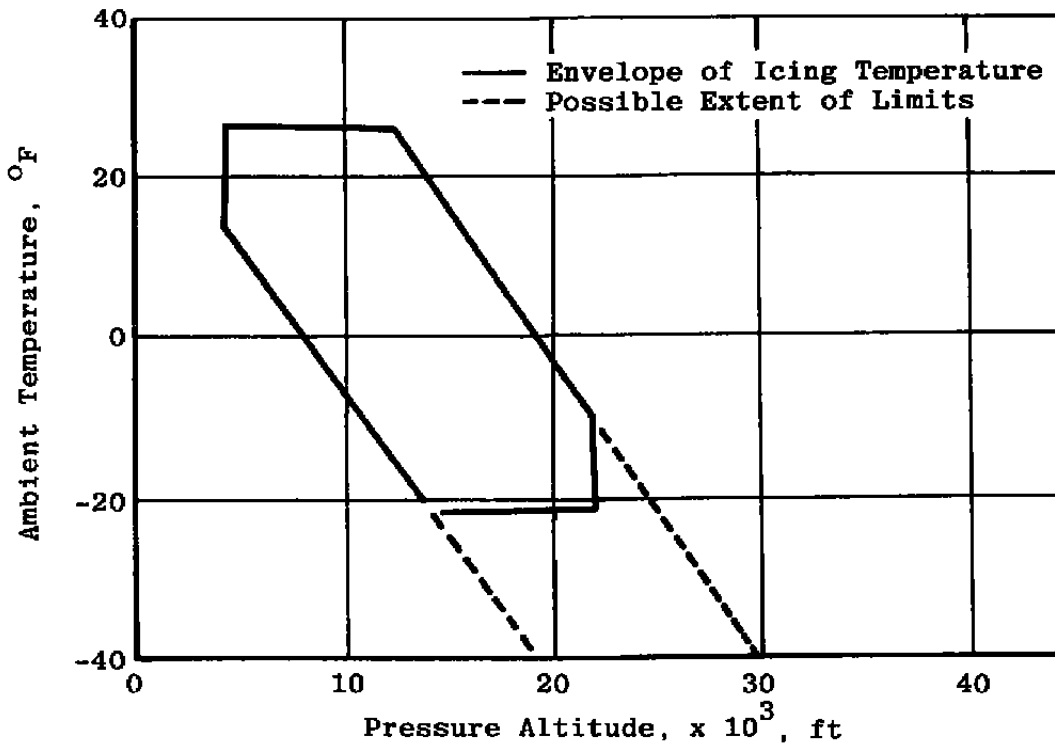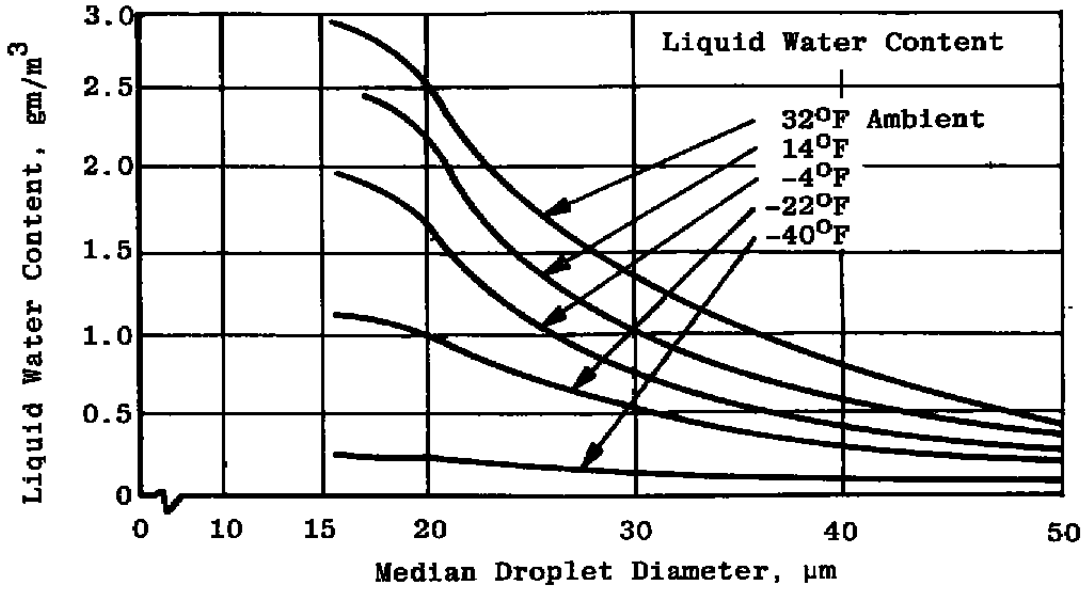
b. Intermittent maximum (cumuliform clouds)
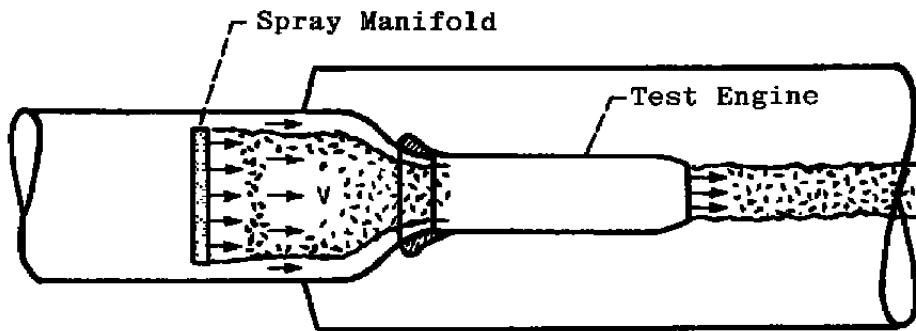FIGURE 1. CLOUD ICING CONDITIONS (CONCLUDED).

a. Inlet Mach number less than flight Mach Number, $LWC_\infty < LWC_{CF}$

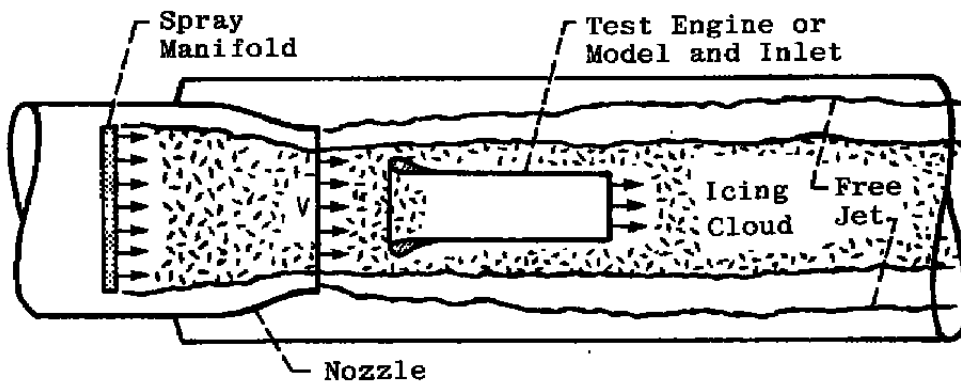b. Inlet Mach number greater than flight Mach number, $LWC_{CF} < LWC_\infty$

FIGURE 2. SCHEMATIC SHOWING POSSIBLE STREAM TUBE CONFIGURATION FOR TURBOFAN ICING CONDITIONS (TAKEN FROM AEDC-TR-73-144).

Spray Manifold

Test Engine

a. Direct connect

Spray
Manifold

Test Engine or
Model and Inlet

Icing
Cloud

Free
Jet

Nozzle

b. Free jet

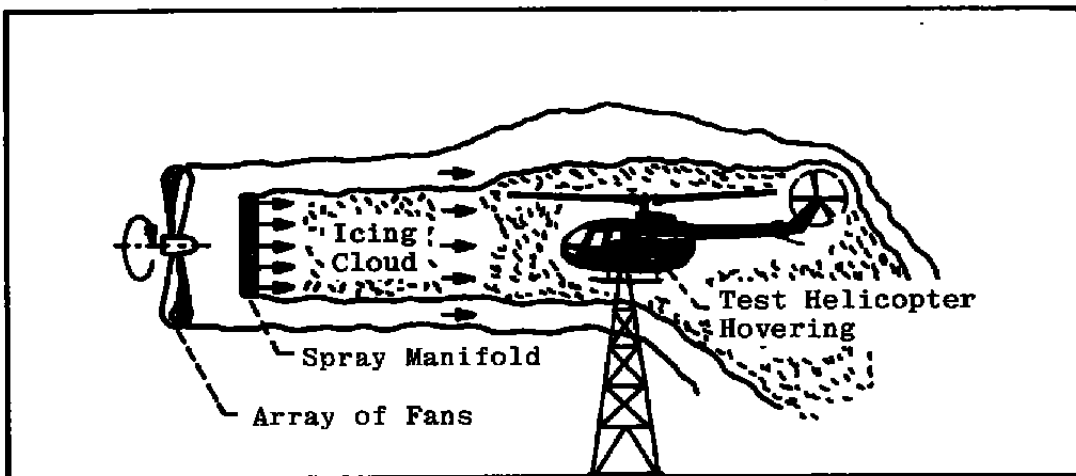**FIGURE 3. ICING CLOUD SIMULATION TEST TECHNIQUES.**

c. Fan blown spray in a large room or outdoors
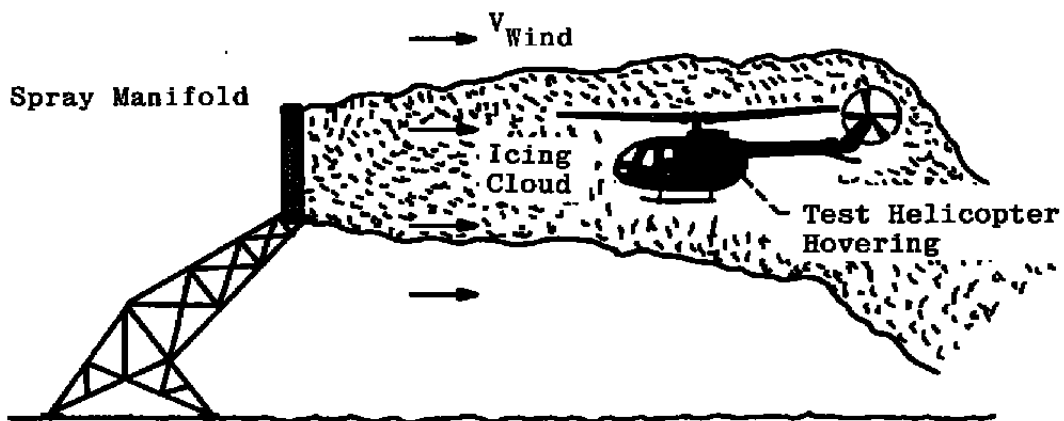
d. Windblown sprays in an outdoor facility

FIGURE 3. ICING CLOUD SIMULATION TEST TECHNIQUES (CONCLUDED).

a. Changes in static pressure

b. Changes in air velocity

FIGURE 4. ICING CONDITION VARIABLE CHANGES REQUIRED FOR
SIMILITUDE AT VARIOUS ICING TEMPERATURES FOR AC
20-73 POINT 1.

c. Changes in liquid water content

d. Changes in droplet diameter

FIGURE 4. ICING CONDITION VARIABLE CHANGES REQUIRED FOR SIMILITUDE AT VARIOUS ICING TEMPERATURES FOR AC 20-73 POINT 1 (CONTINUED).

e. Changes in icing time

FIGURE 4. ICING CONDITION VARIABLE CHANGES REQUIRED FOR SIMILITUDE
AT VARIOUS ICING TEMPERATURES FOR AC 20-73 POINT 1
(CONCLUDED).

a. Changes in static pressure

b. Changes in air velocity

FIGURE 5. ICING CONDITION VARIABLE CHANGES REQUIRED FOR
SIMILITUDE AT VARIOUS ICING TEMPERATURES FOR AC
20-73 POINT 2.
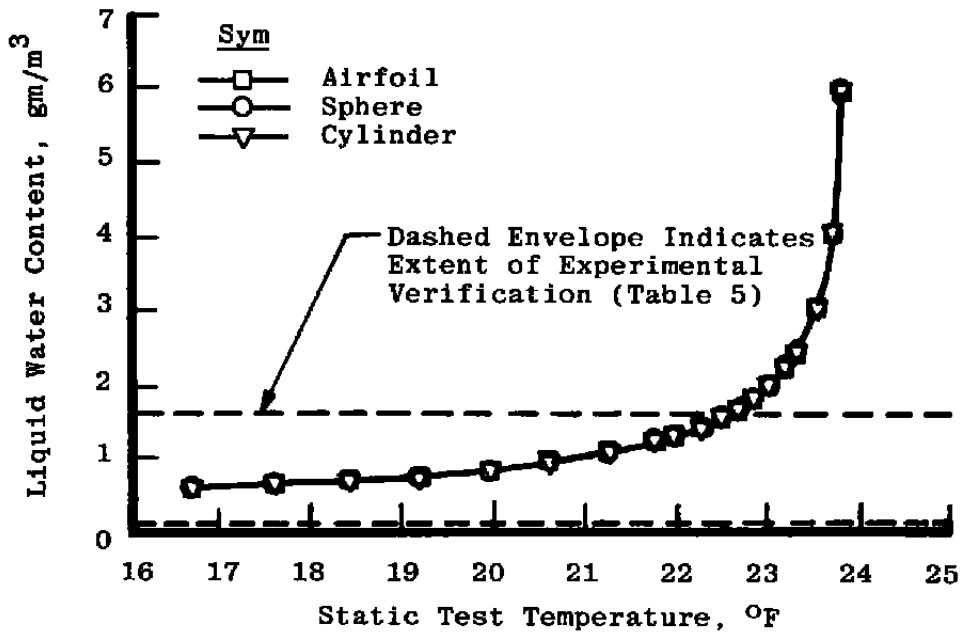
c. Changes in liquid water content
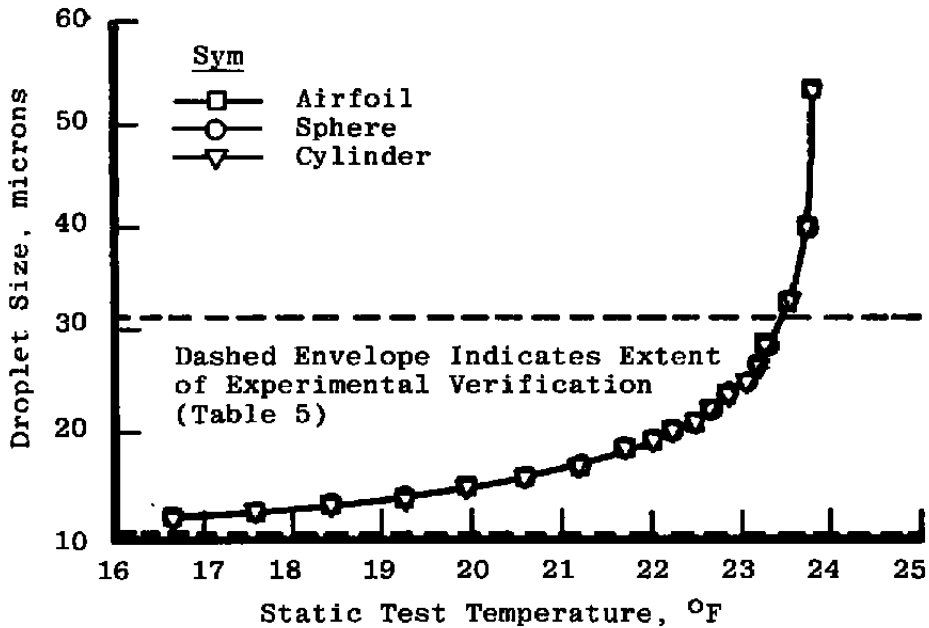
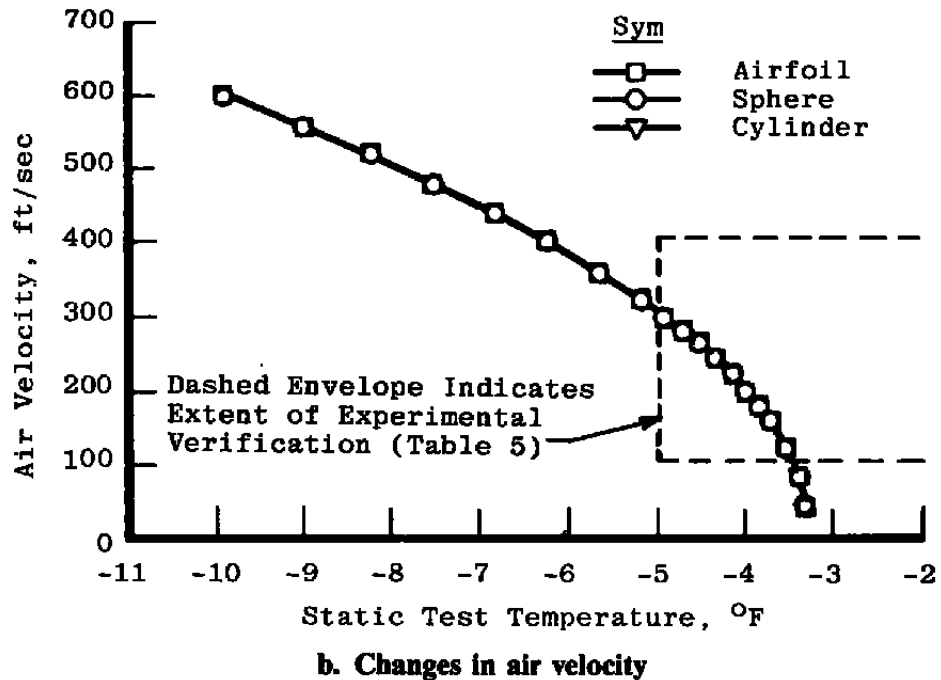d. Changes in droplet diameter

FIGURE 5. ICING CONDITION VARIABLE CHANGES REQUIRED FOR SIMILITUDE AT VARIOUS ICING TEMPERATURES FOR AC 20-73 POINT 2 (CONTINUED).

AEDC-TR-86-26
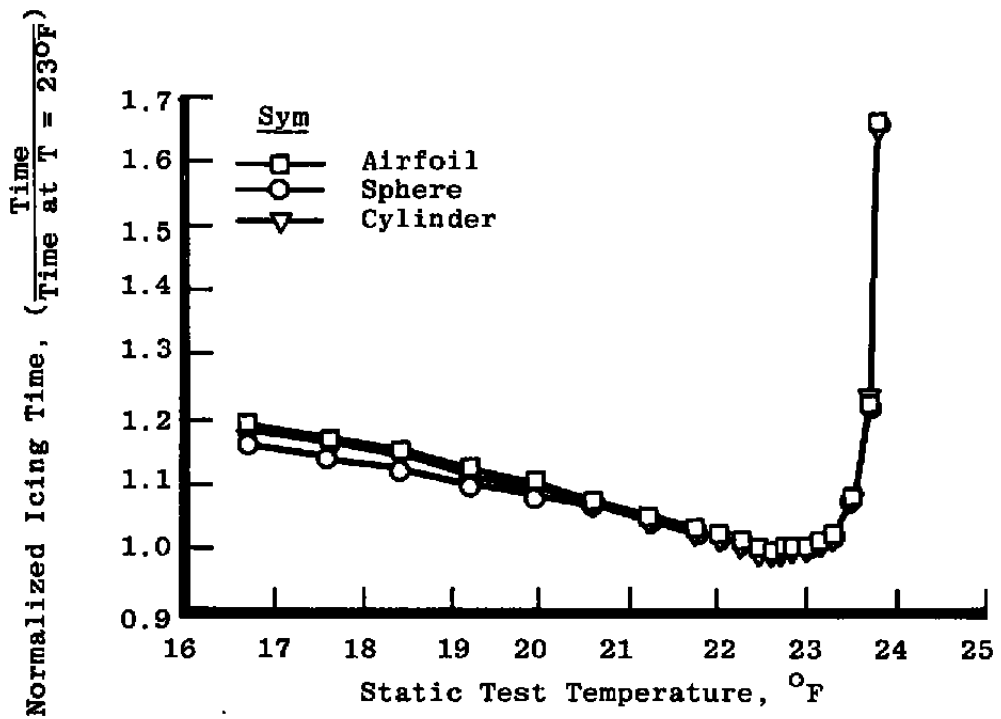
e. Changes in icing time

FIGURE 5. ICING CONDITION VARIABLE CHANGES REQUIRED FOR SIMILITUDE
AT VARIOUS ICING TEMPERATURES FOR AC 20-73 POINT 2
(CONCLUDED).

55
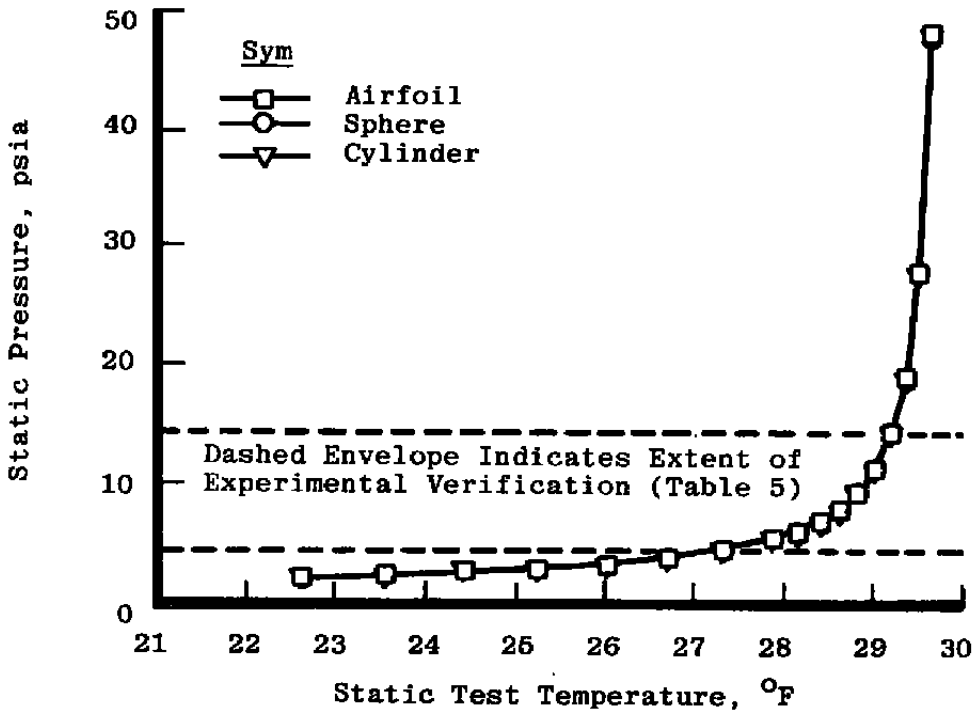
a. Changes in static pressure
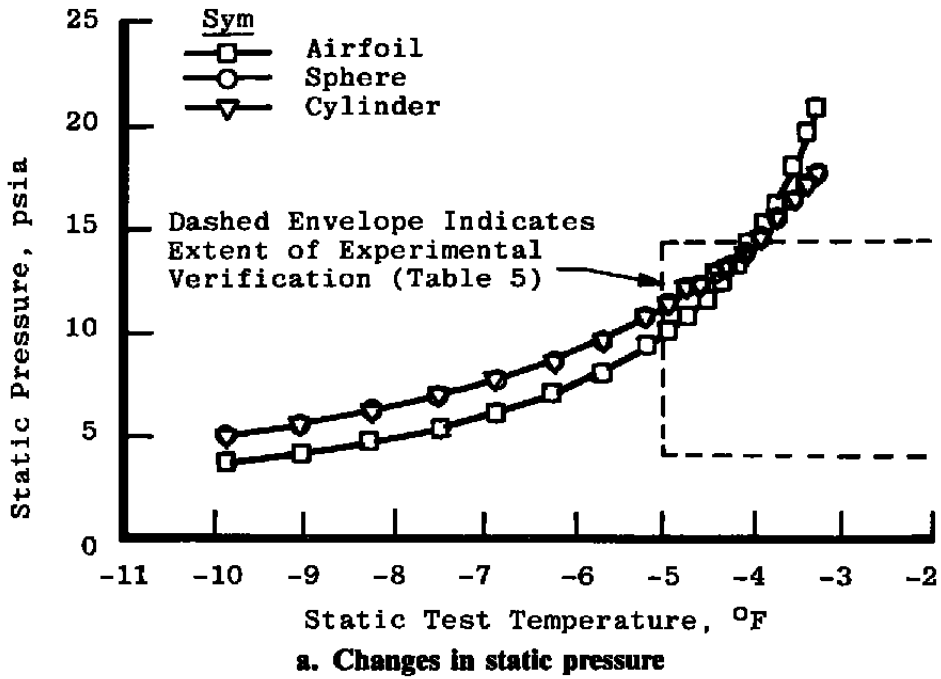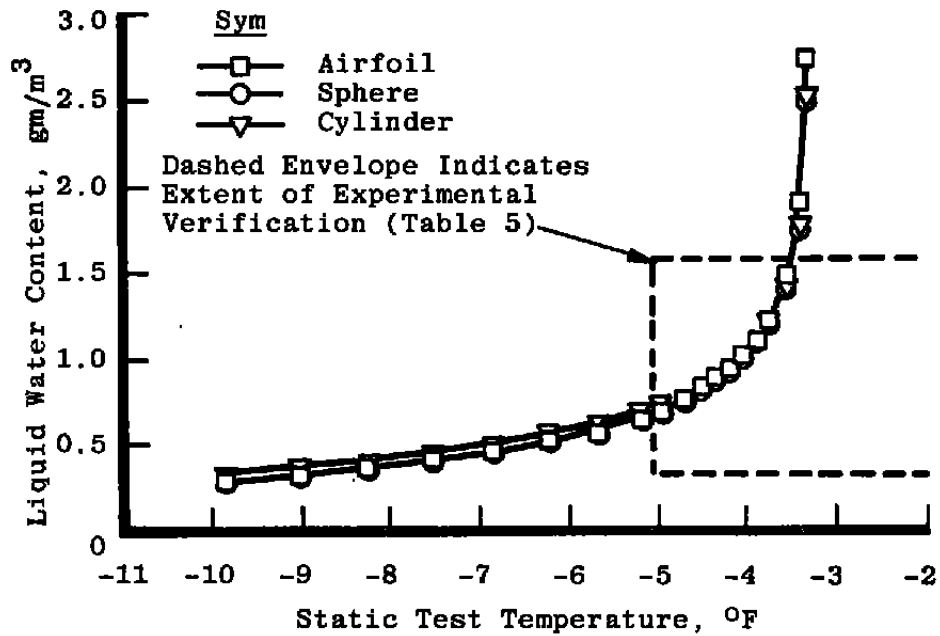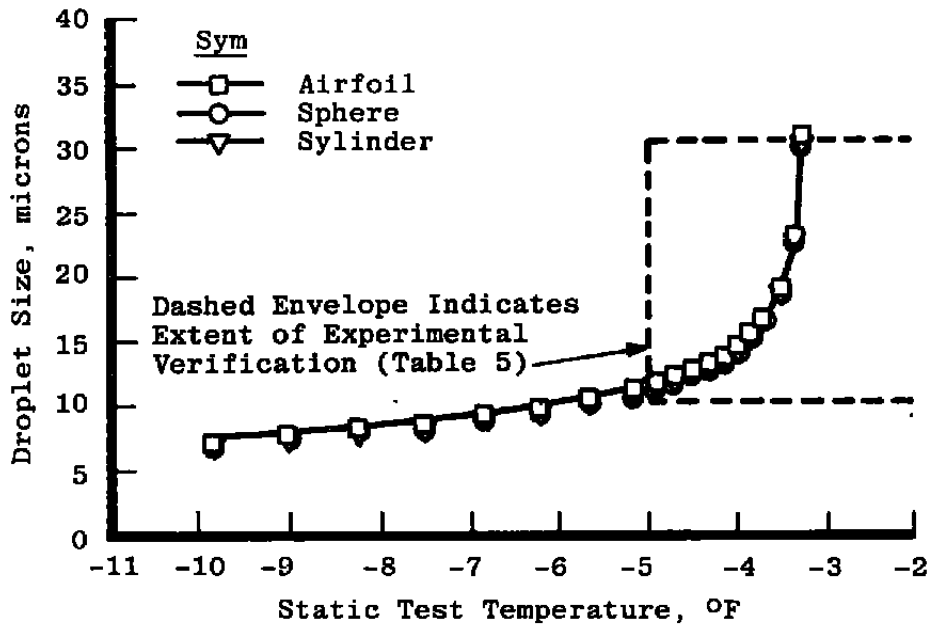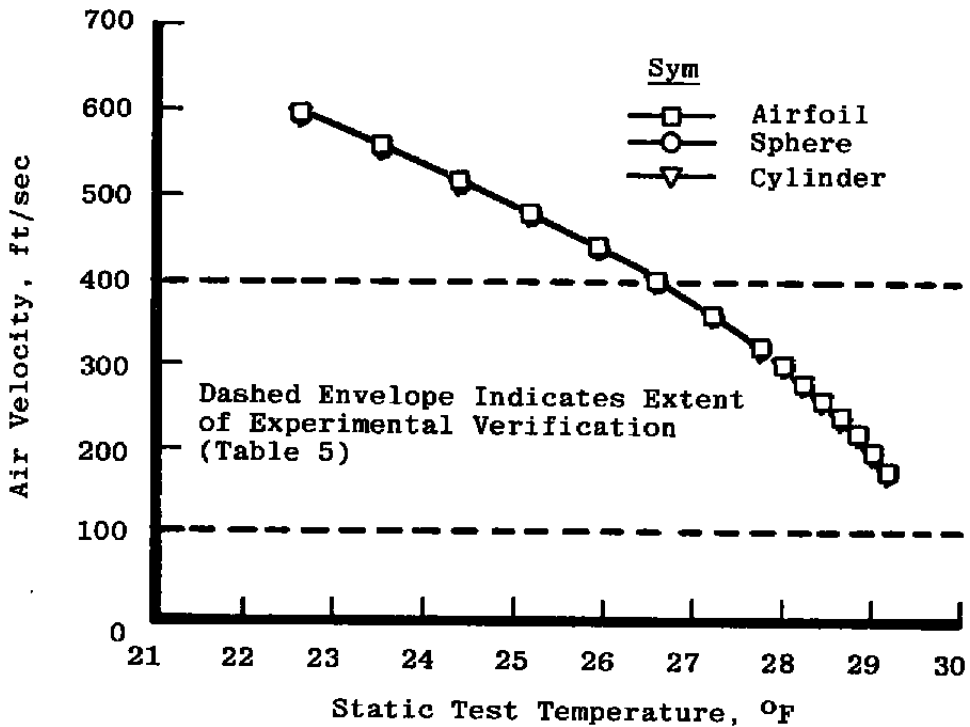

b. Changes in air velocity

FIGURE 6. ICING CONDITION VARIABLE CHANGES REQUIRED FOR SIMILITUDE AT VARIOUS ICING TEMPERATURES FOR AC 20-73 POINT 3.
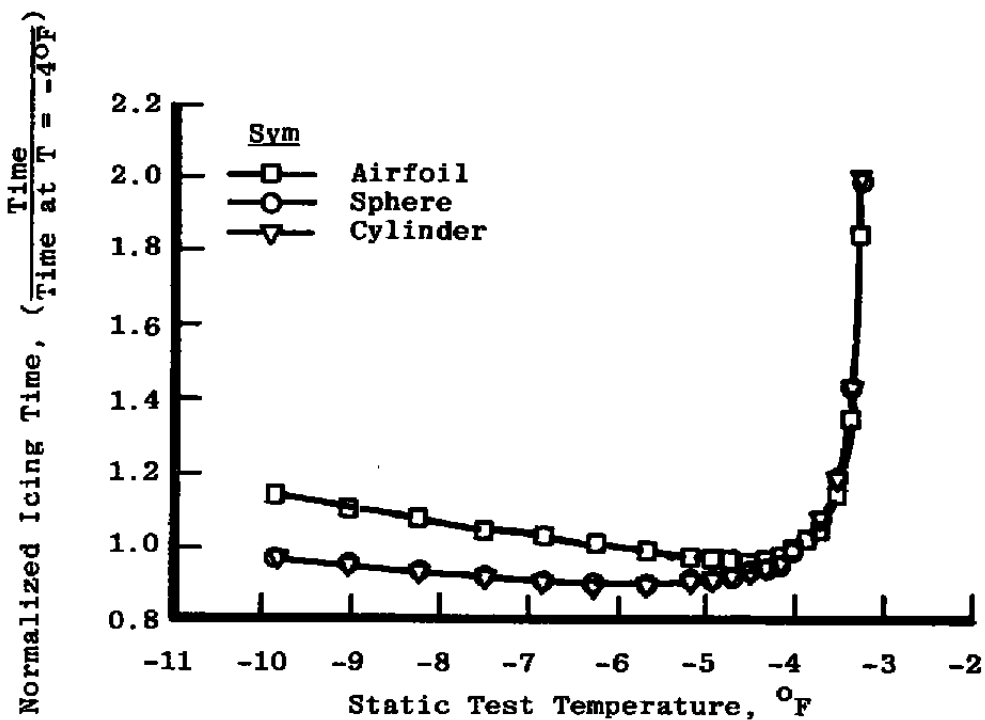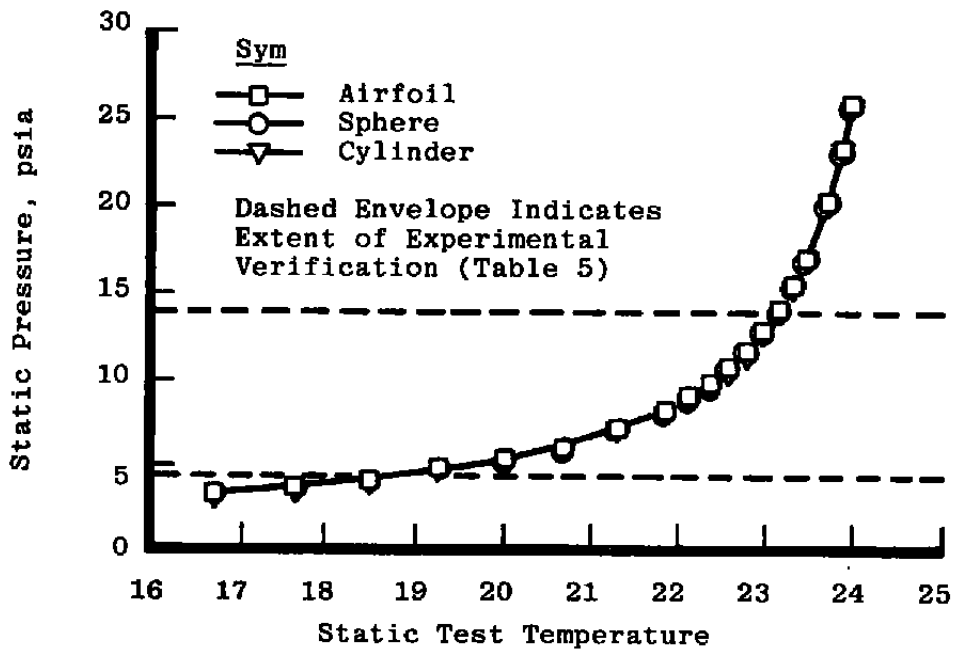
c. Changes in liquid water content
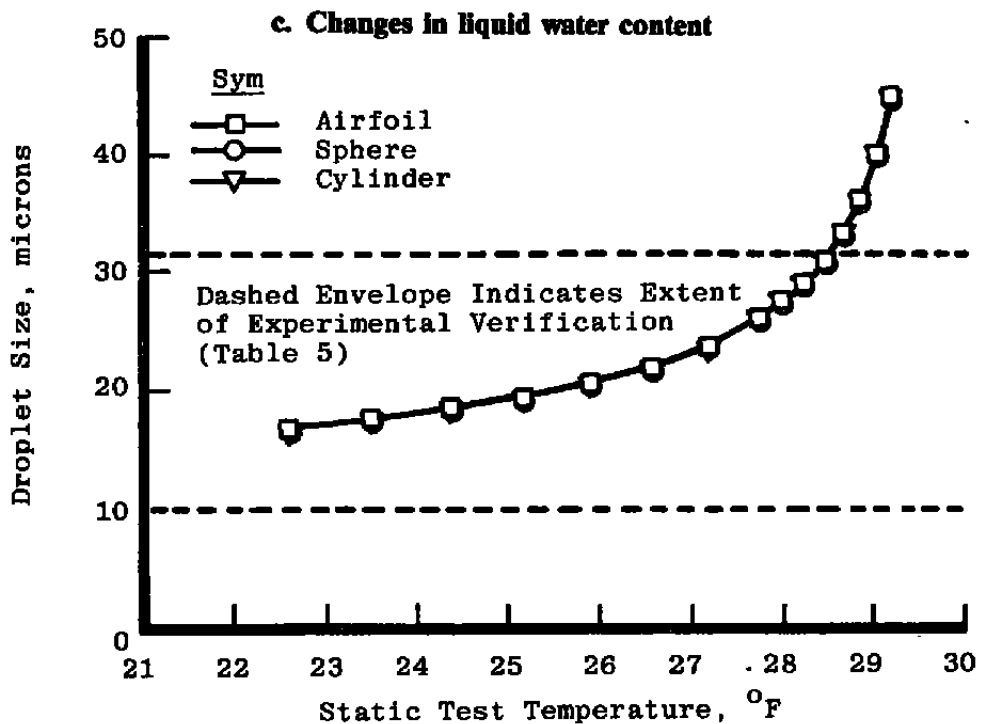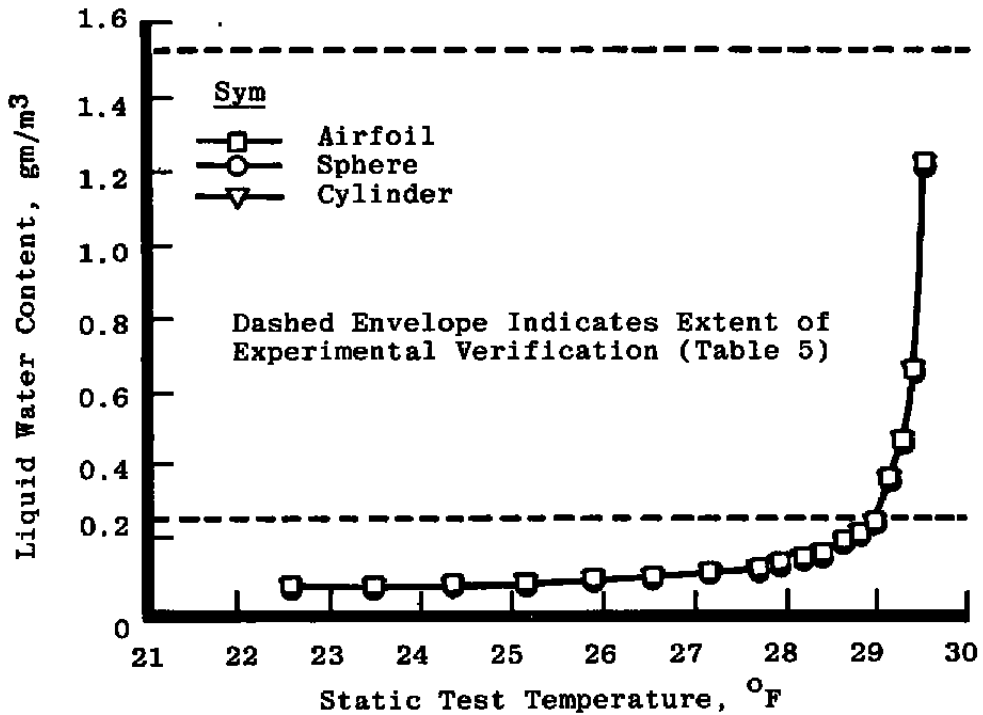
d. Changes in droplet diameter

FIGURE 6. ICING CONDITION VARIABLE CHANGES REQUIRED FOR
SIMILITUDE AT VARIOUS ICING TEMPERATURES FOR AC
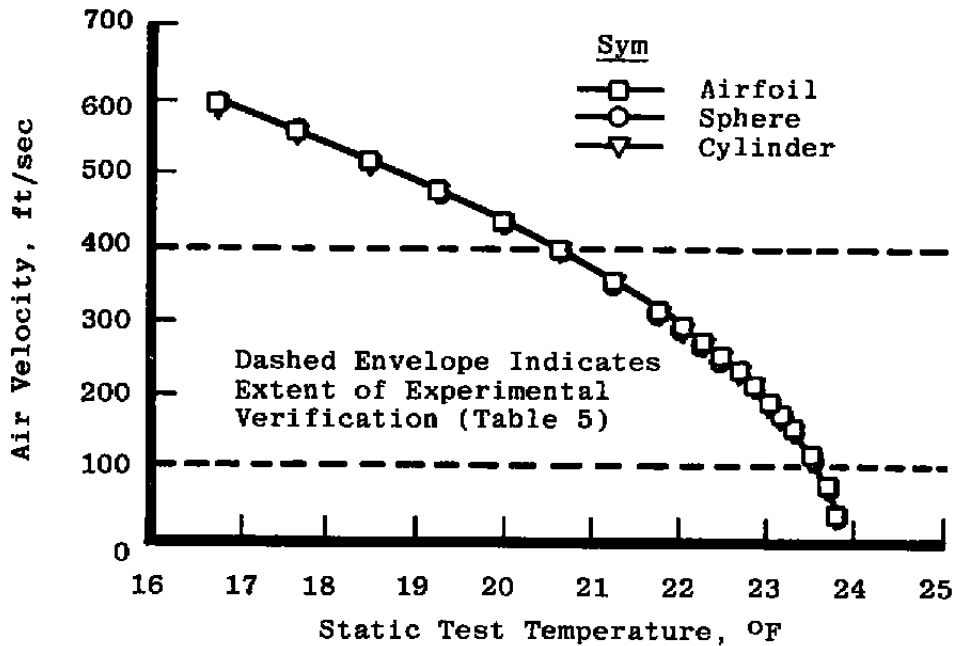20-73 POINT 3 (CONTINUED).
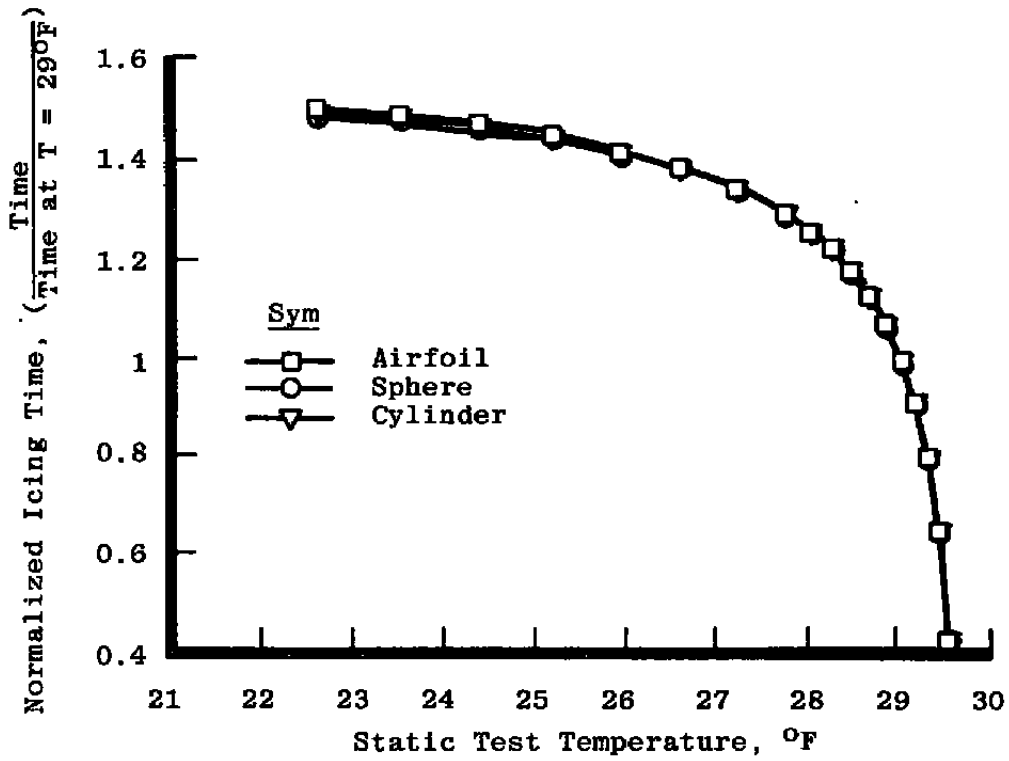
e. Changes in icing time

FIGURE 6. ICING CONDITION VARIABLE CHANGES REQUIRED FOR
SIMILITUDE AT VARIOUS ICING TEMPERATURES FOR AC
20-73 POINT 3 (CONCLUDED).
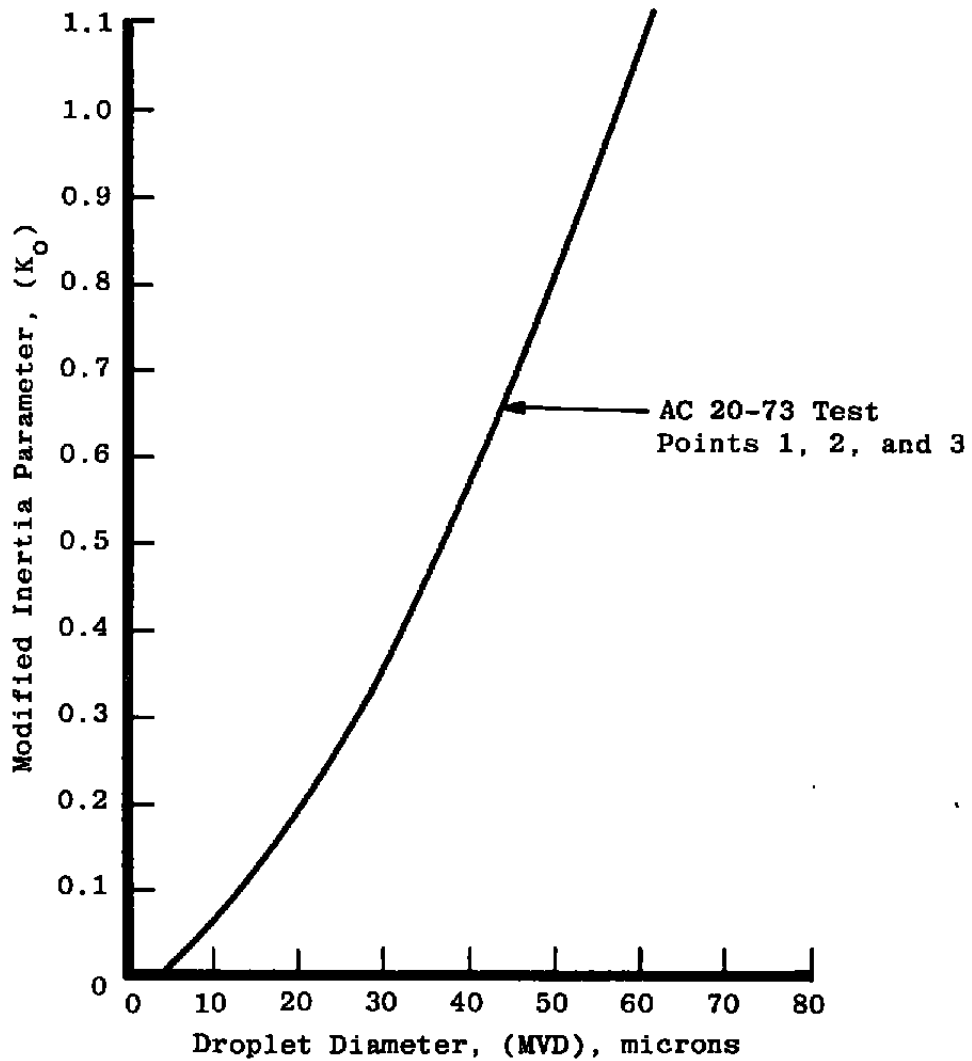
FIGURE 7. EFFECT OF DROP SIZE ON THE MODIFIED INERTIA PARAMETER FOR AN NACA 0012 AIRFOIL (6.0-IN. CHORD) AT 200 FT/SEC FLOW VELOCITY.

Sym
_____ AC 20-73 Point 1
- - - - AC 20-73 Point 2
-- -- -- AC 20-73 Point 3

Freezing Fraction, (N)

Liquid Water
Content, gm/m^3

Static Temperature, ^{o}F

Droplet Diameter, microns

a. Effect of liquid water content   b. Effect of static temperature   c. Effect of drop size
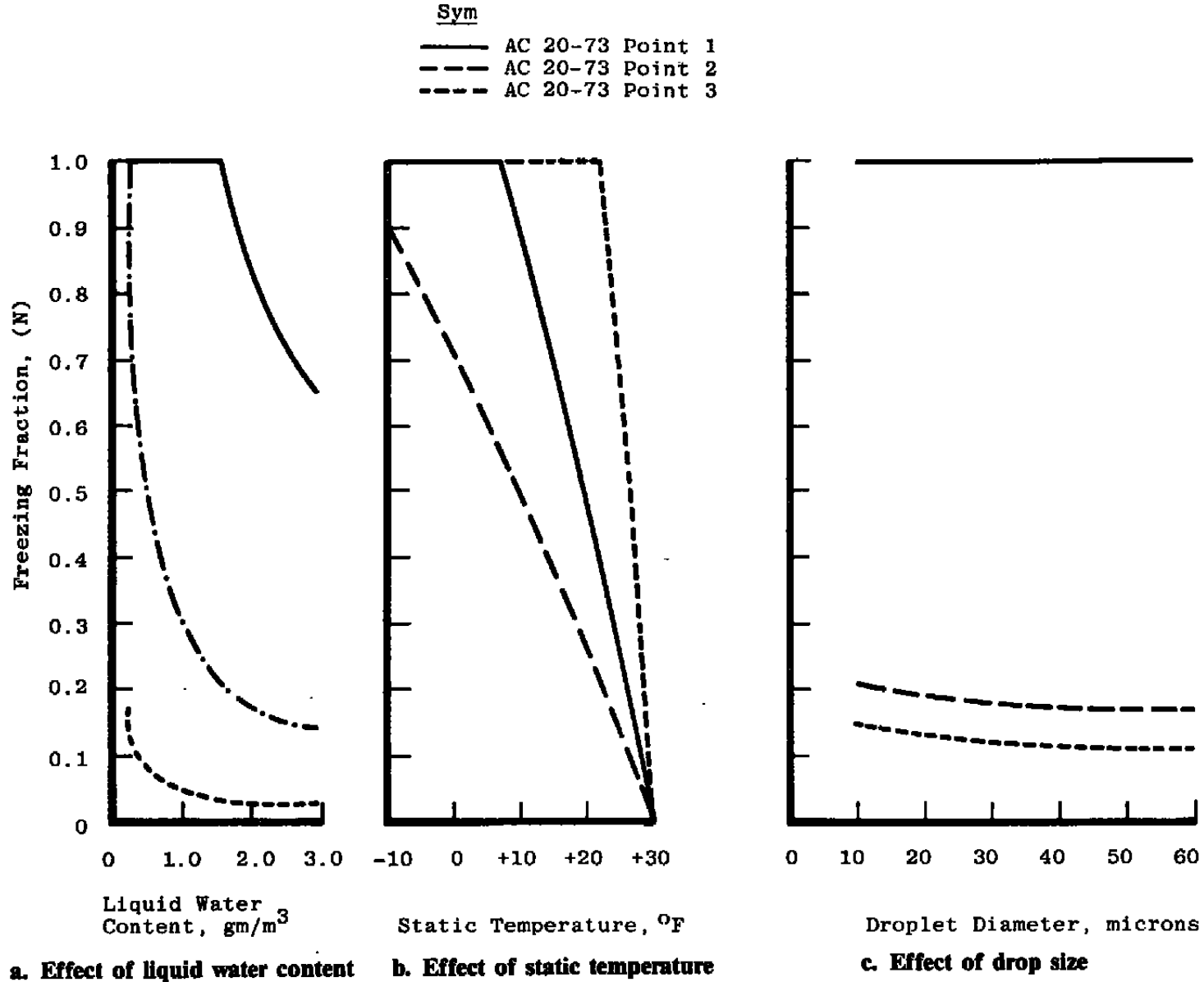
FIGURE 8. EFFECT OF THE TEST CONDITIONS ON FREEZING FRACTION FOR
AN NACA 0012 AIRFOIL (6.0-IN. CHORD) AT 200 FT/SEC FLOW
VELOCITY.
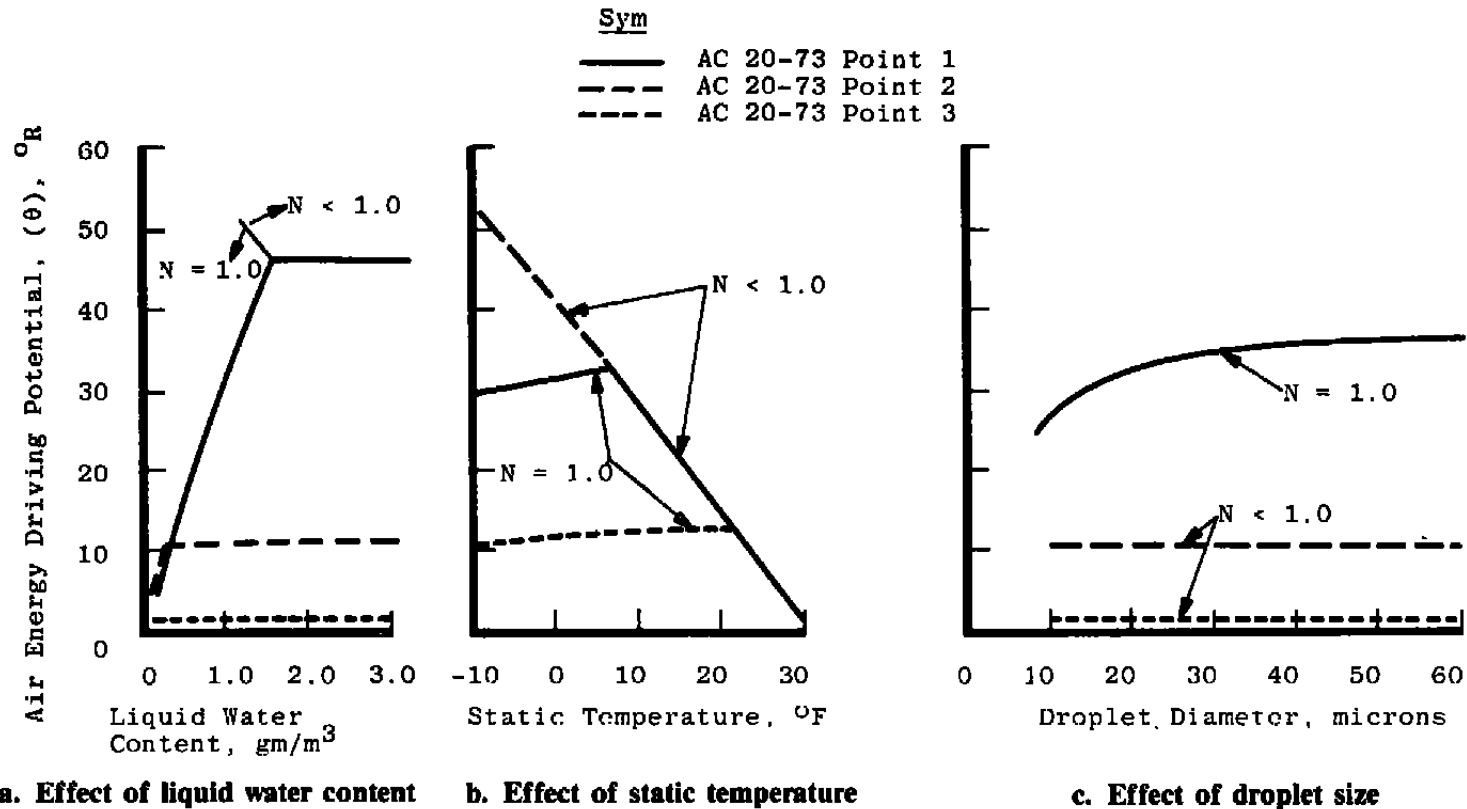
FIGURE 9. EFFECT OF THE TEST CONDITIONS ON AIR ENERGY DRIVING POTENTIAL FOR AN NACA 0012 AIRFOIL (6.0-IN. CHORD) AT 200 FT/SEC FLOW VELOCITY.
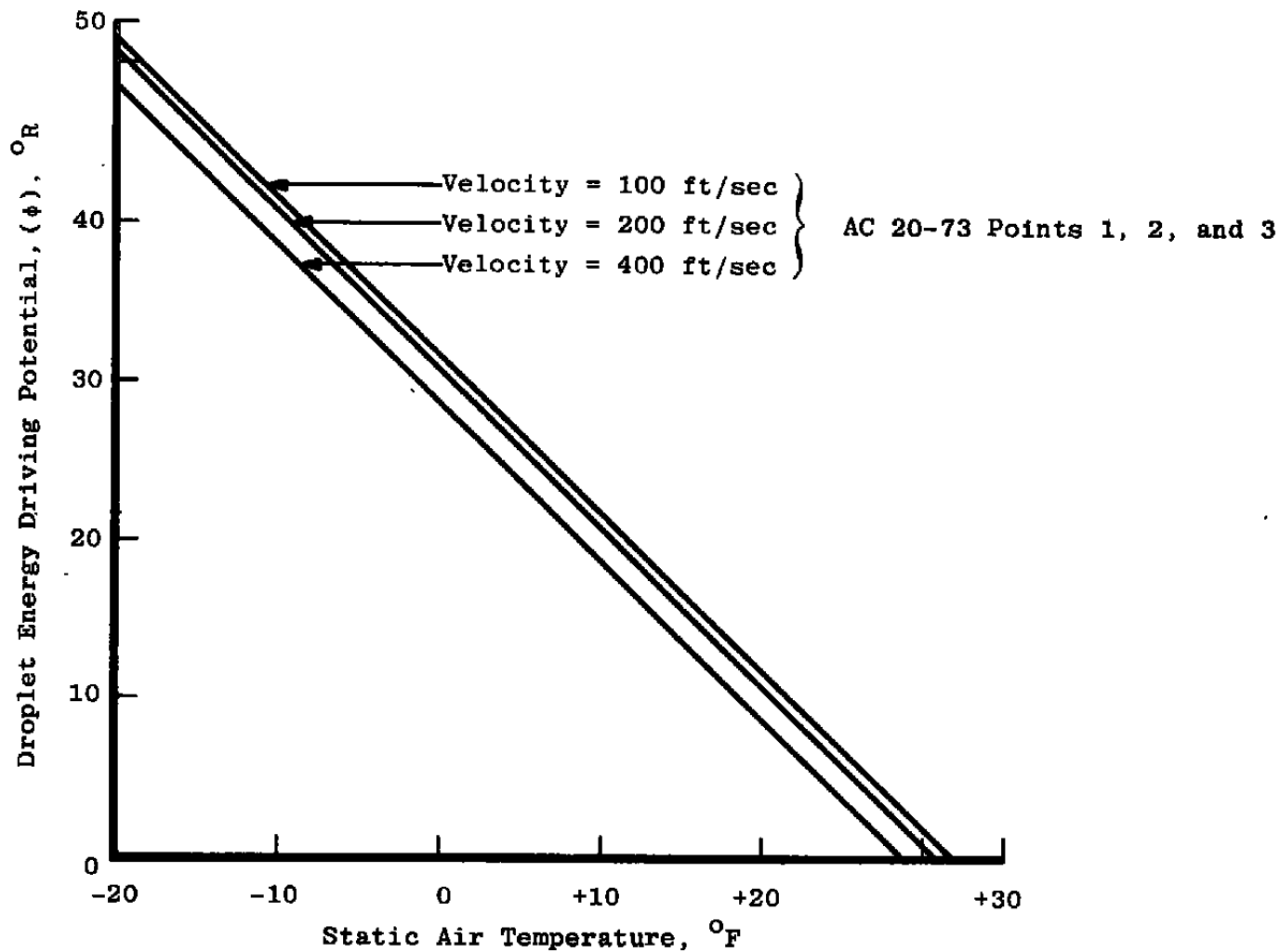
FIGURE 10. EFFECT OF STATIC TEMPERATURE AND VELOCITY ON DROPLET
ENERGY DRIVING POTENTIAL FOR AN NACA 0012 AIRFOIL (6.0-IN.
CHORD) AT 200 FT/SEC FLOW VELOCITY.

a. Effect of liquid water content

b. Effect of droplet size
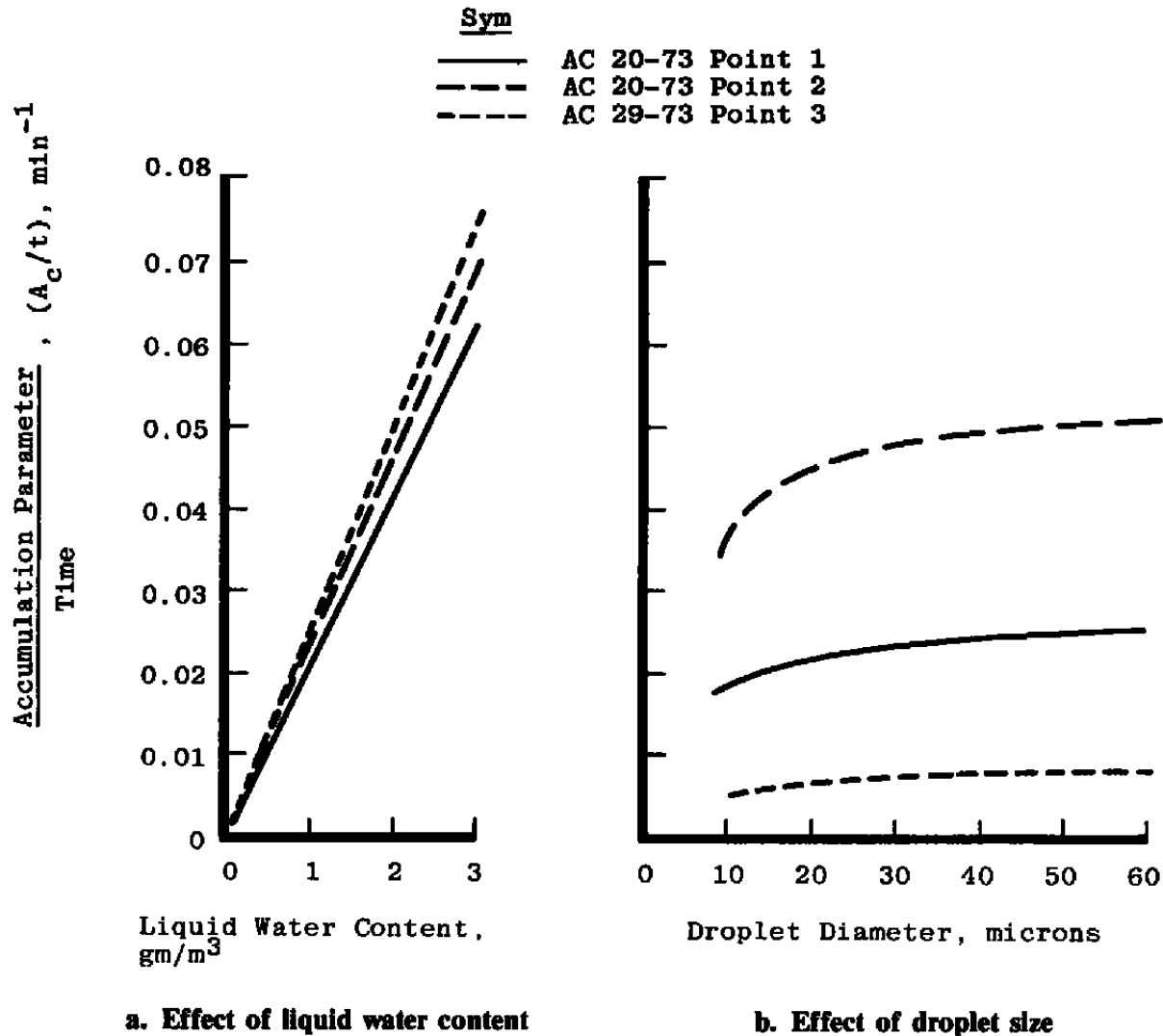
FIGURE 11. EFFECT OF LIQUID WATER CONTENT AND DROP SIZE ON THE
ACCUMULATION PARAMETER RATIOED TO TIME FOR AN NACA
0012 AIRFOIL (6.0-IN. CHORD) AT 200 FT/SEC FLOW VELOCITY.
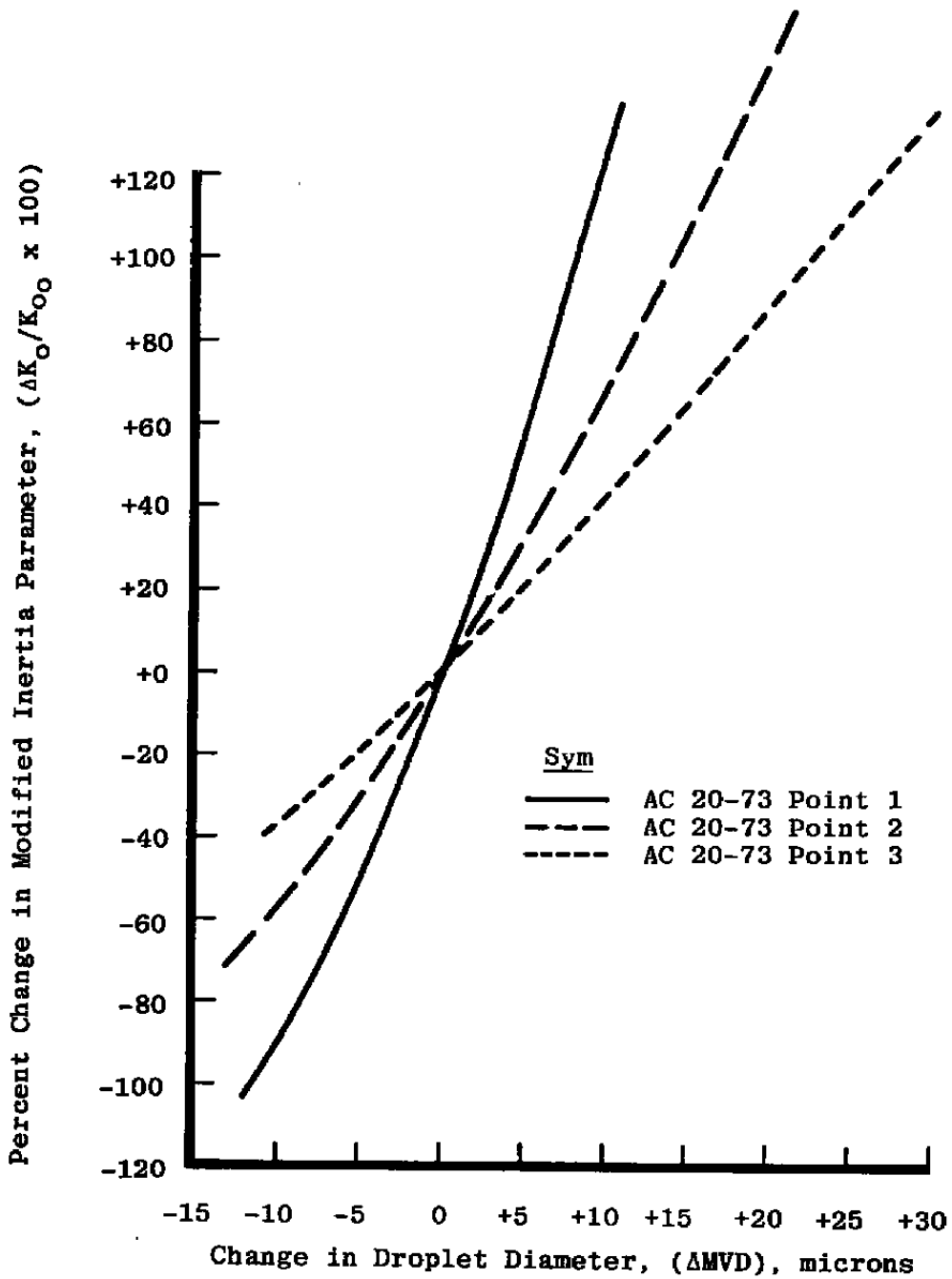
FIGURE 12. PERCENTAGE CHANGE IN MODIFIED INERTIA PARAMETER VERSUS CHANGE IN DROP SIZE FOR AN NACA 0012 AIRFOIL (6.0-IN. CHORD).
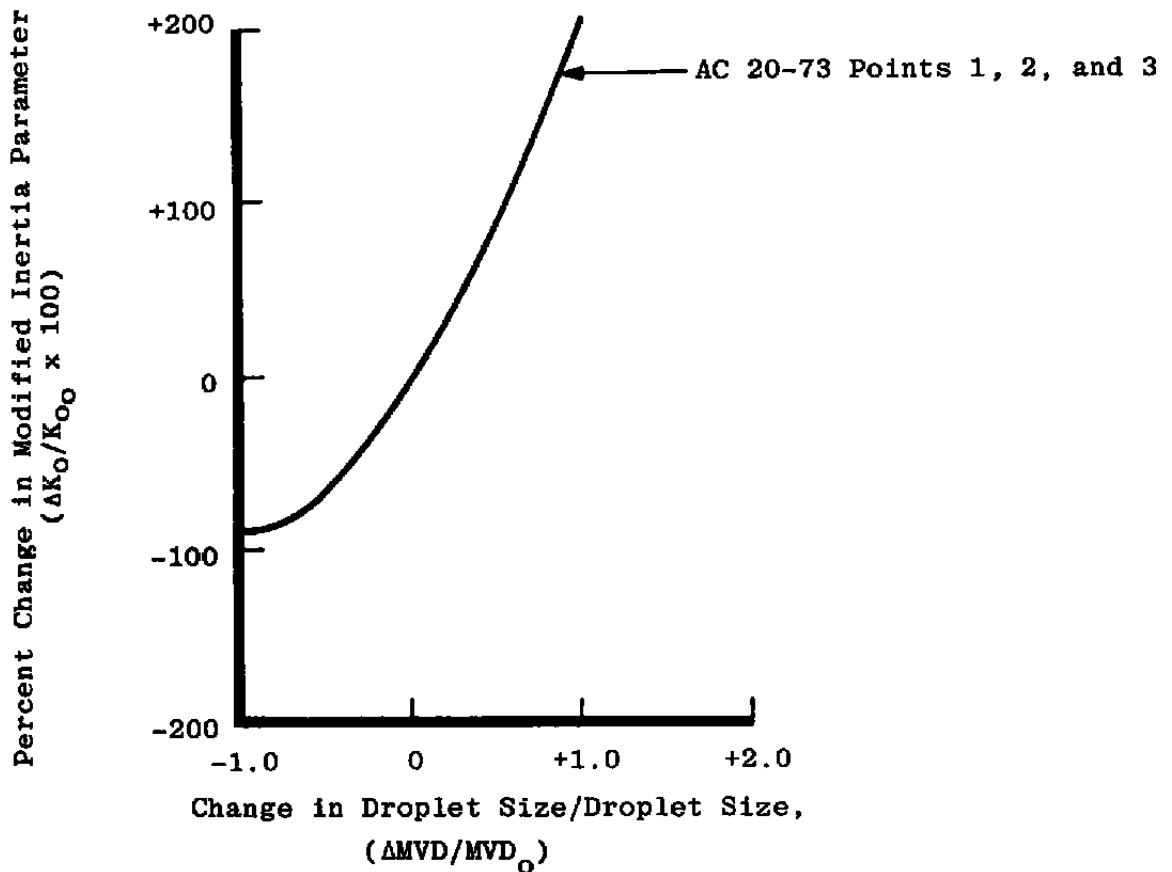
FIGURE 13. PERCENTAGE CHANGE IN MODIFIED INERTIA PARAMETER VERSUS NORMALIZED DROP SIZE FOR AN NACA 0012 AIRFOIL (6.0-IN. CHORD) AT 200 FT/SEC FLOW VELOCITY.
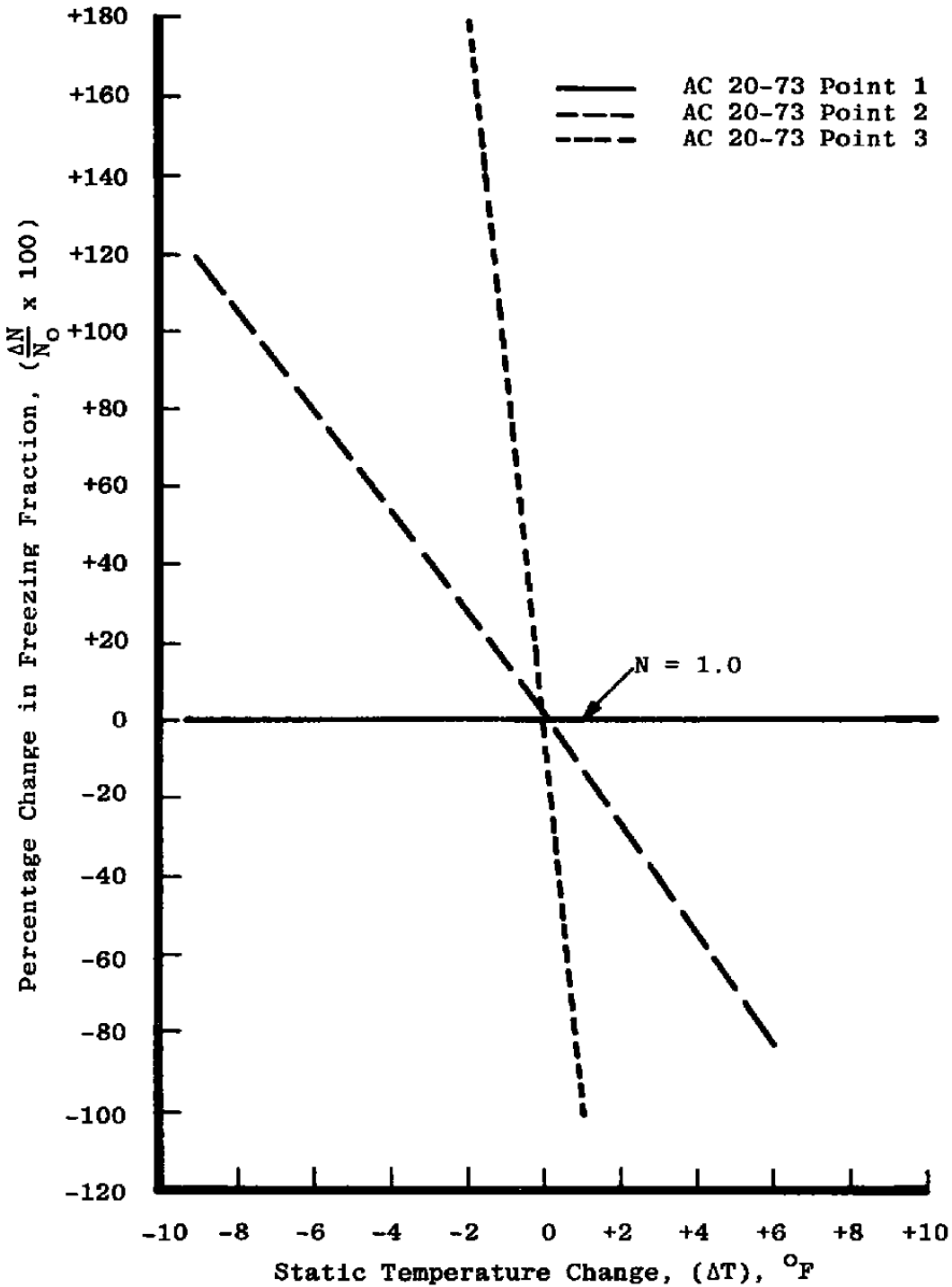
a. Effect of static temperature change

FIGURE 14. PERCENTAGE CHANGE IN FREEZING FRACTION AS TEST
CONDITIONS CHANGE FOR AN NACA 0012 AIRFOIL (6.0-IN.
CHORD) AT 200 FT/SEC FLOW VELOCITY.
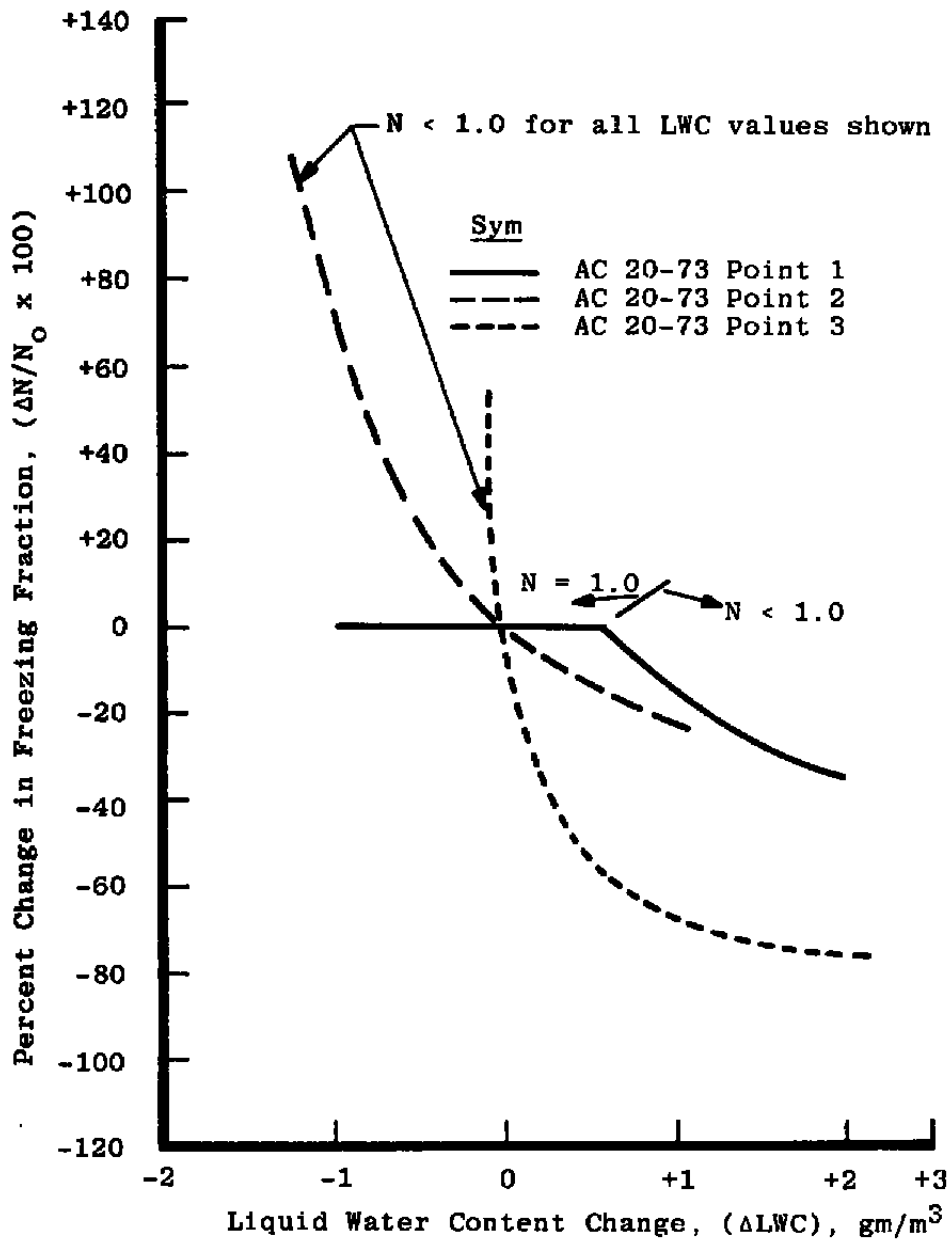
b. Effect of liquid water content changes

FIGURE 14. PERCENTAGE CHANGE IN FREEZING FRACTION AS TEST
CONDITIONS CHANGE FOR AN NACA 0012 AIRFOIL (6.0-IN.
CHORD) AT 200 FT/SEC FLOW VELOCITY (CONTINUED).
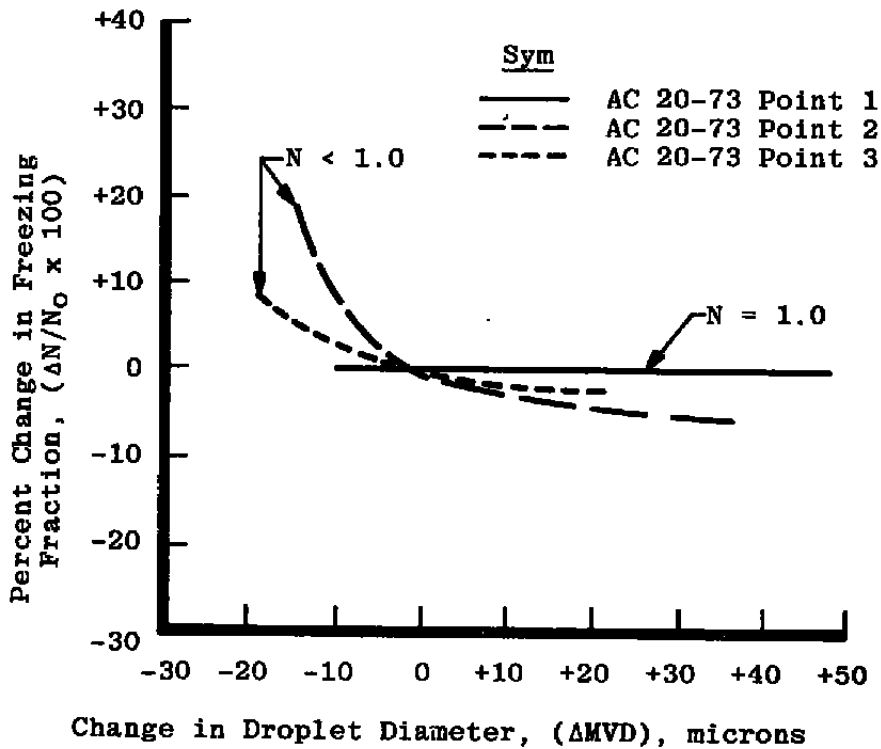
c. Effect of droplet size changes

FIGURE 14. PERCENTAGE CHANGE IN FREEZING FRACTION AS TEST
CONDITIONS CHANGE FOR AN NACA 0012 AIRFOIL (6.0-IN
CHORD) AT 200 FT/SEC FLOW VELOCITY (CONCLUDED).
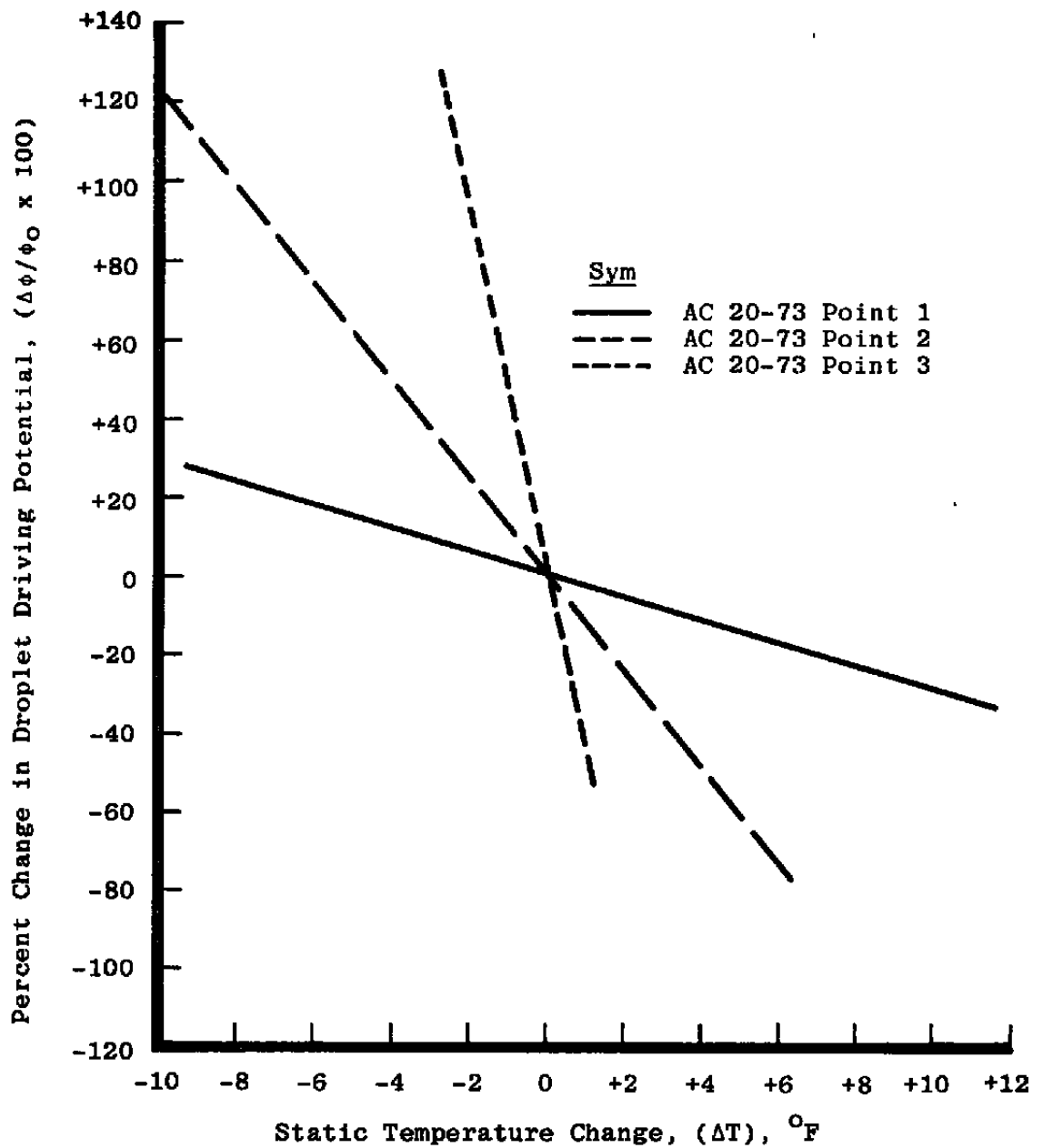
FIGURE 15. PERCENTAGE CHANGE IN DROPLET DRIVING POTENTIAL VERSUS CHANGE IN STATIC TEMPERATURE FOR AN NACA 0012 AIRFOIL (6.0-IN. CHORD) AT 200 FT/SEC FLOW VELOCITY.
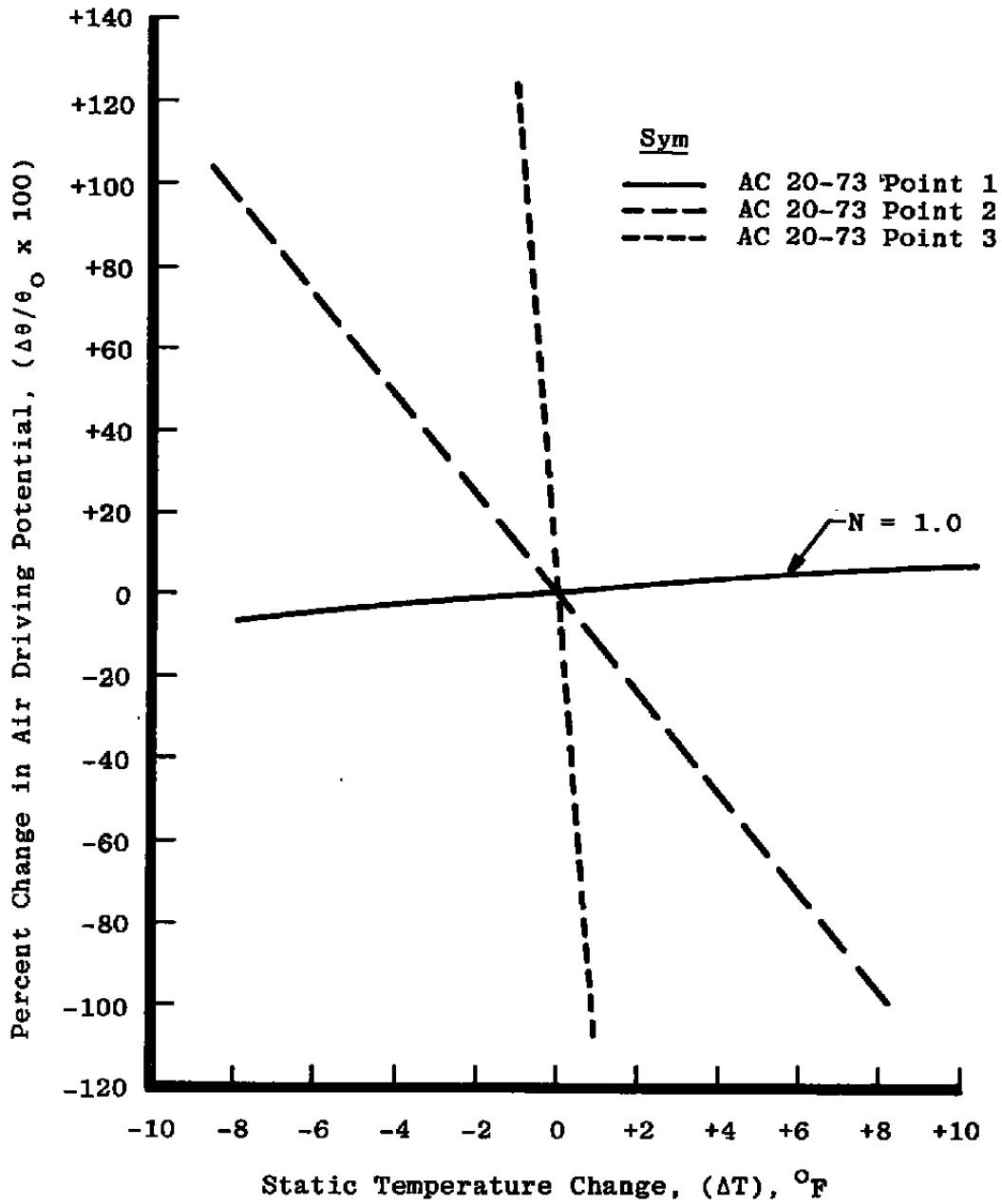
a. Effect of static temperature changes

FIGURE 16. PERCENTAGE CHANGE IN AIR DRIVING POTENTIAL AS THE TEST
CONDITIONS CHANGE FOR AN NACA 0012 AIRFOIL (6.0-IN. CHORD)
AT 200 FT/SEC FLOW VELOCITY.
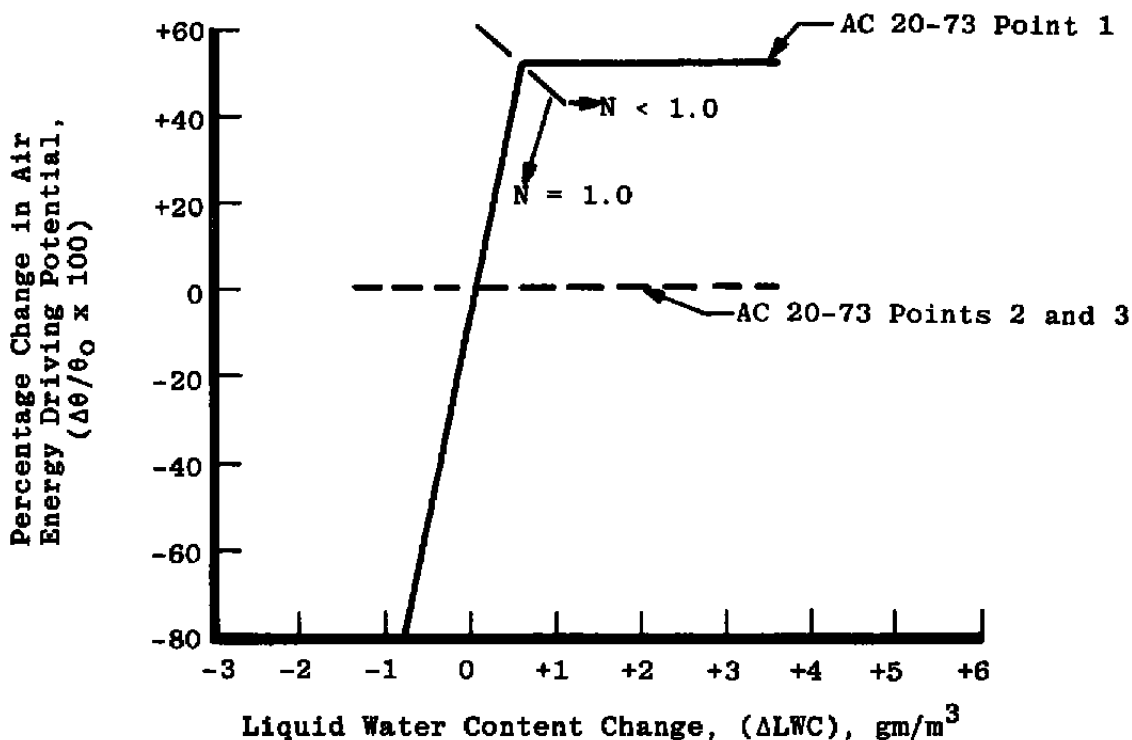
b. Effect of liquid water content
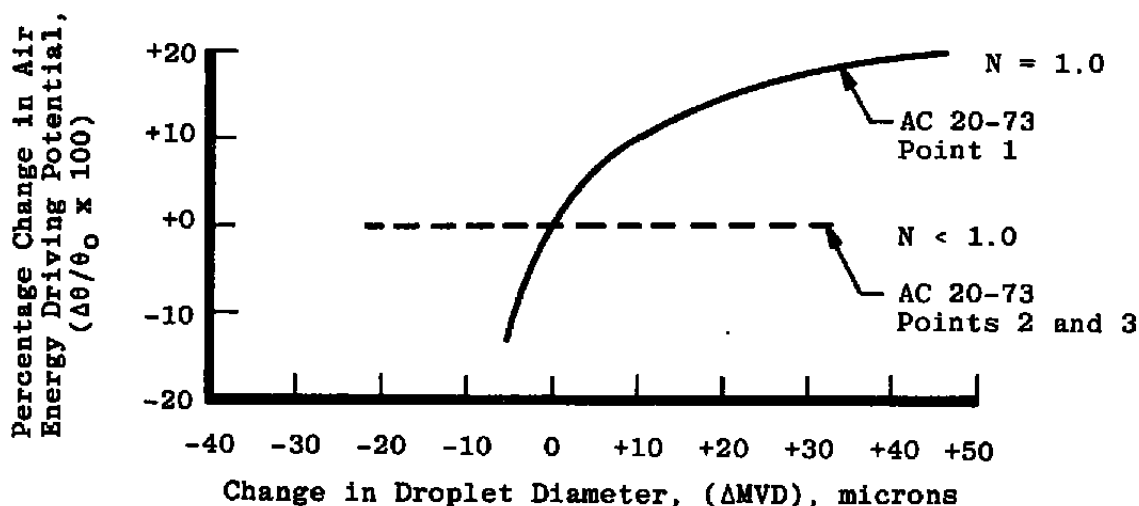
c. Effect of drop size

FIGURE 16. PERCENTAGE CHANGE IN AIR DRIVING POTENTIAL AS THE TEST
CONDITIONS CHANGE FOR AN NACA 0012 AIRFOIL (6.0-IN. CHORD)
AT 200 FT/SEC FLOW VELOCITY (CONCLUDED).
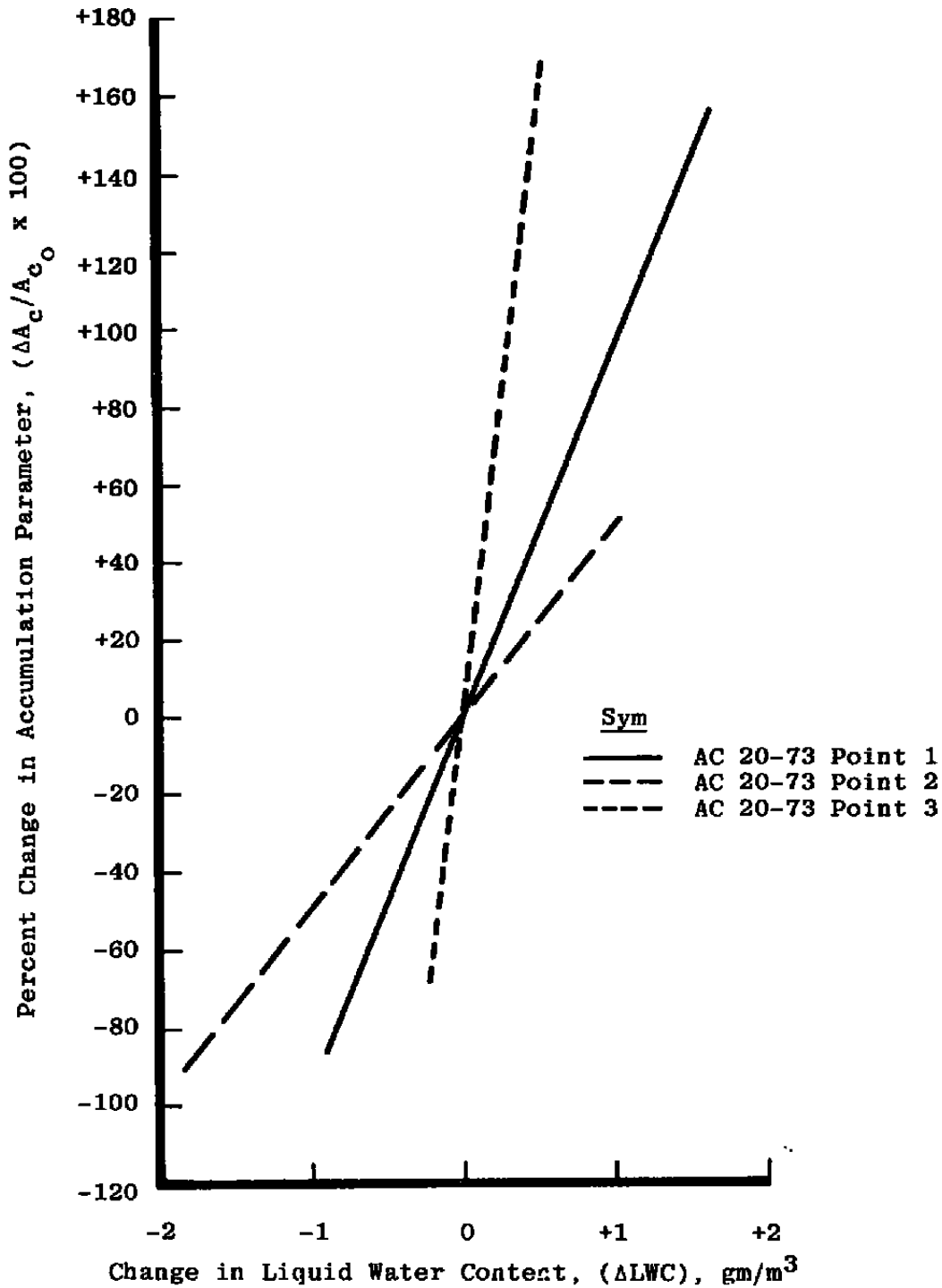
a. Effect of liquid water content changes

FIGURE 17. PERCENTAGE CHANGE IN ACCUMULATION PARAMETER AS TEST CONDITIONS CHANGE FOR AN NACA 0012 AIRFOIL (6.0-IN. CHORD) AT 200 FT/SEC FLOW VELOCITY.
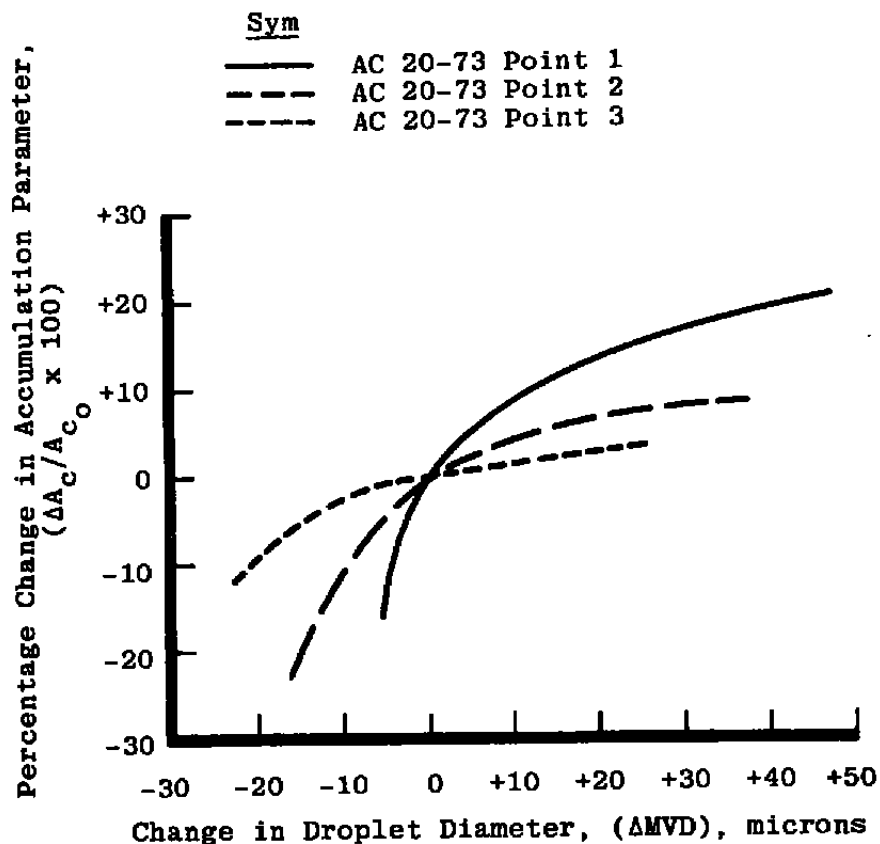
b. Effect of droplet size changes

FIGURE 17. PERCENT CHANGE IN ACCUMULATION PARAMETER AS TEST
CONDITIONS CHANGE FOR AN NACA 0012 AIRFOIL (6.0-IN.
CHORD) AT 200 FT/SEC FLOW VELOCITY (CONCLUDED).

73
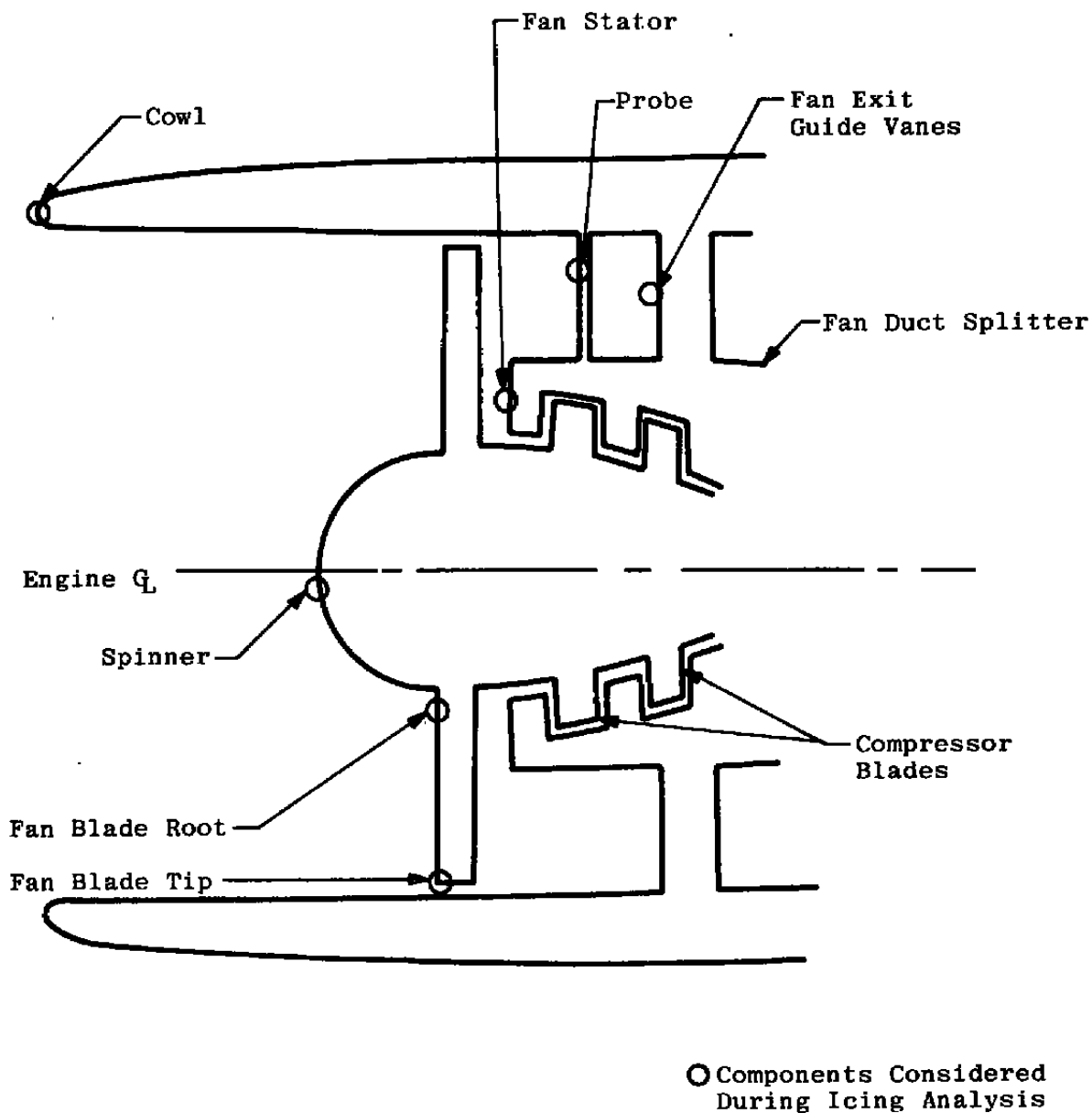
FIGURE 18. SCHEMATIC OF GENERIC ENGINE AND INLET SHOWING ICING COMPONENTS CONSIDERED DURING ANALYSIS.
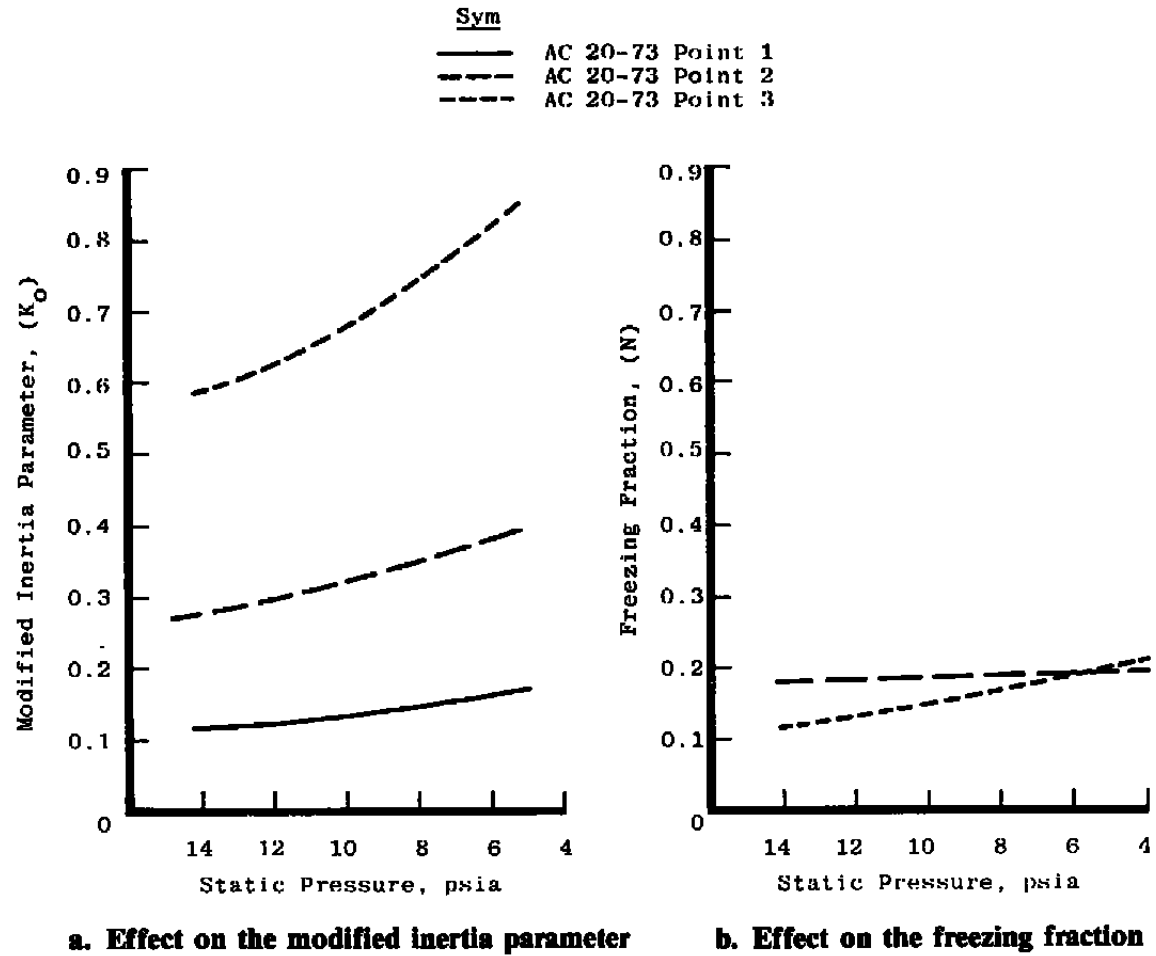
Sym

——— AC 20-73 Point 1
—— — AC 20-73 Point 2
— — — AC 20-73 Point 3

a. Effect on the modified inertia parameter   b. Effect on the freezing fraction

FIGURE 19. EFFECT OF STATIC PRESSURE ON THE SCALING PARAMETERS FOR AN NACA 0012 AIRFOIL (6.0-IN. CHORD) AT 200 FT/SEC FLOW VELOCITY.

Sym

—————— AC 20-73 Point 1
— — — AC 20-73 Point 2
- - - - AC 20-73 Point 3
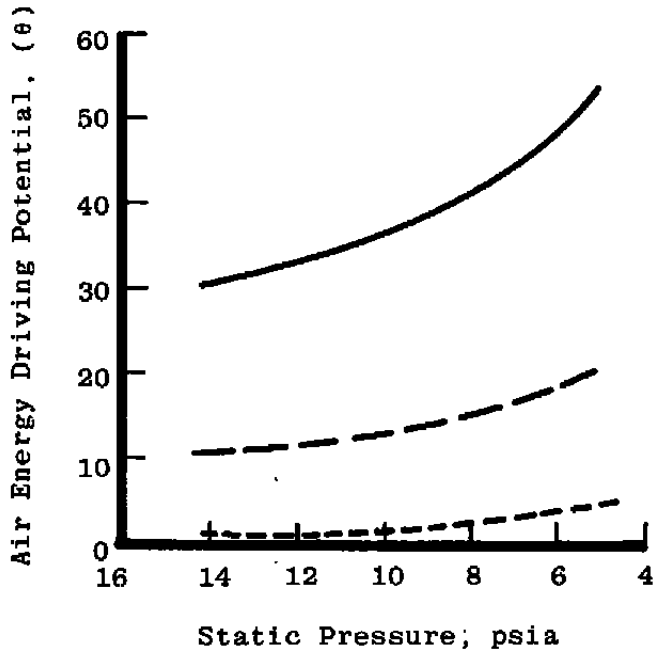
c. Effect on the air energy driving potential
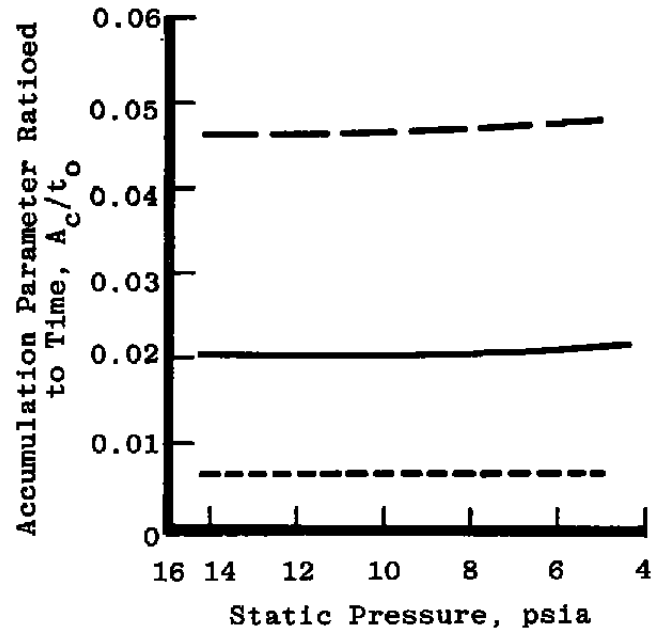
d. Effect on the accumulation parameter ratioed to time

FIGURE 19. EFFECT OF STATIC PRESSURE ON THE SCALING PARAMETERS FOR AN NACA 0012 AIRFOIL (6.0-IN. CHORD) AT 200 FT/SEC FLOW VELOCITY (CONCLUDED).
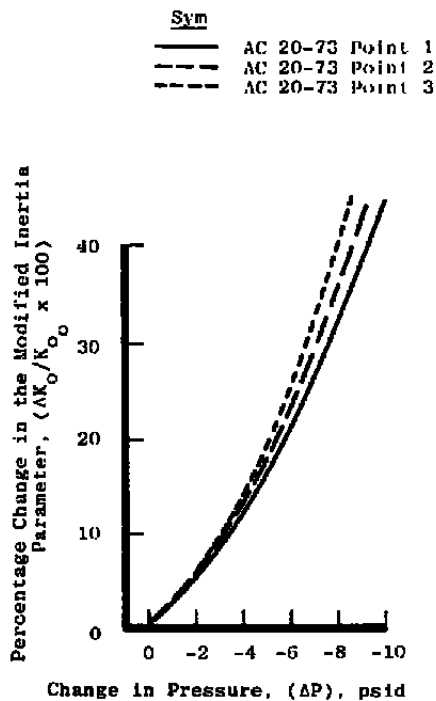
a. Effect on the modified inertia parameter
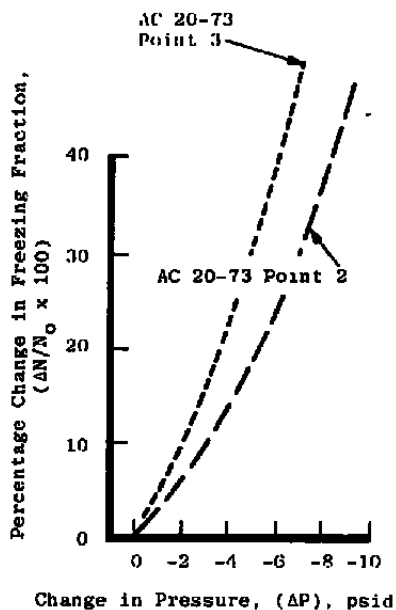
b. Effect on the freezing fraction

FIGURE 20. PERCENTAGE CHANGES IN THE SCALING PARAMETERS AS STATIC PRESSURE CHANGES FOR AN NACA 0012 AIRFOIL (6.0-IN. CHORD) AT 200 FT/SEC FLOW VELOCITY.

Sym

——— AC 20-73 Point 1
— — — AC 20-73 Point 2
— — — — AC 20-73 Point 3

Percentage Change in the Air Energy Driving Potential, ($\Delta\theta/\theta_o$ x 100)

110
100
90
80
70
60
50
40
30
20
10
0

0 -2 -4 -6 -8 -10

Change in Pressure, (ΔP), psid

c. Effect on the air energy driving potential

Percentage Change in Accumulation Parameter, ($\Delta A_c/A_{co}$ x 100)

6
5
4
3
2
1
0

0 -2 -4 -6 -8 -10

Change in Static Pressure, (ΔP), psid
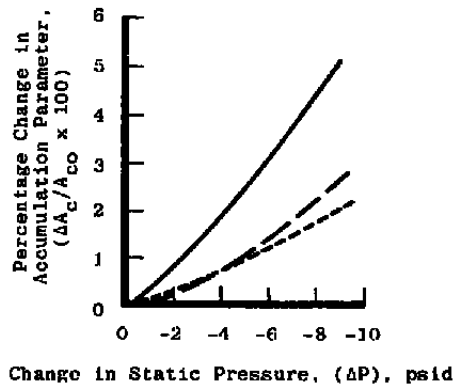
d. Effect on the accumulation parameter

FIGURE 20. PERCENTAGE CHANGES IN THE SCALING PARAMETERS AS STATIC PRESSURE CHANGES FOR AN NACA 0012 AIRFOIL (6.0-IN. CHORD) AT 200 FT/SEC FLOW VELOCITY (CONCLUDED).

TABLE 1. AC 20-73 ACCEPTABLE MEANS OF COMPLIANCE TEST POINTS AS USED FOR THIS STUDY

Icing Condition			
AC 20-73 Point	Liquid Water Content, gm/m^3	Static Temperature, °F	Droplet Diameter, microns
Point 1	1.0	−4	15
Point 2	2.0	23	25
Point 3	0.3	29	40

TABLE 2. ICING CONDITION VARIABLE VALUES TO OBTAIN ICING SIMILITUDE AT VARIOUS ICING TEMPERATURES FOR AN NACA 0012 AIRFOIL OF 6.0-IN. CHORD FOR AC 20-73 TEST POINT 1

Static Temperature T, °F	Static Pressure P, psia	Velocity V, ft/sec	Liquid Water Content LWC, gm/m³	Mean Volume Drop Diameter MVD, μm	Normalized Icing Time *
−3.5	18.4	112	1.52	19.9	1.18
−4.0**	14.2	200	1.00	15.0	1.00
−4.5	11.6	258	0.8	13.0	0.97
−5.0	9.7	307	0.67	11.7	0.98
−5.5	8.4	347	0.58	10.8	0.99
−6.0	7.4	385	0.52	10.0	1.00
−6.5	6.6	418	0.47	9.5	1.02
−7.0	5.9	450	0.43	9.1	1.04
−7.5	5.3	479	0.4	8.7	1.05
−8.0	4.9	507	0.37	8.3	1.07
−8.5	4.5	533	0.34	8.1	1.09
−9.0	4.1	560	0.32	7.8	1.11
−9.5	3.8	585	0.3	7.5	1.13
−10.0	3.5	610	0.29	7.3	1.15

Scaling Parameter Values: K_o = 0.119, A_c = 0.021, N = 1.00, ϕ = 35.3°R, θ = 30.5°R

* Normalized Icing Time = $\left(\dfrac{\text{Time}}{\text{Time At T} = -4°\text{F Conditions}}\right)$, t/t_o

** Initial Conditions

TABLE 3. ICING CONDITION VARIABLE VALUES TO OBTAIN ICING SIMILITUDE AT VARIOUS ICING TEMPERATURES FOR AN NACA 0012 AIRFOIL OF 6.0-IN. CHORD FOR AC 20-73 TEST POINT 2

Static Temperature T, °F	Static Pressure P, psia	Velocity V, ft/sec	Liquid Water Content LWC, gm/m³	Mean Volume Drop Diameter MVD, μm	Normalized Icing Time *
23.5	19.8	125	2.99	32.4	1.07
23.0**	14.2	200	2.00	25.0	1.00
22.5	11.2	253	1.58	21.6	1.00
22.0	9.1	300	1.31	19.3	1.02
21.5	7.8	338	1.14	17.8	1.04
21.0	6.7	375	1.01	16.5	1.06
20.5	6.0	408	0.91	15.6	1.08
20.0	5.4	436	0.84	14.9	1.09
19.5	4.9	465	0.77	14.2	1.11
19.0	4.5	490	0.72	13.7	1.13
18.5	4.2	515	0.68	13.2	1.14
18.0	3.9	538	0.64	12.8	1.16
17.5	3.6	563	0.61	12.4	1.17
17.0	3.4	585	0.58	12.1	1.18

Scaling Parameter Values: K_o = 0.274, A_c = 0.047, N = 0.18, ϕ = 8.19°R, θ = 10.9°R

* Normalized Icing Time = $\left(\dfrac{\text{Time}}{\text{Time At T} = 23°\text{F Condition}} \right)$, t/t_o

** Initial Conditions

TABLE 4. ICING CONDITION VARIABLE VALUES TO OBTAIN ICING SIMILITUDE AT VARIOUS ICING TEMPERATURES FOR AN NACA 0012 AIRFOIL OF 6.0-IN. CHORD FOR AC 20-73 TEST POINT 3

Static Temperature T, °F	Static Pressure P, psia	Velocity V, ft/sec	Liquid Water Content LWC, gm/m³	Mean Volume Drop Diameter MVD, μm	Normalized Icing Time *
29.5	29.5	131	0.82	77.00	0.56
29.0**	14.2	200	0.30	40.00	1.00
28.5	8.1	255	0.20	31.70	1.17
28.0	6.0	297	0.16	27.90	1.26
27.5	4.8	337	0.13	25.30	1.32
27.0	4.1	370	0.12	24.60	1.39
26.5	3.7	400	0.11	22.30	1.42
26.0	3.3	433	0.10	21.13	1.44
25.5	3.0	463	0.09	20.18	1.45
25.0	2.7	489	0.08	19.45	1.47
24.5	2.6	514	0.08	18.82	1.48
24.0	2.4	537	0.08	18.30	1.48
23.5	2.3	556	0.07	17.87	1.48
23.0	2.2	580	0.07	17.30	1.49

Scaling Parameter Values: $K_o = 0.581$, $A_c = 0.007$, $N = 0.12$, $\phi = 2.18°R$, $\theta = 1.44°R$

* Normalized Icing Time $= \left(\dfrac{\text{Time}}{\text{Time At T} = 29°\text{F Condition}} \right), t/t_o$

** Initial Conditions

TABLE 5. PARAMETER RANGES OF VERIFICATION FOR THE ICE SCALING MODEL

Parameter	Low	High
Velocity, (V), ft/sec	100	400
Static Pressure, (P), psia	4.4	14.2
Static Temperature, (T), °F	-5	32
Liquid Water Content, (LWC), gm/m^3	0.26	1.54
Droplet Diameter, (MVD), microns	10	31.0
Icing Time, (t), min	1.5	6.0

TABLE 6. FUNCTIONAL DEPENDENCIES OF THE SCALING PARAMETERS TO THE TEST CONDITION PARAMETERS

	T	P	LWC	MVD	V	t	c.
Droplet Energy Driving Potential (ϕ)	X	---	---	---	X	---	---
Air Energy Driving Potential (θ)	X	X	X	X	X	---	---
Modified Inertia Parameter (K_o)	—	X	---	X	X	—	X
Freezing Fraction (N)	X	X	X	X	X	---	X
Accumulation Parameter (A_c)	—	X	X	X	X	X	X

TABLE 7. SUMMARY OF PAST ICE SCALING INVESTIGATIONS

Scaling Analysis	Scaling Parameters					
	K_o	A_c	N	b	θ	ϕ
Douglas Aircraft Co., 1954 (Ref. 7)	X	X	---	---	---	—
Lockheed Aircraft Corp., 1955 (Ref. 8)	X	X	X	X	—	---
Boeing Airplane Co., 1962 (Ref. 9)	X	X	—	---	---	---
British Aircraft Corp., 1967 (Ref. 10)	X	X	X	X	---	---
ONERA Modane Centre, France, 1977 (Ref. 11)	X	X	X	X	X	X

TABLE 8. GENERIC ENGINE COMPONENTS AND SIMPLE MODELING GEOMETRIES

Component	Approximating Geometry	Characteristic Length, in. (See text)	Chord, in.
Cowl	NACA 0012 Airfoil	5	160
Spinner	Sphere	34	N/A
Fan Blade	NACA 0012 Airfoil	0.07	4.75
Fan Stator	NACA 0012 Airfoil	0.06	2.35
Exit Vane	NACA 0012 Airfoil	0.37	4.2
Probe	Cylinder	0.5	N/A

TABLE 9. GROUND IDLE ICING ANALYSIS RESULTS

Component	T_∞	T	P	V	LWC	MVD	K_0	THETA	PHI	A_c	N
Cowl (Flight Free-Stream Conditions)	−4	−4	13.2	209	1	15	0.01	29.8	35.2	0.0004	1.00
	1	1		210				31.0	30.2		1.00
	6	6		211				32.2	25.2		1.00
	11	11		212				28.1	20.1		0.86
	16	16		214				21.2	15.1		0.64
	21	21	13.2	215	1	15	0.01	13.8	10.1	0.0004	0.43
Spinner	−4	−1.7	13.4	127	1.23	15	0.03	24.2	33.4	0.0005	1.00
	1	3.3		127				25.0	28.4		1.00
	6	8.4		127				25.7	23.3		1.00
	11	13.4		128				26.8	18.3		1.00
	16	18.4		129				20.3	13.3		0.76
	21	23.4	13.4	129	1.23	15	0.03	12.8	8.3	0.0005	0.48
Fan Root	−4	−1.7	13.4	184	3.15	14.6	0.14	44.8	33.1	0.235	0.88
	1	3.3		184	3.16			38.8	28.1		0.71
	6	8.4		184	3.16			32.4	23.0		0.59
	11	13.4		185	3.15			25.7	17.9		0.46
	16	18.4		186	3.18			18.7	12.9		0.33
	21	23.4	13.4	186	3.18	14.6	0.14	11.6	7.9	0.235	0.20
Fan Tip	−4	−1.7	13.4	217	3.15	14.6	0.16	43.6	32.8	0.28	0.76
	1	3.3		217	3.16			37.6	27.8		0.65
	6	8.4		217	3.16			31.2	22.7		0.53
	11	13.4		218	3.15			24.5	17.7	0.28	0.41
	16	18.4		218	3.18			17.5	12.7	0.29	0.29
	21	23.4	13.4	218	3.18	14.6	0.16	9.4	7.6	0.29	0.17
Stator	−4	−0.2	13.5	117	2.83	14.4	0.2	41.2	31.9	0.28	1.00
	1	5.2		118				37.4	26.5	0.28	0.92
	6	10.3						31.0	21.4	0.28	0.76
	11	15.3			2.83	14.4		24.9	16.4	0.29	0.58
	16	20.3		118	2.85	14.3		17.7	11.4	0.29	0.41
	21	25.4	13.5	118	2.85	14.4	0.2	9.8	6.3	0.29	0.23
Exit Vane	−4	−0.2	13.5	117	2.83	14.3	0.11	44.8	31.9	0.15	0.60
	1	5.2		118	2.85			38.2	26.5	0.16	0.50
	6	10.3			2.89			31.7	21.4	0.19	0.41
	11	15.3			2.85			24.9	16.4		0.32
	16	20.3		118	2.87			17.7	11.4		0.22
	21	25.4	13.5	118	2.87	14.3	0.11	9.8	6.3	0.19	0.12
Probe	−4	−0.2	13.5	117	2.83	14.3	1.88	44.8	31.9	1.26	0.54
	1	5.2		118	2.85		1.88	38.2	26.5	1.26	0.46
	6	10.3			2.85		1.88	31.7	21.4	1.26	0.37
	11	15.3			2.85		1.89	24.9	16.4	1.28	0.29
	16	20.3		118	2.87		1.89	17.7	11.4	1.28	0.20
	21	25.4	13.5	118	2.87	14.3	1.89	9.8	6.3	1.28	0.11

TABLE 10. 0.5 MCT SEA-LEVEL ICING ANALYSIS RESULTS

Component	T_∞	T	P	V	LWC	MVD	K_0	THETA	PHI	A_c	N
Cowl (Flight	−20	−20	13.2	411	1	15	0.01	51.1	49.0	0.0013	1.00
Free-Stream	−15	−15	↓	413	↓	↓	↓	47.3	43.9	↓	0.91
Conditions)	−10	−10		415				41.6	38.9		0.79
	−4	−4		418				34.7	32.7		0.65
	1	1		420				28.5	27.6		0.54
	6	6		423				22.2	22.5		0.42
	11	11		425				15.7	17.5		0.31
	16	16	↓	427	↓	↓	↓	8.7	12.4	↓	0.19
	21	21	13.2	429	1	15	0.01	1.2	7.3	0.0013	0.06
Spinner	−20	−17.6	13.4	374	1.04	15	0.06	52.9	47.1	0.0035	0.82
	−15	−12.5	13.4	↓	1.04	↓	↑	47.4	42.0	↓	0.73
	−10	−7.3	13.5		1.05			41.6	36.7		0.64
	−4	−1.1						34.3	30.5		0.52
	1	4		↓				28.2	25.3		0.43
	6	9.3		374	↓			21.5	20.0	0.0035	0.33
	11	14.4		373	1.05			14.7	14.9	0.0031	0.23
	16	19.6	↓	373	1.06	↓	↓	7.3	9.6	0.0031	0.13
	21	24.8	13.5	373	1.06	15	0.06	−0.7	4.4	0.0031	0.07
Fan Root	−20	−17.6	13.4	671	1.76	14.5	0.3	24.8	41.5	0.52	0.60
	−15	−12.5	13.4	671	1.76	↓	↓	19.3	36.3	↓	0.49
	−10	−7.3	13.5	671	1.76			13.5	31.0		0.38
	−4	−1.1		670	1.78			6.4	24.7		0.25
	1	4			1.78			0.2	19.4	↓	0.14
	6	9.3			1.78			−6.5	14.0	0.52	0.03
	11	14.4			1.79			−7.7	8.8	0.53	0
	16	19.6	↓	↓	1.80	↓	↓	−7.2	3.5	0.53	0
	21	24.8	13.5	670	1.80	14.5	0.3	−6.5	−1.9	0.53	0
Fan Tip	−20	−17.6	13.4	822	1.76	14.5	0.34	4.6	37.5	0.64	0.34
	−15	−12.5	13.4	↓	1.76	↓	↓	−1.0	32.2	0.64	0.24
	−10	−7.3	13.5		1.76			−6.7	26.8	0.64	0.13
	−4	−1.1			1.78			−9.1	20.4	0.65	0.01
	1	4		↓	1.78			−10.8	15.2	0.65	0
	6	9.3		822	1.78			−11.7	9.7	0.65	0
	11	14.4		824	1.79			−11.8	4.4	0.66	0
	16	19.6	↓	821	1.80	↓	↓	−10.8	−1.0	0.66	0
	21	24.8	13.5	821	1.80	14.5	0.34	−9.6	−6.5	0.66	0

TABLE 10. 0.5 MCT SEA-LEVEL ICING ANALYSIS RESULTS (CONCLUDED)

Component	T_∞	T	P	V	LWC	MVD	K_0	THETA	PHI	A_c	N
Stator	−20	−1.4	14.6	529	1.60	14.3	0.49	21.0	28.1	0.72	0.52
	−15	6.5		529	1.60		0.50	11.8	20.1		0.32
	−10	11.7		529	1.61		0.50	5.2	14.9		0.18
	−4	17.9		528	1.62		0.51	−3.4	8.6		0.01
	1	23		528	1.62		0.51	−3.6	3.4		0
	6	28.3	14.6	528	1.62	14.3	0.51	−3.3	−2.1	0.72	0
	11	>32									
	16	>32									
	21	>32									
Exit Vane*	−20	−1.4	14.6	529	1.60	14.1	0.28	21	28.1	0.42	0.34
	−15	6.5		529	1.60			11.6	20.1	0.42	0.22
	−10	11.7		529	1.61			4.4	14.9	0.42	0.14
	−4	17.9		528	1.63			−3.4	8.6	0.43	0.04
	1	23		528	1.63			−6.6	3.4	0.43	0
	6	28.3	14.6	528	1.63	14.1	0.28	−6.2	−2.1	0.43	0
	11	>32									
	16	>32									
	21	>32									
Probe	−20	−1.4	14.6	529	1.62	14.1	4.74	21.6	28.1	3.6	0.32
	−15	6.5		529	1.62		4.74	11.6	20.1	3.6	0.21
	−10	11.7		529	1.62		4.74	4.9	14.9	3.6	0.13
	−4	17.9		528	1.63		4.70	−3.4	8.6	3.7	0.04
	1	23		528	1.63		4.70	−7.3	3.4	3.7	0
	6	28.3	14.6	528	1.63	14.1	4.70	−6.8	−2.1	3.7	0
	11	>32									
	16	>32									
	21	>32									

TABLE 11. VARIATIONS OF ICING CONDITION PARAMETERS AND SCALING PARAMETERS FOR VARIOUS ENGINE COMPONENTS AT GI

Component	T_∞	T	P	V	LWC	MVD	K_0	N	THETA	PHI	A_c
Free-Stream	−4	−4.0	13.2	209	1.00	15.0	---	---	---	---	---
Cowl		−4.0	13.2	209	1.00	15.0	0.01	1.00	29.8	35.2	0.0004
Spinner		−1.7	13.4	127	1.23	15.0	0.03	1.00	34.2	33.4	0.0005
Fan Root		−1.7	13.4	184	3.15	14.6	0.14	0.83	44.8	33.1	0.2350
Fan Tip		−1.7	13.4	217	3.15	14.6	0.16	0.76	43.6	32.8	0.2800
Stator		−0.2	13.5	117	2.83	14.4	0.20	1.00	41.2	31.9	0.2800
Exit Vane		−0.2	13.5	117	2.83	14.3	0.11	0.60	44.8	31.9	0.1500
Probe	−4	−0.2	13.5	117	2.83	14.3	1.88	0.54	44.8	31.9	1.2600

TABLE 12. VARIATIONS OF ICING CONDITION PARAMETERS AND SCALING PARAMETERS FOR VARIOUS ENGINE COMPONENTS AT 50-PERCENT MAXIMUM CONTINUOUS THRUST

Component	T_∞	T	P	V	LWC	MVD	K_0	N	THETA	PHI	A_c
Free-Stream	−4	−4	13.2	418	1.00	15.0	---	---	---	---	---
Cowl		1.1	13.2	418	1.00	15.0	0.01	0.65	34.7	32.7	0.0013
Spinner			13.5	374	1.05	14.5	0.06	0.52	34.3	30.5	0.0035
Fan Root			13.5	670	1.78	14.5	0.30	0.25	6.4	24.7	0.5200
Fan Tip		−1.1	13.5	822	1.78	14.5	0.34	0.01	−9.1	20.4	0.6400
Stator		17.9	14.6	529	1.61	14.3	0.51	0.01	−3.4	8.6	0.7200
Exit Vane		17.9	14.6	529	1.61	14.1	0.28	0.04	−3.4	8.6	0.4200
Probe	−4	17.9	14.6	529	1.63	14.1	4.74	0.04	−3.4	8.6	3.6000

TABLE 13. ICING CONDITION PARAMETER VALUES TO OBTAIN ICING SIMILITUDE AT VARIOUS PRESSURE ALTITUDES FOR AN NACA 0012 AIRFOIL OF 6.0-IN. CHORD FOR AC 20-73 TEST POINT 1

Altitude, ft	P, psia	T, °F	V, ft/sec	LWC, gm/m^3	MVD, μm	t/t_o
1,000	14.2	−4	200	1.00	15.0	1.00
5,000	12.4	−4.3	239	0.85	13.6	0.98
10,000	10.1	−4.9	297	0.69	11.9	0.97
15,000	8.3	−5.5	350	0.58	10.8	0.99
20,000	6.8	−6.4	409	0.48	9.7	1.01
25,000	4.3	−8.7	542	0.34	8.0	1.10

TABLE 14. ICING CONDITION PARAMETER VALUES TO OBTAIN ICING SIMILITUDE AT VARIOUS PRESSURE ALTITUDES FOR AN NACA 0012 AIRFOIL OF 6.0-IN. CHORD FOR AC 20-73 TEST POINT 2

Altitude, ft	P, psia	T, °F	V, ft/sec	LWC, gm/m^3	MVD, μm	t/t_o
1,000	14.2	23.0	200	2.00	25.0	1.00
5,000	12.4	22.7	230	1.74	22.9	1.00
10,000	10.1	22.3	275	1.44	20.4	1.01
15,000	8.3	21.7	321	1.21	18.4	1.03
20,000	6.8	21.0	373	1.01	16.6	1.06
30,000	4.3	18.8	504	0.70	13.4	1.14

TABLE 15. ICING CONDITION PARAMETER VALUES TO OBTAIN ICING
SIMILITUDE AT VARIOUS PRESSURE ALTITUDES FOR AN
NACA 0012 AIRFOIL OF 6.0-IN. CHORD FOR AC 20-73 TEST
POINT 3

Altitude, ft	P, psia	T, °F	V, ft/sec	LWC, gm/m^3	MVD, μm	t/t_o
1,000	14.2	29.0	200	0.30	40.0	1.00
5,000	12.3	28.9	212	0.27	37.7	1.04
10,000	10.1	28.7	231	0.23	34.7	1.11
15,000	8.3	28.5	252	0.20	32.1	1.16
20,000	6.8	28.2	279	0.18	29.4	1.22
30,000	4.4	27.2	358	0.12	24.2	1.34

TABLE 16. ICING CONDITION PARAMETER VALUES TO OBTAIN ICING
SIMILITUDE AT ALTITUDE DESCENT FOR AN NACA 0012 AIR-
FOIL OF 6.0-IN. CHORD FOR AC 20-73 TEST POINT 2

Altitude, ft	P, psia	T, °F	V, ft/sec	LWC, gm/m^3	MVD, μm	t/t_o
20,000	6.8	23.0	200	2.00	25.0	1.00
19,000	7.0	23.2	179	2.16	26.4	1.04
18,500	7.5	23.4	145	2.47	29.0	1.12
16,000	8.0	23.6	100	3.08	34.2	1.30
15,000	8.33	23.7	64	3.92	41.3	1.59
14,000	8.50	23.8	30	5.79	56.8	2.30

APPENDIX A

ICE SCALING SYNOPSIS

Ice scaling is a test procedure which is used to form similar ice accretions on ice collection geometries under different icing test conditions of temperature (T), liquid water content (LWC), droplet size (MVD), air velocity (V), and static pressure (P). In Ref. 5, Ruff fully describes the ice scaling process, limitations, experimental verification, and math model used to predict ice scaling. This is an involved and detailed report, parts of which will be presented here to aid in the understanding of ice scaling technique.

The ice scaling parameters are reference quantities obtained from modeling the physical process of ice accretion. The ice scaling parameters, when held constant between two different icing test conditions, allow the results of one condition to predict the results of the other condition. For scaling to be effective, four areas of the physical process are evaluated: (1) flow field about the body; (2) droplet trajectory and impingement; (3) surface mass collection; and (4) surface thermodynamics.

Each of these areas must be considered in the ice scaling process.

Assumptions made and limitations existing in the scaling work are presented here. The icing surfaces are unheated surfaces reaching equilibrium surface temperature. The conductive heat-transfer rate between different test conditions is the same. Complex geometries and high angles of attack are not considered. The assumption is also made that similarity of ice shapes is held. As will be seen in the following sections, if similarity is not held many of the analysis techniques are invalid.

This report addresses only icing caused by supercooled clouds and does not address other icing hazards that may exist such as freezing rain, hail, ice storms, or snow storms.

FLOW FIELD SCALING.

Since the concept discussed here concerns possible parameter substitution for a particular set of engine hardware, it can be assumed that the flow field about the body will be similar since the body itself is not changed. As long as similar geometric ice shapes are formed between different test conditions, which must be criteria for successful ice scaling, the flow field will also be scaled. All ice scaling equations used have been experimentally verified in the AEDC icing research wind tunnel for simple geometries such as cylinders, spheres, and NACA

0012 airfoils at low angles of attack. For complex geometries or high angles of attack, flow field scaling has not been verified and is not necessarily applicable in ice scaling work.

DROPLET TRAJECTORY SCALING.

A droplet trajectory scaling parameter is required to produce similar mass distributions and droplet impingement on the collection surface. The distribution and impingement scaling can be ensured by maintaining the local (β) and total (E_m) surface collection efficiency constants (see Fig. A-1), and by holding the droplet impingement limits equal at different test conditions. Much work has been done on study of droplet trajectories (Ref. 12). The modified inertia parameter (K_o) is used as a scaling parameter to ensure similar values of β and E_m, thereby ensuring similar droplet distribution on the collection surface (Ref. 13). K_o is given by:

$$K_o = (\lambda/\lambda_s)\, K$$

where

$$K = \frac{2}{9}\, \frac{\varrho_w r_d^2\, U_\infty}{\mu_a c}$$

and λ/λ_s is defined as the range parameter in Ref. 12.

SURFACE MASS COLLECTION SCALING.

The accumulation parameter A_c can be described as the total mass of impinging water W_w divided by the ice density and based on a per characteristic length (c) basis where

$$W_w = LWC(U_\infty)\, \beta t$$

and

$$A_c = \frac{LWC(U_\infty)\, \beta t}{\varrho_i c}$$

Holding A_c constant ensures the total mass of water catch is the same. In parameter substitution scaling where the body geometry and thus the characteristic length (c) is constant, and similar ice with corresponding similar density is formed, the A_c parameter can be held constant by holding the product of LWC, U_∞, and t constant between different test points.

The A_c term does assume that the droplet impingement between test points is scaled; therefore, A_c can be applied only if K_o is held constant.

SURFACE THERMODYNAMICS SCALING.

The first law of thermodynamics is used to develop the model of the ice accretion surface thermodynamics. The control volume is taken as the icing surface. The surface mass balance (Fig. A-2) can be given as

$$w_w - w_e - w_r = w_i \qquad \text{where} \qquad w_w \rightarrow \text{impinging liquid}$$

$$w_e \rightarrow \text{evaporation}$$

$$w_r \rightarrow \text{runback}$$

$$w_i \rightarrow \text{ice accumulation}$$

The energy balance can be given generally as

$$Q_{C.V.} + \Sigma m_i \left(i_i + \frac{U_i^2}{2g_c J} + Z_i \frac{g}{g_c} \right) = \Sigma m_e \left(i_e + \frac{U_e^2}{2g_c J} + Z_e \frac{g}{g_c} \right) + E_{stored} + W_{C.V.}$$

Specifically, for an unheated icing surface the equation for the energy balance (see Fig. A-3) can be given by

$$W_w i_{w,T} \Delta s = W_e i_{v,sur} \Delta s + w_r i_{w,sur} + W_i i_{i,sur} \Delta s + q_c \Delta s + q_k \Delta s$$

The evaluation of the above terms has been taken from Ref. 5. The resulting equation, similar to that derived by Messinger (Ref. 14) can be given by

$$W_w \overset{\text{impinging liquid}}{\left| c_{P_{w,s}} (T_s - 32) + \frac{U_\infty^2}{2g_c J} \right|} = W_e \overset{\text{evaporation}}{\left| c_{P_{w, sur}} (T_{sur} - 32) + L_v \right|}$$

93

runback

$$+ \left| (1 - n) W_w - W_e \right| c_{P_{w, sur}} (T_{sur} - 32)$$

ice accumulation   convection

$$+ MW_w \left| c_{P_{i,sur}} (T_{sur} - 32) - L_f \right| + h_c \left| T_{sur} - T_s - \frac{U_\infty^2}{2g_c J \, c_{pair}} \right| + q_k$$

where

c_p	~	specific heat	subscripts: e	~	evaporative
L_f	~	latent heat of fusion	w	~	liquid water
L_v	~	latent heat of vaporization	i	~	ice
W	~	mass flux	s	~	static
U_∞	~	free-stream velocity	sur	~	surface
n	~	freezing fraction			
h_c	~	convective heat-transfer coefficient			
q_k	~	conductive heat transfer			

rearranging

$$-B\phi = \theta + (1 - n) \frac{W_w}{h_c} \left| c_{P_{w,sur}} (T_{sur} - 32) \right| + n \frac{W_w}{h_c} \left| c_{P_{i,sur}} (T_{sur} - 32) - L_f \right|$$

where

$$B = \frac{W_w c_{P_{w,s}}}{h_c} \qquad \sim \quad \text{relative heat factor}$$

$$\phi = 32 - T_s - \frac{U_\infty^2}{2g_c J \, c_{P_{w,s}}} \qquad \sim \quad \text{droplet driving potential}$$

$$\theta = \left| T_{sur} - T_s - \frac{U_\infty^2}{2g_c J \, c_{P_{air}}} \right| + \frac{W_e}{h_c} L_v \quad \sim \quad \text{air driving potential}$$

The relative heat factor (B) is defined as a measure of the ratio of the sensible heat absorbing capacity of the impinging supercooled liquid per unit area to the convective heat dissipating

capacity of the surface. This term is geometry dependent since it depends on the convective heat-transfer coefficient. (B) may also be written as

$$B = \frac{LWC\beta U_\infty c_{p_{W,S}}}{h_c}$$

showing that, for everything else held constant, an increase in LWC requires a decrease in U_∞ for B to remain constant.

The droplet driving potential (ϕ) and the air driving potential (θ) describe the energy transfer potential of the droplets and air, respectively. They are analogous to the ΔT term of the classic heat-transfer equation

$$q_c = h_c \, A \, (\Delta T)$$

One should note that (θ) is dependent on the value of pressure through the evaporation terms, while both ϕ and θ are functions of T_s since this term appears explicitly in the definitions.

The freezing fraction (N) is defined as the fraction of the total impinging liquid which freezes at any point on impact with the surface. The results of analytical and empirical studies indicate that rime ice corresponds to a freezing fraction of unity, and as (N) approaches zero the ice tends to become more glaze-like in appearance. For values of (N) less than ≈ 0.3, the ice characteristics are completely glaze.

Recall that the above analysis is for an unheated icing surface; that is, there is no external heat added to the icing surface. A different analysis must be performed for heated surfaces. The conductive heat-transfer term (q_k) is dependent on the thermal conductivity of the skin. In parameter substitution the thermal conductivity of the collection surface is constant. It is assumed that the conductive heat flow rate between different test conditions will be the same, and to simplify the energy balance the conductive heat-transfer term was dropped. This assumption will not change similitude conditions but the absolute value of the surface temperature and freezing fraction may be affected.

SUMMARY.

In Ref. 5 Ruff shows that similitude between different icing conditions can be obtained if the following scaling parameters are maintained as constant values.

K_o ~ modified inertia parameter

A_c ~ accumulation parameter

ϕ ~   droplet driving potential

θ ~   air driving potential

N   ~   freezing fraction

Maintaining the values of these parameters has been shown to be sufficient, although they may or may not all be necessary.

A limitation on the velocity range for applicability of the icing scaling method will be imposed. A lower limit of free-stream velocity corresponding to a free-stream Reynolds number of ~200,000 and an upper limit of ~400 ft/sec will be used since these values were used by Ruff (Ref. 5). Table 5 gave the ranges over which the scaling process was experimentally verified. The upper range limits set by Ruff were attributable to facility constraints encountered during experimental verification of scaling laws and do not necessarily represent a limit of the scaling laws themselves.

SAMPLE CASE.

A sample case of the icing scaling code follows.

The specified icing test point conditions are

T =   23.00°F

P =   14.2 psia

LWC   =   2.0 gm/m^3

MVD   =   25 μm

t =   1.0 min

V =   200 ft/sec

The test article is an NACA 0012 air foil of 6-in. chord and 0.19-in. leading edge diameter.

At this condition the following values of the scaling parameters are calculated by the model.

K_o =   0.274

N =   0.181

θ =   10.94

ϕ =   8.19

A_c =   0.046

For some reason the value of V cannot be met, and the value that must be used is V = 120 ft/sec. The icing scaling code maintains the value of the scaling parameters and calculates new values of the icing conditions to achieve V = 120 ft/sec.

The new test conditions are:

$$
\begin{aligned}
V &= 120 \ \text{ft/sec} \\
T &= 23.51°F \\
P &= 20.22 \ \text{psia} \\
LWC &= 3.08 \ \text{gm/m}^3 \\
MVD &= 33.1 \ \mu\text{m} \\
t &= 1.08 \ \text{min}
\end{aligned}
$$
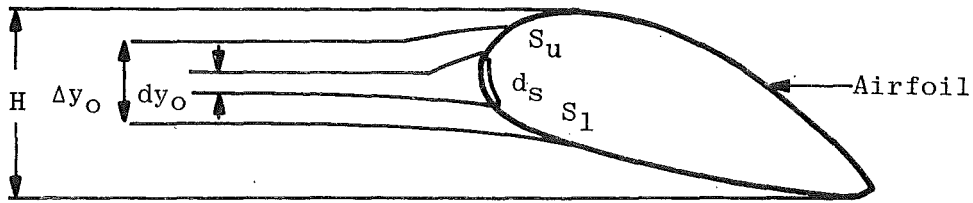
H $\sim$ projected height of airfoil

S_u $\sim$ upper surface impingement limit for given droplet size

S_1 $\sim$ lower surface impingement limit for given droplet size

Δy_0 $\sim$ projected impingement height

dy_0 $\sim$ projected incremental impingement height

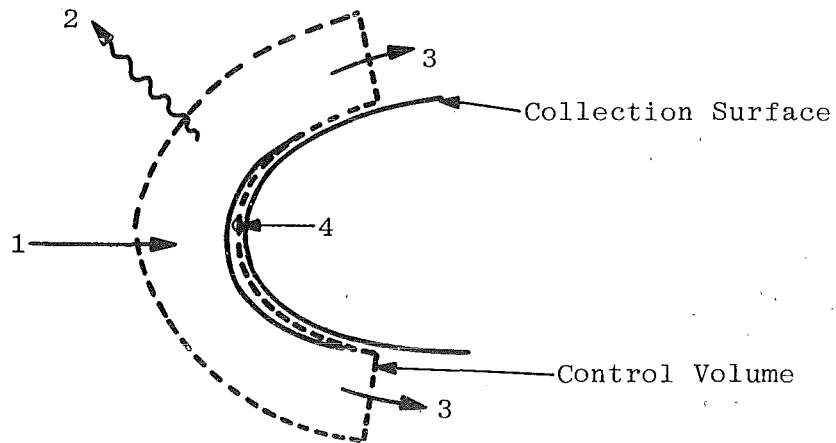d_s $\sim$ incremental impingement limits

Total Collection Efficiency

$$EM = \frac{\Delta y_0}{H}$$

Local Collection Efficiency

$$\beta = \frac{dy_0}{ds}$$

$$EM = \frac{1}{H} \int_{S_1}^{S_u} \beta \, ds$$

FIGURE A-1. ILLUSTRATION OF TOTAL AND LOCAL DROPLET COLLECTION EFFICIENCIES.

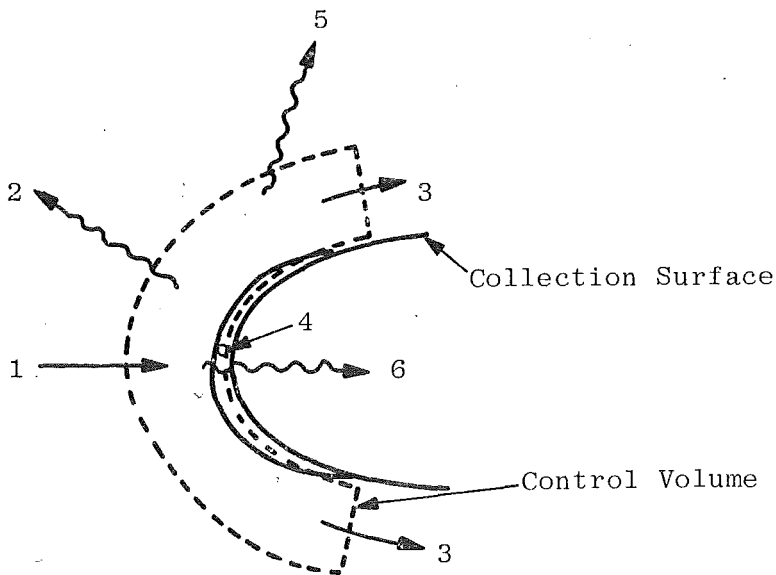Mass Balance, Icing Surface

$$w_w - w_e - w_r = w_c$$

where 	w_w = Impinging liquid 	(1)

	w_e = Evaporation 	(2)

	w_r = Runback 	(3)

	w_i = Ice accumulation 	(4)

FIGURE A-2. MASS BALANCE ON A SURFACE EXPOSED TO AN ICING CLOUD.

Energy Balance, Unheated Icing Surface

$$W_w \, i_{w,t} \, \Delta S = W_e \, i_{v,sur} \, \Delta S + W_r i_{w,sur} + W_i \, i_{i,sur} \, \Delta S + q_c \Delta S + q_k \Delta S$$

where

$$W_w i_{w,t} \; \Delta S = \text{Impinging liquid} \quad (1)$$

$$\dot{W}_e i_{v,sur} \; \Delta S = \text{Evaporation} \quad (2)$$

$$W_r i_{w,sur} = \text{Runback} \quad (3)$$

$$W_i i_{i,sur} \; \Delta S = \text{Ice accumulation} \quad (4)$$

$$g_c \; \Delta S = \text{Convection} \quad (5)$$

$$g_k \; \Delta S = \text{Conduction} \quad (6)$$

FIGURE A-3. ENERGY BALANCE ON AN UNHEATED SURFACE EXPOSED TO AN ICING CLOUD.

APPENDIX B

CLOUD INGESTION AND ICE ACCUMULATION

This section briefly describes some of the analytical procedures used to study the behavior of the icing cloud as it is ingested by the engine. The effects of engine flow path blockage and droplet impingement on engine hardware are important in the determination of LWC and MVD throughout the engine. Some discussion of ice accumulation is also given.

The analyses are similar to those of Ref. 5. The interested reader should consult this work for a more detailed approach and analysis.

The amount of water ingested by the inlet is dependent on the aircraft flight speed, the engine airflow requirements, the amount of liquid water present in the atmosphere, the size of the water drops, and the geometry of the inlet. The ratio of the inlet air velocity to the free-stream flight velocity will help determine whether the engine/inlet is gulping or spilling air. These processes are depicted by the stream tubes in Fig. B-1 taken from Ref. 3.

With knowledge of the flight and inlet velocities, and that the airflow through the stream tube is constant, the location of the stream tube boundaries may be found. For the compressor face (CF) and flight (∞) conditions

$$\varrho_\infty A_\infty V_\infty = \varrho_{CF} A_{CF} V_{CF}$$

rearranged as

$$\frac{V_\infty}{V_{CF}} = \frac{\varrho_{CF} A_{CF}}{\varrho_\infty A_\infty}$$

If $V_\infty/V_{CF} > 1$, the engine is gulping. If $V_\infty/V_{CF} < 1$, the engine is spilling.

If the engine is gulping, the LWC at the inlet is greater than the free-stream value; the reverse is true if the engine is spilling.

Knowledge of the droplet trajectories is also of importance since small drops tend to follow streamlines and large drops do not. To help define the role that drop size has in the water ingestion process, the concentration factor (C_t) is used (Ref. 6) and the effect of droplet size is shown in Fig. B-1 (Ref. 15). Infinitely small drops will follow streamlines, making the C_t

101

approximately equal to the ratio of inlet velocity to free-stream velocity while infinitely large drops will make the C_t equal to 1.0. Actual icing clouds contain droplets that fall somewhere in between.

Utilizing C_t and assuming LWC is uniform through a stream tube cross section, the water catch may be calculated. The factor C_t is the ratio of water ingested by the engine inlet (area A_I) to the water contained in the free-stream tube (A_∞) as shown in Fig. B-1. The water ingestion can be found from the following equations.

The rate of water ingestion in the inlet is given by

$$m_{W_I} = LWC_I \, A_I \, V_I$$

and the concentration factor C_t is given by

$$C_t = \frac{LWC_I \, A_I \, V_I}{LWC_\infty \, A_\infty \, V_\infty}$$

rearranging, the relationship of inlet LWC (LWC_I) to free-stream LWC (LWC_∞) is

$$LWC_I = C_t \, LWC_\infty \, \frac{V_\infty}{V_I}$$

To determine the LWC at various components, one must consider both the area ratios (which are proportional to the volume ratios in the mass per volume term LWC), the mass rate of water lost from the airstream due to the impingement, and accumulation of drops on objects upstream of the component under consideration. The airflow bypass ratio should also be considered for bypass engines. Components throughout the induction system and inlet will selectively remove drops at rates depending on the component geometry, the droplet size, and the velocity at which the drops are approaching the component.

Using collection efficiency as defined in Fig. B-2, the ratio of the portion of the stream tube area (A_{ST}) which will impinge on a particular component to the component projected area (A_{proj}) for a particular drop size (d_i) is given by

$$E_{m_{d_i}} = \frac{A_{st,d_i}}{A_{proj}}$$

If MF_{d_i} is the mass fraction of total liquid mass of a projected area which is contained in all droplets of size d_i, the amount of liquid water removed by impingement on a component (MF_{d_i},rem) is given by

$$M_{d_i,rem} = MF_{d_i} \, M_{total} \, \frac{A_{ST,d_i}}{A_{proj}}$$

or

$$M_{d_i,rem} = MF_{d_i} \, M_{total} \, E_{m_{d_i}}$$

and the remaining liquid is given by

$$M_{remain} = M_{total} - \Sigma \, (M_{d_i,rem})$$

summed over all droplet diameters.

For the remaining liquid passing into an area (A) at a velocity (V), the LWC is given by

$$LWC = \frac{M_{remain}}{VA}$$

For a constant mass of liquid (that is, no impingement has taken place) as the area is changed the LWC will change proportionately. The MVD will also be reduced, by removal of the drops of size d_i contained in the area $A_{ST_{d_i}}$, depending on $E_{m_{d_i}}$.

Procedures similar to these may be used to determine the effective LWC and MVD for engine and induction system components. As mentioned earlier, Ref. 4 gives detail on this type of procedure.

An initial attempt to determine the amount of ice accreted on a surface can be made by assuming the accretion does not change the effective capture area of the collection surface. For a surface per unit width, the rate of liquid impingement for the total wetted area is

$$W_w = LWC \, V \, A_{eff}$$

where

$$A_{eff} = A_{proj} \, (E_m)$$

which may also be expressed on a local stagnation line basis as

$$A_{eff} = A_{proj} \, (\beta)$$

103

For ice accumulation analysis, the freezing fraction (N) can be included to account more accurately for the amount of impinging liquid (W_w) that freezes and accumulates as ice. Ice accumulation is sometimes given as

$$W_i = W_W (N)$$

It is sometimes assumed that if N is unity, a conservative value of ice accumulation will be the result. This is not always a good assumption. For N close to 1.0 (rime ice), the accretion is generally smooth and aerodynamically streamlined, but for values of N close to zero (glaze ice), the accretion forms well-defined horns, as shown in Fig. B-3. A rise in temperature leading to a reduction in N may well lead to a large increase in the effective capture area leading to a greater amount of water captured, thereby overcoming the reduction in the amount of impinging water which freezes. The growth of ice on a surface does change the collection characteristics of that surface due to changes in shape and surface texture which will, in turn, affect the capture area, collection efficiency, and heat transfer values. This invalidates the assumption that a lower freezing fraction will result in a smaller ice accumulation. Reference 5 gives some probable guidelines for the limits of accumulation allowable for engine components.

No mention of ice shedding has been made. Obviously, the shedding characteristics of ice formations are important in icing tests. Nonsymmetrical shedding on rotating bodies may lead to rotor imbalance and excessive vibration. Continuous shedding of ice from engine and induction system components of which the engine is tolerant is not an icing problem, but shedding of ice in pieces large enough to cause damage is a problem. If no shedding occurs, the flow passage may become blocked and choke off airflow, causing engine operating problems. Shedding characteristics will certainly affect the shape and, thus, the capture properties of a component, but detailed discussion is beyond the scope of this report. Study of shedding was reported in Ref. 16.
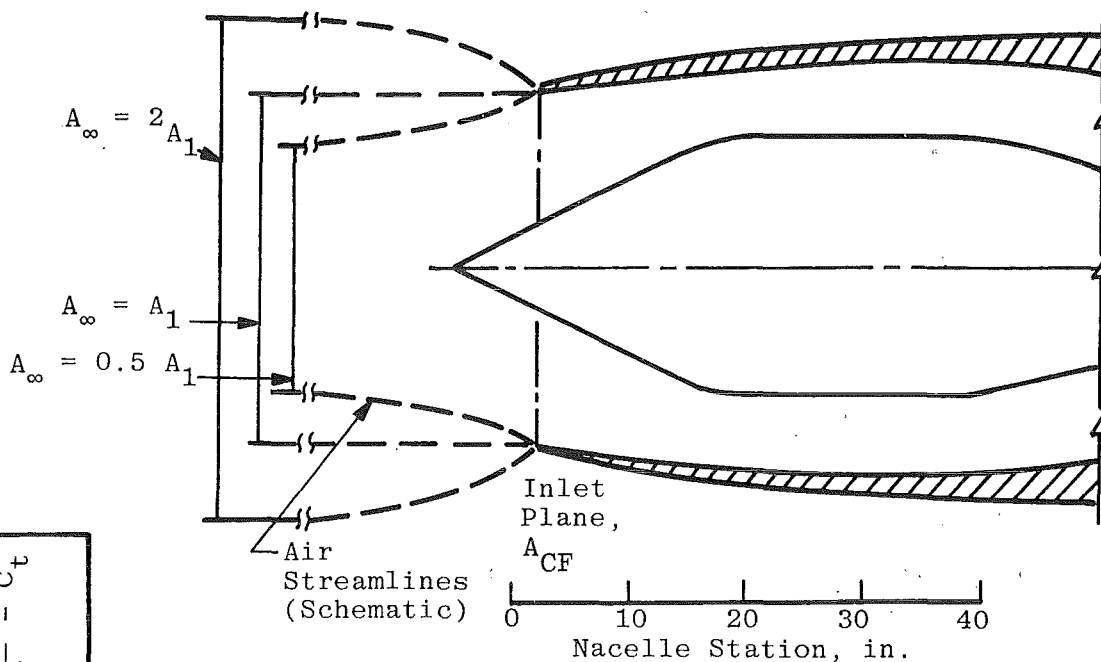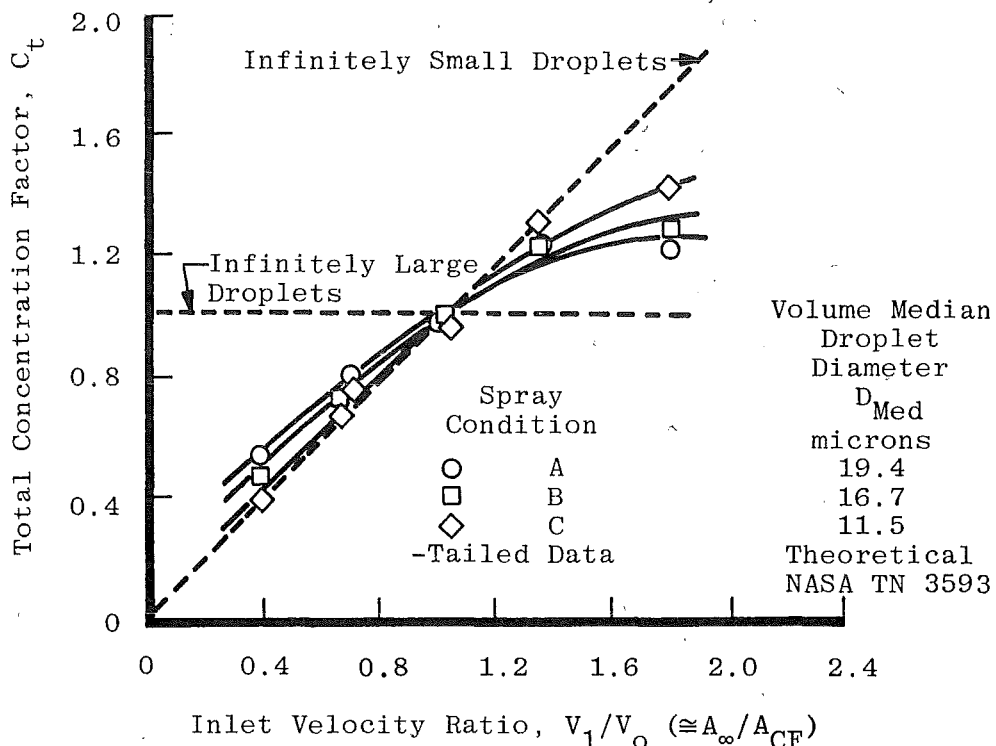
FIGURE B-1. INLET CATCH EFFICIENCY.

M_{total} = Total Liquid Mass Captured by (A_{proj})

M_{d_i} = Mass, captured by A_{proj}, contained in droplets of diameter d_i

$$MF_{d_i} = \frac{M_{d_i}}{M_{total}}$$

Projected Area (A_{proj})

Projected Stream Tube Area for Droplet Diameter d_i $\left(A_{ST_{d_i}}\right)$

Projected Height of Stream Tube $H_{ST_{d_i}}$

Projected Height of Airfoil, H_{proj}
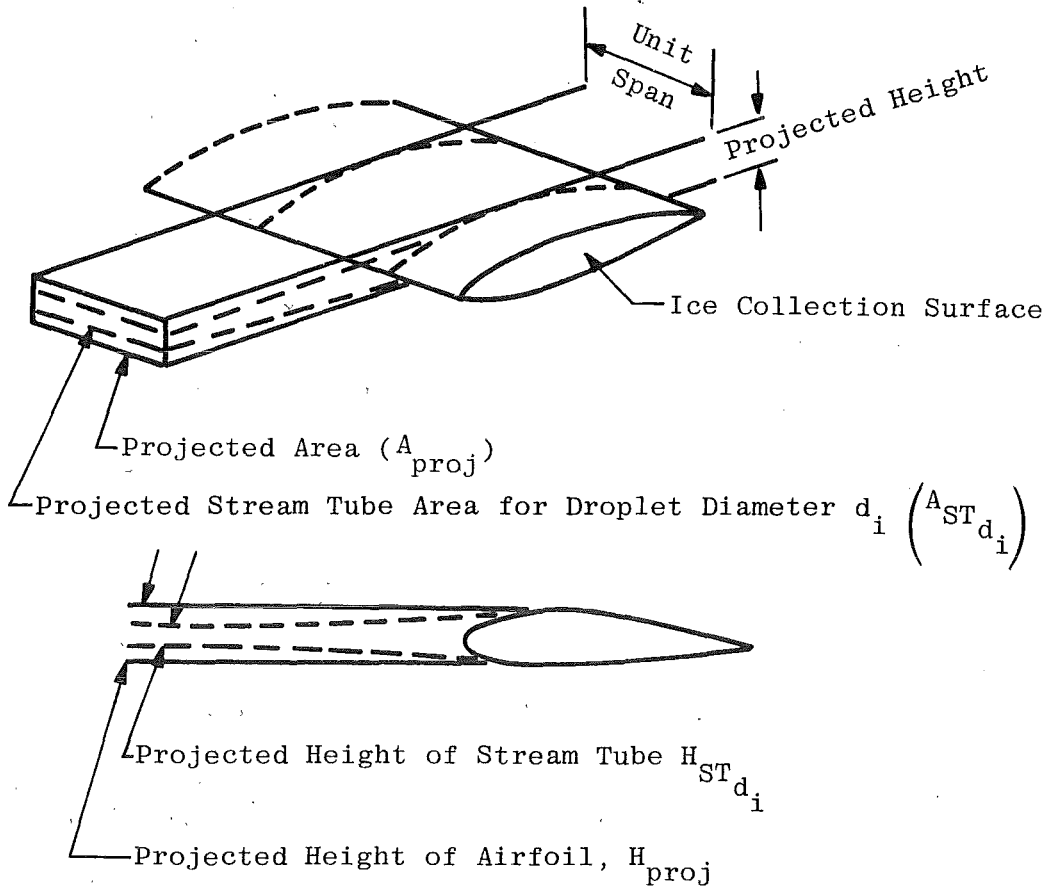
Collection Efficiency for Droplets of Diameter (Size) d_i

$$E_{m_{d_i}} = \frac{H_{ST_{d_i}}}{H_{proj}}$$

on a per unit width basis $E_{m_{d_i}}$ can be given by

$$E_{m_{d_i}} = \frac{A_{ST_{d_i}}}{A_{proj}}$$

FIGURE B-2. COLLECTION EFFICIENCY FOR DROPLETS OF DIAMETER d_i

o   Sketches shown on same scale for ease of comparison

o   Shaded areas represent rime ice

LWC, gm/m^3	V_∞, ft/sec	T_s, °F	P_s, psia	MVD, μm	τ, min	K_o	n	b	ϕ, °F	θ, °F	
1.2	200	23	14.2	20	7.5	2.29	0.15	0.78	8.2	10.9	(Glaze)
1.2	200	5	14.2	20	7.5	2.29	0.50	0.83	26.2	35.5	(Mixed)
0.58	200	0	12.2	15.4	10	0.79	0.90	0.48	31.2	43.6	(Rime)

FIGURE B-3. COMPARISON OF GLAZE, MIXED, AND RIME ICE ACCRETIONS SHOWING FREEZING FRACTION VALUES (TAKEN FROM AEDC-TR-85-30).